ANTI-PARKINSONIAN DRUG DELIVERY ACROSS THE BLOOD-BRAIN BARRIER

A THESIS SUBMITTED TO
THE GRADUATE SCHOOL OF NATURAL AND APPLIED SCIENCES
OF
MIDDLE EAST TECHNICAL UNIVERSITY

BY

ZEYNEP BARÇİN

IN PARTIAL FULLFILLMENT OF THE REQUIREMENTS
FOR
THE DEGREE OF MASTER OF SCIENCE
IN
BIOTECHNOLOGY

FEBRUARY 2014

Approval of the thesis:

ANTI-PARKINSONIAN DRUG DELIVERY ACROSS THE BLOOD-BRAIN BARRIER

submitted by **ZEYNEP BARÇİN** in partial fulfillment of the requirements for the degree of **Master of Science in Biotechnology Department, Middle East Technical University by,**

Prof. Dr. Canan Özgen _____
Dean, Graduate School of **Natural and Applied Sciences**

Prof. Dr. Filiz Bengü Dilek _____
Head of Department, **Biotechnology**

Assoc. Prof. Dr. Dilek Keskin _____
Supervisor, **Engineering Sciences Dept., METU**

Assist. Prof. Dr. Seval Korkmaz _____
Co-Supervisor, Cell Culture and In Vitro Screening Supervisor, **Abdi Ibrahim Inc.**

Examining Committee Members:

Assoc. Prof. Dr. Ayşen Tezcaner _____
Engineering Sciences Dept., METU

Assoc. Prof. Dr. Dilek Keskin _____
Engineering Sciences Dept., METU

Assist. Prof. Dr. Seval Korkmaz _____
Cell Culture and In Vitro Screening Supervisor, Abdi Ibrahim Inc.

Assoc. Prof. Dr. Can Özen _____
Biotechnology Dept., METU

Assist. Prof. Dr. İrem Erel Göktepe _____
Chemistry Dept., METU

Date: _____

I hereby declare that all information in this document has been obtained and presented in accordance with academic rules and ethical conduct. I also declare that, as required by these rules and conduct, I have fully cited and referenced all material and results that are not original to this document.

Name, Last name: Zeynep Barçin

Signature:

ABSTRACT

ANTI-PARKINSONIAN DRUG DELIVERY ACROSS THE BLOOD-BRAIN BARRIER

Zeynep Barçin

M.Sc., Department of Biotechnology

Supervisor: Assoc. Prof. Dr. Dilek Keskin

Co-Supervisor: Assist. Prof. Dr. Seval Korkmaz

February 2014, 121 pages

Localized and controlled delivery of drugs at their site of action is necessary to increase its efficiency. Current study was designed on the development of a brain targeted liposomal Levodopa delivery system for the treatment of the Parkinson's disease. Size and surface charge of the liposomes were modified and optimized to increase the bioavailability and effectiveness of the liposomes. The liposomes were produced in sizes to be administrated intravenously (D: 100-150 nm). In initial optimization studies, the conventional Large Unilamellar Vesicles (LUVs) were prepared with three different molar lipid compositions (DPPC:Cho; 8:2, 7:3, and 6:4) at four different temperatures (38, 40, 42 and 44^{o}C). Among the conventional LUVs, DPPC:Cho (7:3) liposomes prepared at 40^{o}C with the highest Levodopa encapsulation efficiency and slowest cumulative Levodopa release was PEGylated with two different ratios (2 and 4 mole percentage of DPPC). PEGylated liposomes (i.e. 2% PEG/LUV and 4% PEG/LUV) had slower *in vitro* cumulative percent Levodopa release than conventional liposomal formulations. The targeted liposomes were prepared with two different mole percentage of maltodextrin (i.e. 0.35 and 0.7 mole percentage of DPPC) conjugation to 4% PEG/LUV (i.e. 0.35% MD-4% PEG/LUV and 0.7% MD-4% PEG/LUV). Maltodextrin conjugated liposomes are promising for brain drug delivery via receptor-mediated endocytosis. This study is novel for developing maltodextrin conjugated liposomes as a brain targeted delivery system for the first time. Later, the targeted liposomal formulation 0.7% MD-4%

PEG/LUV was loaded with both Levodopa and GSH (LD-20μM GSH-0.7% MD-4% PEG/LUV and LD-40μM GSH-0.7% MD-4% PEG/LUV). The antioxidant GSH was incorporated to improve liposome stability and drug bioavailability. This study is also new for bringing Levodopa and GSH in the same liposomal formulation. Among all experimental groups, LD-40μM GSH-0.7% MD-4% PEG/LUV had the slowest *in vitro* cumulative percent Levodopa release (19.12 ± 0.97% and 31.07 ± 1.98% at 24 and 48 hours, respectively). *In vitro* cytotoxicity experiments revealed that percent viabilities of the 3T3 and SH-SY5Y cells were higher than 80% after 48 hours incubation with liposomal formulations. Among experimental groups, LD-40μM GSH-0.7% MD-4% PEG/LUV had the highest Levodopa passage in Parallel Artificial Membrane Permeability Assay for Blood-Brain Barrier (PAMPA-BBB) and had superior binding to MDCK cells via receptor mediated association. LD-40μM GSH-0.7% MD-4% PEG/LUV was found quite stable at 4^{o}C after 5 months with good particle size distribution and drug encapsulation efficiency. These data suggest that designed dual loaded maltodextrin conjugated liposomal formulation is promising in brain targeted drug delivery with controlled and sustained drug release property, low cellular cytotoxicity, good BBB delivery, and good stability. This brain targeted liposomal delivery system will bring a novel approach for the delivery of Levodopa to increase brain transition with decreased drug side effects.

Keywords: Parkinson’s disease, Blood-Brain Barrier (BBB), liposome, brain targeted liposome, Levodopa (L-Dopa), Glutathione (GSH), maltodextrin.

ÖZ

KAN-BEYİN BARİYERİNDEN BEYİNE ANTİ-PARKİNSON İLAÇ TAŞINMASI

Zeynep Barçin
Master, Biyoteknoloji
Tez Yönetici: Doç. Dr. Dilek Keskin
Ortak Tez Yöneticisi: Y. Doç. Dr. Seval Korkmaz
Şubat 2014, 121 sayfa

Hasta organa hedefli ve kontrollü ilaç salamı yapan ilaç taşıma sistemleri yüksek tedavi etkinliğine sahip olmalarından dolayı gereklidirler. Bu çalışmanın amacı Parkinson hastalığının tedavisine yönelik geliştirilmiş beyine hedeflendirilmiş bir lipozomal Levodopa taşıma sistemi geliştirilmesidir. Lipozomların boyut ve yüzey yükleri etkinlik ve biyoyararlılıklarını artıracak şekilde değiştirilmiş ve en uygun hale getirilmiştir. Lipozomlar damar içine uygulanabilecek boyutlarda üretilmişlerdir (D: 100-150 nm). Ön optimizasyon çalışmaları dört farklı sıcaklıkta (38, 40, 42 ve 44^{o}C) üç farklı lipit kompozisyonu (DPPC:Kol; 8:2, 7:3 ve 6:4) ile hazırlanan konvensiyonel Büyük Tek Tabakalı Lipozomlar (LUV) ile yapılmıştır. Konvensiyonel LUV'ler arasından en yüksek ilaç hapsetme verimliliğine ve en yavaş kümülatif Levodopa salımına sahip olan 40^{o}C'de hazırlanan DPPC:Kol 7:3 iki farklı oranda PEGile edilmiştir (DPPC'nin molar olarak % 2 ve 4'ü oranında). PEGile lipozomlar (% 2 PEG/LUV ve % 4 PEG/LUV) konvensiyonel lipozomlardan daha yavaş *in vitro* kümülatif yüzde ilaç salımına sahip olmuşlardır. Hedefli lipozomlar, PEGile lipozomal formülasyon %4 PEG/LUV'ye iki farklı oranda maltodekstrin (DPPC'nin molar olarak yüzde 0.35 ve 0.7'si oranında) bağlanması ile oluşturulmuştur (% 0.35 MD-% 4 PEG/LUV ve (% 0.7 MD-% 4 PEG/LUV). Maltodekstrin bağlanmış olan lipozomlar beyine reseptör aracılığı ile endositoz yoluyla ilaç taşıyabileceği için umut vericidir.Bu çalışma lipozomların maltodekstin bağlanması ile beyine hedeflendirilmesi açısından yenilikçi bir çalışmadır.

Sonrasında hedefli lipozom formülasyonuna % 0.7 MD-% 4 PEG/LUV hem Levodopa hem de GSH hapsedilmiştir (LD-20μM GSH- % 0.7 MD-% 4 PEG/LUV and LD-40μM GSH- % 0.7 MD-% 4 PEG/LUV). Antioksidan GSH hem lipozom stabilitesini hem de ilaç biyoyararlımını artırmak için eklenmiştir. Bu çalışma Levodopa ve GSH'ın aynı lipozomal formuülasyon içinde hapsedilmesi açısından yenilikçidir. Bütün deney grupları arasında, LD-40μM GSH- % 0.7 MD-% 4 PEG/LUV en yavaş *in vitro* kümülatif yüzde Levodopa salımına sahip olmuştur (24 ve 48 saatin sonunda sırasıyla % 19.12 ± 0.97 ve % 31.07 ± 1.98 ilaç salımı). *In vitro* sitotoksisite deneylerinde lipozomalarla inkübe edilen 3T3 ve SH-SY5Y hücreleri 48 saatin sonunda %80'in üzerinde canlılığa sahip olmuşlardır. Deney grupları arasında, LD-40μM GSH- % 0.7 MD-% 4 PEG/LUV Kan-beyin Bariyeri Paralel Yapay Membran Geçirgenlik Deneyinde (PAMPA-BBB) en yüksek Levodopa geçişini ve reseptör aracılığıyla MDCK hücrelerine bağlanma özelliğini göstermiştir. 4^{o}C'de saklanan LD-40μM GSH- % 0.7 MD-% 4 PEG/LUV'nin 5 aya kadar boyut dağılımını ve ilaç hapsetme verimliliğini koruyarak oldukça sağlam kalmıştır. Bu sonuçlar, geliştirilen ikili yüklenmiş maltodekstrin bağlanmış lipozomal formülasyonun, kontrollü ve sürekli ilaç salımı yapan, düşük sitotoksisiteye sahip olan, KBB'yi geçebilen, hücresel bağlanma özelliği fazla olan ve iyi stabiliteye sahip olan umut verici bir lipozomal ilaç sistemi olduğunu göstermektedir. Geliştirilen beyine hedefli lipozomal bu ilaç taşıma sistemi Levodopa'nın beyindeki konsantrasyonunu artırabilecek ve yan etkilerini de azaltabilecek bir sistemdir.

Anahtar kelimeler: Parkinson hasalığı, Kan-beyin Bariyeri (KBB), lipozom, beyin hedefli lipozom, Levodopa (L-Dopa), Glutatyon (GSH), maltodekstrin.

to my family for always being with me and supporting me in all conditions

ACKNOWLEDGEMENTS

I would like to express my special appreciation and thanks to my advisor Assoc. Prof. Dr. Dilek Keskin for her guidance, encouragement, and support throughout my thesis study. I would like to thank my co-advisor Assist. Prof. Dr. Seval Korkmaz for her advice and assistance in my thesis study. I also would like to express my special thanks to Assoc. Prof. Dr. Ayşen Tezcaner for her corcern, contribution, and encouragement in my thesis study from beginning to the end.

I would like to thank my thesis committee members, Assoc. Prof. Dr. Can Özen and Assist. Prof. Dr. İrem Erel Göktepe for their interest in my thesis study and their assistances and recommendations.

I would like to thank Middle East Technical University Graduate School of Natural and Applied Sciences for supporting my thesis study for the financial support by the Project BAP-03-10-2013-002. I would like to thank Abdi Ibrahim Pharmaceuticals Incorporation for supplying raw materials and cell culture ingredients for my thesis study. I also would like to thank to Halil Memiş at Middle East Technical University Chemical Storeroom for chemical supply. I also would like to thank Leyla Kaya at Middle East Technical University Engineering Sciences Secretarial for her assistance in payments.

I would like to thank Middle East Technical University Central Laboratory Research and Development Education and Measurement Center and Molecular Biology and Biotechnology Research and Development Center for performing some important analysis in my thesis study. I would like to thank Ibrahim Çam for particle size and zeta potential analysis, Binnur Özkan and Elif Unsal for Fourier Transform Infrared and Raman (FTIR) Spectroscopy analysis, Tuğba Endoğan Tanır and Seçkin Öztürk for Transmission Electron Microscopy (TEM) analysis, and Fatma Gül for Laser Scanning Confocal Microscopy (LSCM) analysis.

I would like to acknowledge the asisstance of my laboratory friends. I would like to thank Ayşegül Kavas, Özge Erdemli, Ömer Aktürk, and Sibel Ataol for their guidance in my laboratory studies. I also would like to express my very special thanks for Aslı Erdoğ and Mert Baki for training me in liposome preparation.

I also would like to thank my other laboratory friends for allowing me to grow as a multi oriented research scientist. I would like to represent my deepest love for Deniz Atila for being my extraordinary and imaginative fiend, Ali Deniz Dalgıç for being my open-minded and nature lover friend, Nil Göl for being my innocent and pure-minded friend, Merve Güldiken for being my creative and designer friend, Engin Pazarçeviren for being my sophisticated friend, Reza Moonesirad and Aydın Tahmasebifar for being my Azeri Turkish friends and teaching me their culture and civilization, Hazal Aydoğdu for being my surprizing and traveller friend, Bengi Yılmaz for being my intelligent and researcher friend, Alişan Kayabölen for being my energetic and sportive friend, Bora Onat for being my philharmonic friend, and Yağmur Çalışkan for being my polite and elegant friend.

I also would like to thank my childhood friends Esra Daş, İnci Ulay, Nisa Tuzcu, Çidem Argunhan, and Gözde Çoban for always being with me regardless.

I would to state my special thanks to Fatih Furkan Gürtürk for being my greatest support not only during my thesis study but also during my lifetime.

A special thanks to my family. I would like to express my grateful feelings for my father Ömer Barçin, my mother Sevim Nuran Barçin, my brother Kutay Barçin, and my sister İpek Barçin for supporting me in all aspects all the time...

Once and for all, I would like to thank to Mustafa Kemal Atatürk for founding the civilized Turkish Republic, upgrading the education level of the community, and ensuring the participation of the women in society. I owe my twenty year-old modern education life to his incredible reformations.

TABLE OF CONTENTS

LIST OF TABLES

TABLES

LIST OF FIGURES

FIGURES

LIST OF ABBREVIATIONS

3T3: Anl Swiss albino mouse fibroblast cell line

ABS: Absorbance

ANOVA: Analysis of Variance

ATR-FTIR: Attenuated Total Reflectance Fourier Transform Infrared Spectroscopy

BBB: Blood-Brain Barrier

CF: Corrected Fluorescence

CFS: Cerebrospinal Fluid

Cho: Cholesterol

CNS: Central Nervous System

Conj. Eff.: Conjugation efficiency

CTEM: Contrast Transmission Electron Microscopy

DCC: N,N-Dicyclohexylcarbodiimide

DLS: Dynamic Light Scattering

DMEM: Dulbecco‘s Modified Eagle‘s Medium

DMSO: Dimethyl Sulphoxide

DPPC: PC (1,2-dipalmitoyl-*sn*-glycero-3-phosphocholine, 16:00)

DSPE-mPEG(2000): 1,2-distearoyl-*sn*-glycero-3-phosphoethanolamine-N-methoxy(polyethylene glycol)-2000

DSPE-PEG(2000)Amine: 1,2-distearoyl-*sn*-glycero-3-phosphoethanolamine-N-[amino(polyethylene glycol)-2000] (ammonium salt)

EE: Encapsulation Efficiency

ELISA: Enzyme-linked Immunosorbent Assay

EPC: Egg Yolk Phosphotidylcholine

EPR: Enhanced Permeability and Retention Effect

FBS: Fetal Bovine Serum

FDA: Food and Drug Administration

FSU: Fluorescent Standard Unit

FTIR/ATR: Fourier Transform Infrared Spectrometer/Attenuated Total Reflectance

GSH: Glutathione

HPLC: High Performance Liquid Performance

LD: Levodopa

L-Dopa: Levodopa

LSCM: Laser Scanning Confocal Microscopy

LUVs: Large Unilamellar Vesicles

mAbs: Monoclonal Antibodies

MAOIs: Monoamino Oxidase Inhibitors

MD: Maltodextrin

MDCK: Madin-Darby Canine Kidney epithelial cells

MIR: Mid Infrared

MLVs: Multilamellar Vesicles

mPEG: Methoxy Polyethylene Glycol

MPS: Mononuclear Phagocyte System

MTT: 3-(4,5-Dimethylthiazol-2-yl)-2,5-diphenyltetrazolium bromide

MW: Molecular Weight

MWCO: Molecular Weight Cut-Off

NHS: N-Hydroxysuccinimide

PAMPA-BBB: Parallel Artificial Membrane Permeability Assay for Blood-brain Barrier

PB: Phosphate Buffer

PBS: Phosphate Buffer Saline

PC: Polycarbonate

PdI: Polydispersity Index

PEG: Polyethylene Glycol

PP: Polypropylene

RES: Reticuloendothelial System

RMT: Receptor-mediated Transporters

RPM: Revolutions per Minute

SH-SY5Y: Neuronal tumor cell line with human neuroblastoma cells

SUVs: Small Unilamellar Vesicles

TEM: Transmission Electron Microscopy

TfR: Transferring Receptor

z-average diameter: Average hydrodynamic diameter

CHAPTER 1

INTRODUCTION

1.1.Parkinson's disease

1.1.1. Origin and Symptoms of the Disease

Parkinson's disease is a progressive neurodegenerative disorder. The disease primarily results from the death of dopamine-generating cells in the substantia nigra, the middle part of the brain. The reason of cell death has not been completely identified yet [1, 2]. The possible reasons for neuronal death were clarified as oxidative stress, neuroinflammation, abnormal protein accumulation, change in protein degradation via various pathways, mitochondrial dysfunction, and dysregulated kinase signaling [1, 2].

Parkinson's disease is geriatric disease that is most commonly observed after the age of 55 [1]. There is no certain test to identify this disease. It is diagnosed from some motor and non-motor symptoms associated with the disease [3]. The most common motor symptoms are tremor, brandykinesia, rigidity, postural instability, postural deformity, and freezing. The non-motor symptoms include autonomic dysfunction (i.e. sweating, sphincter, and erectile dysfunction, and orthostatic hypotension), cognitive, neurobehavioral, and sensory abnormalities, and sleep disorders [3].

The symptoms vary from patient to patient according to the degree of the disease. The patient having complaints about some motor or non-motor symptoms must be well checked before having being diagnosed for the Parkinson's disease. An authorized neurologist who is experienced in the field of movement disorders should carry out the medical examination. The accurate diagnosis of the disease is very important before starting treatment considering that other diseases may show the same symptoms [4].

1.1.2. Treatment of the Disease

Parkinson's disease is a permanent disease that cannot be completely cured. The treatment of the disease can be accomplished by either medical or surgical treatment. The medical treatment is only used to control the symptoms while minimizing the side effects [5]. The medication treatment program varies from patient to patient. Each patient follows an individual drug therapy program according to degree of disability and ability to tolerate the medication [5].

The patients with mild motor disability and no cognitive impairment take monoamino oxidase inhibitors (MAOIs), dopamine agonists (DAs), Catechol-O-methyl Transferase Inhibitors (COMTIs) or anti-cholinergics [6, 7]. MAOs are the enzymes inactivating certain monoamines including dopamine. MAOIs increase the availability of the dopamine by inhibiting the activity of the MAOs. Dopamine agonists simulate the action of dopamine by activating the dopamine receptors. They simulate the activity of the dopamine in the brain by imitating the dopamine characteristics at the cells using dopamine [6, 7]. The Catechol-O-methyl Transferases are the enzymes degrading the catecholamines including dopamine. COMTIs improve the effect of the dopamine by preventing its breakdown by the COMTs. Anti-cholinergics act to reduce the action of the acetylcholines that prevent the dopamine activity in the brain [6, 7]. The patients having cognitive impairment or age more than 70 with moderate or severe disability take dopamine replacement therapy. Levodopa (L-Dopa) is the most commonly used drug in the dopamine replacement therapy. In the brain Levodopa is converted to dopamine and stored in nerve cells to replace deficient dopamine [8].

In Table 1.1 the medications used in the Parkinson's disease therapy are listed. All of these medications are taken orally at high doses and cause side effects such as low blood pressure, nausea, dyskinesia, and dizziness [9]. They later become ineffective and more powerful treatment techniques are required.

Table 1.1. The medications used in Parkinson's disease therapy (modified from www.neurotransmitter.net and www.parkinsons.about.com)

Generic Name	**Trade Name**	**Company Name**	**Mechanism of Action**
Amantadine hydrochloride	Symmetrel	Endo	Anti-cholinergic
Apomorphine hydrochloride	Apokyn	Mylan Bertek	Dopamine agonist
Benztropine mesylate	Cogentin	Merck	Anti-cholinergic
Biperiden hydrochloride	Akineton	Abbott, Par	Anti-cholinergic
Bromocriptine mesylate	Parlodel	Novartis	Dopamine agonist
Carbidopa	Lodosyn	Bristol-Myers Squibb	Aromatic L-amino acid decarboxylase
Carbidopa, entacapone, and **Levodopa**	Stalevo	Orion	Dopamine replacement
Carbidopa/ **Levodopa**	Sinemet	Bristol-Myers Squibb	Dopamine replacement
Carbidopa/**Levodopa** orally disintegrating tablet	Parcopa	SRZ Properties, *Inc*.	Dopamine replacement
Entacapone	Comtan	Orion (marketed by Novartis)	Catechol-O-methyl Transferase Inhibitor
Pergolide mesylate	Permax	Eli Lilly	Dopamine agonist
Pramipexole dihydrochloride	Mirapex	Boehringer Ingelheim (marketed by Pfizer)	Dopamine agonist
Procyclidine hydrochloride	Kemadrin	Monarch	Anti-cholinergic
Rasagiline	Azilect	Teva Neuroscience, Inc.	Monoamino oxidase inhibitor
Ropinirole hydrochloride	Requip	GlaxoSmithKline	Dopamine agonist
Rotigotine (transermal system)	Neupro	Aderis Pharmaceuticals. (marketed by Schwarz Pharma)	Dopamine agonist
Selegiline hydrochloride	Eldepryl	Somerset	Monoamino oxidase inhibitor
Tolcapone	Tasmar	Valeant	Catechol-O-methyl Transferase Inhibitor
Trihexyphenidyl	Artane	Lederle Pharmaceuticals	Anti-cholinergic
Trihexyphenidyl hydrochloride	Broflex	Alliance	Anti-cholinergic

In case of very severe symptoms or when the medications are no longer sufficient, surgical operations are used in the treatment of Parkinson's disease [10]. In the surgical operations some electrodes are implanted into the brain and they are controlled by an electric pulse generator. This generator is also implanted into the body. The high frequency deep brain stimulation improves even very severe symptoms of the Parkinson's disease. However, the brain surgery operations have risk of infections, stroke, and brain hemorrhage [10].

1.1.2.1.Levodopa

Levodopa is the most effective medication in treatment of Parkinson's disease symptoms, especially brandykinesia and rigidity [8]. It was first synthesized by Casimir Funk in 1911 and it was approved by the US Food and Drug Administration in 1970 [11]. Since then, it has been widely used for the treatment of Parkinson's disease. The chemical formula of Levodopa is L-3,4-dihydroxyphenylalanine and its chemical structure is as shown in Figure 1.1.

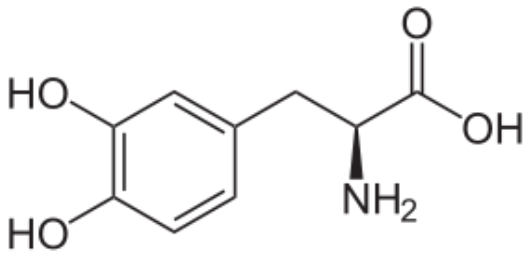

Figure 2.1. Chemical Structure of the Levodopa [8]

The Levodopa has great importance in the body cycle. It is involved in the catecholamine biosynthesis pathway [12]. Figure 1.2 shows synthesis of dopamine, norepinephrin (noradrenalin), and epinephrine (adrenalin) from Levodopa. Dopamine is the first catecholamine produced from Levodopa. Later norepinephrine and epinephrine are generated in further modifications of the dopamine [12]. In Parkinson's disease treatment, Levodopa is used as precursor of dopamine. When it gets into the brain, it is rapidly converted to dopamine by the enzyme DOPA decarboxylase [8].

All patients eventually need Levodopa (L-Dopa) in their medical treatment in Parkinson's disease, as it is a progressive disease. The Levodopa drug formulations involve other chemicals such as carbidopa and bensarizide in order to prevent its conversion to dopamine outside the brain [13]. These formulations cause side effects including dyskinesias (i.e. involuntary movements), nausea, vomiting, and hypotension [13]. Moreover, high-dose administration of Levodopa causes cytotoxicity inducing oxidative stress. The cytotoxicity results from autooxidation of the Levodopa by the free radicals [13]. At this point, it is important to develop new drug strategies with low cytotoxicity and other side effects.

The efficiency of the Levodopa reduces in time due to metabolism, low bioavailability, and the fluctuations in its plasma level [14]. This can be overcome by liposome formulations. The aim of designed Levodopa delivery systems is to increase drug bioavailability and to maintain the required plasma level for a longer time. Continuous drug concentration is required to produce continuous dopaminergic stimulation in the brain. An effective targeted delivery system can overcome all these problems by delivering the Levodopa to the brain inside a proper carrier with prolonged drug circulation [14].

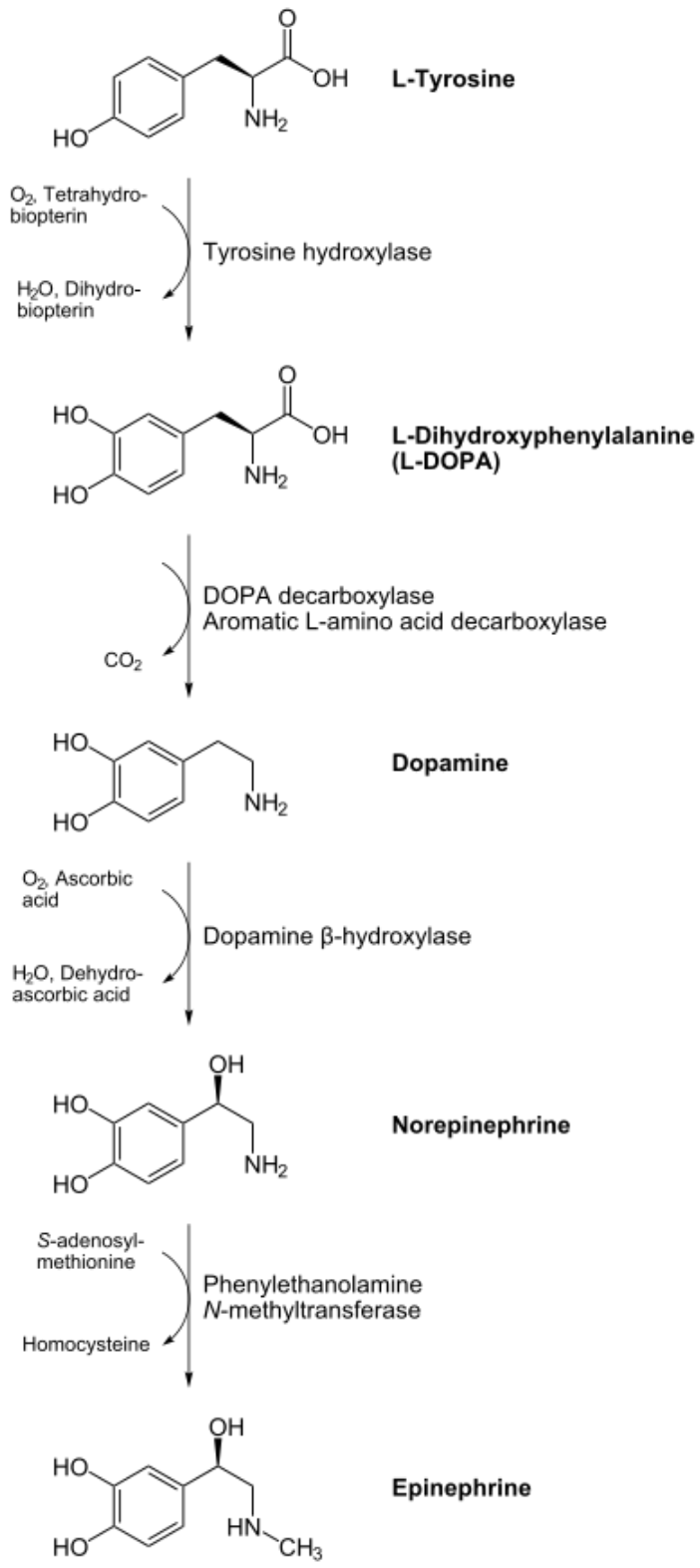

Figure 1.2. Biosynthesis pathway of catecholamines [modified from life-enhancement.com]

1.2.Brain Drug Delivery

Brain is one of the most vital organs in the body. It must be protected against pathogen microorganisms and toxic chemicals. Moreover, its shape and volume has to be kept constant, as it is hold in a rigid bony skull. Molecule flow to the brain is strictly controlled. Most of the therapeutics designed for the brain diseases cannot access the brain due to presence of the physiological barriers [15]. The same problem is encountered in delivery of diagnostic agents to the Central Nervous System (CNS) for medical imaging of the brain [15].

In brain, there are mainly three physiological barriers, which are namely Blood-Brain Barrier (BBB), Blood-Cerebrospinal Fluid Barrier (BCSFB), and arachnoid barrier (Figure 1.3) [16]. These barriers selectively allow transport of the molecules to the brain. The conventional drug delivery systems release the drug into blood circulation system and aim its delivery to the brain. These conventional drug delivery systems fail in delivery of the drugs to the brain due to high protection of the brain [17]. At this point, design of brain targeted drug delivery systems is necessary for the effective delivery of the drugs to the brain.

1.2.1. Barriers of the Brain

The barriers of the brain are the most challenging obstacles in brain drug delivery. The barriers separate the circulating blood stream from the brain extracellular fluid in the central nervous system (CNS) [16]. The ultimate goal of the barriers is to maintain a constant environment (i.e. homoestasis) for the brain [17]. It allows establishment of an optimum extracellular fluid environment in the CNS [18].

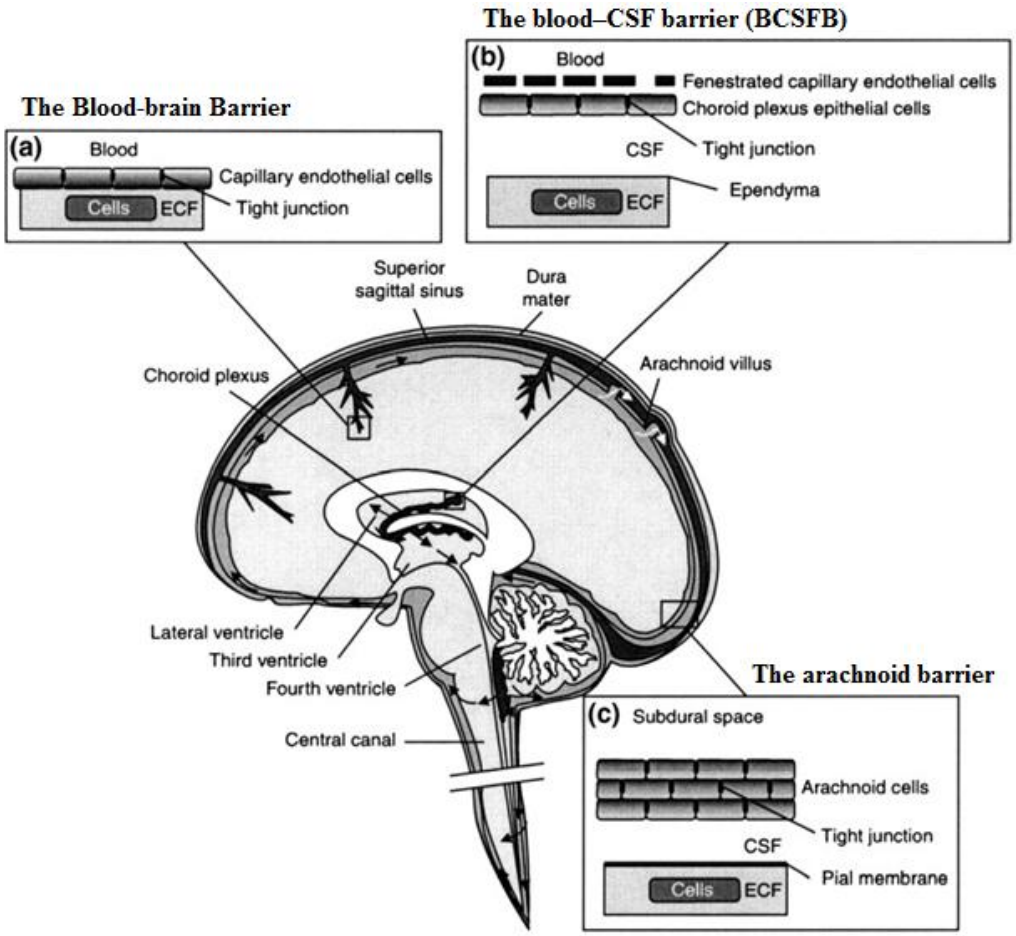

Figure 1.3. Barriers of the brain [18]

The Blood-Brain Barrier (BBB) structure includes endothelial cells and some perivascular elements such as astrocytic foot processes, perivascular neurons, pericytes, and microglial cells (Figure 1.4) [19]. Brain endothelial cells have very different morphology, chemistry, and function from any other endothelial cells in the body. They are strictly interconnected with tight junctions created by the interaction of several transmembrane proteins. The brain endothelial cells have extremely low permeability and fluid-state endocytosis. They allow transport of only nutrients into the CNS and toxic metabolites out of the CNS with some specific transport systems [19, 20].

The astrocytic foot processes (also known as astrocytic feet or glia limitants) surround the brain endothelial cells and provide biochemical structural support to those cells. These processes sustain maintenance of function and tightness of the BBB [19, 20]. The pericytes and microglia cells protect the CNS from changes in physiological and pathological conditions. The neurons regulate the BBB functioning by expressing enzymes [19, 20].

The Cerebrospinal Fluid (CFS) (Figure 1.3) provides the mechanical and immunological protection of the brain regulating the cerebral blood flow [21]. The ion and nutrient transport into the CSF and toxic metabolites out of the CFS are strictly controlled by various transport systems [21]. The regulation of the transport molecules through the Blood-Cerebrospinal Fluid Barrier (BCSFB) sustains the chemical stability of the brain. The changes in the homeostatic regulation of the neuroendocrine factors can damage the nervous system and cause severe problems [18, 22]. BCSFB is located at the tight junctions surrounding and connecting the cuboidal epithelial cells on the choroid plexus surface. The tight junctions between the choroid plexus epithelial cells inhibit the diffusion of paracellular water-soluble molecules across the BCSFB [18, 22].

The Arachnoid barrier (Figure 1.3) has a multi-layered avascular arachnoid epithelium with tight junctions [18]. It completely surrounds the CNS by the arachnoid epithelium and forms a barrier layer. The arachnoid epithelium does not represent a significant exchange surface because it has relatively small area between the blood and CNS [18, 23].

The barriers tightly control the flow of the molecules into the brain by protecting the brain from the changes in ion, amino acid, and peptide level in the blood [24]. The barriers allow the uptake of the essential nutrients, vitamins, and hormones to maintain cerebral growth and metabolism [24]. Moreover, the barriers are responsible for the protection of the brain from circulating neuroactive chemicals such as glycine, glutamate, epinephrine, norepinephrine, and peptide hormones whose concentration in the blood can change with stress, diet, injury, or disease [25].

The barriers have a very vital role for healthy brain functioning. If the barriers become leaky due to trauma or infection, fatal problems can develop. The penetrated water and salts cause swelling (i.e. cerebral oedema) and pressure increase in the brain [26].

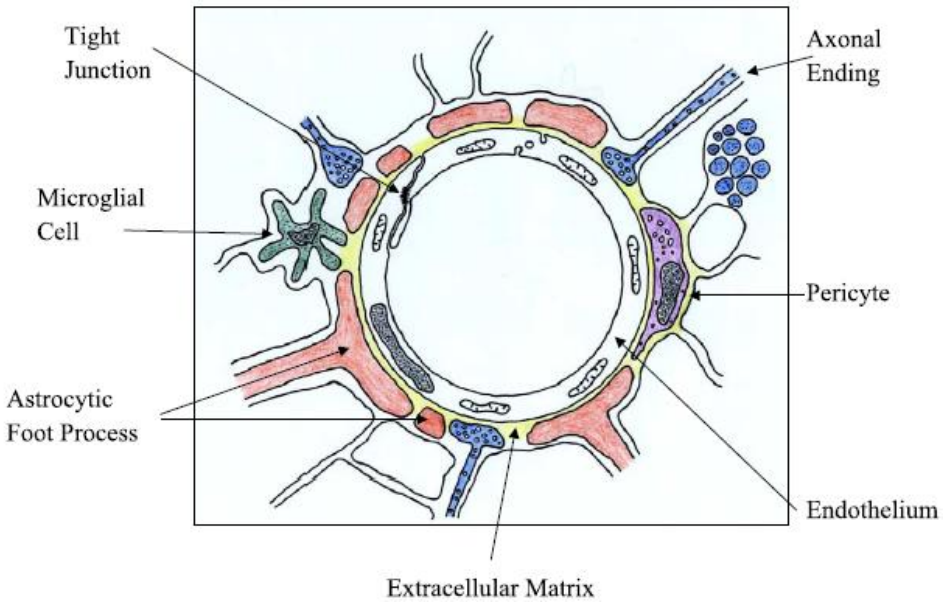

Figure 1.4. Structure of the Blood-Brain Barrier (BBB) [19]

1.2.2. Brain Drug Delivery Strategies

Most of the neurotherapeutics designed for brain diseases cannot get into brain due to Blood-Brain Barrier [27]. Approximately 100% of large-molecule drugs and more than 98% of small-molecule drugs cannot cross BBB [27]. The molecules can get into the brain either by free diffusion (i.e. small lipid soluble molecules with MW<400 Da) or by catalyzed transport in specific transport systems [27]. In order to deliver the pharmaceuticals into the brain, intelligent drug therapies should be designed for the efficient delivery of the drugs into the brain. The drugs should be reformulated in order to access the endogenous BBB transport system and enter the brain.

The endogenous BBB transporter systems can be classified as Carrier-mediated transporters (CMT), Active efflux transporters (AET), and Receptor-mediated transporters (RMT) [28] (Figure 1.5). These transporters are located on the luminal and abluminal membranes of brain capillary endothelium and have specific membrane transporters and carrier molecules with selective permeability and polarity in order to deliver certain molecules [28]. Carrier-mediated transporters (CMT) have glucose transporter (GLUT1), large neutral amino-acid transporter (LAT1), cationic amino-acid transporter (CAT1), monocarboxylic acid or lactate transporter (MCT1), and the adenosine transporter (CNT2) [28]. Receptor-mediated transporters (RMT) have insulin receptor (IR), transferring receptor (TfR), insulin-like growth factor receptor (IGF-R), leptin receptor (OB-R), neonatal Fc receptor (FcRn), and BI scavenger receptor (SR-BI) [28]. Adsorptive-mediated transytosis has plasma protein transporters for cationic protein transport through the barrier via electrostatic interactions [29].

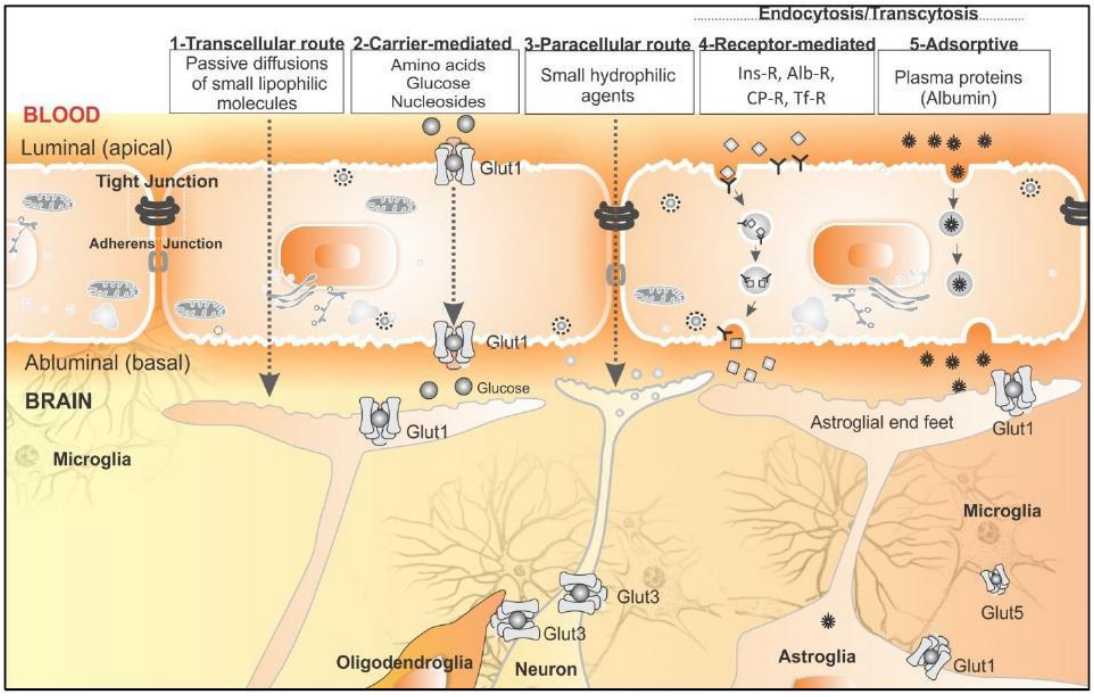

Figure 1.5. Endogenous Blood-Brain Barrier (BBB) transport systems [28]

The pharmacological formulations should be optimized in order to be transported via one of the BBB transporter systems and retain the drug's biological activity in the brain. Drugs may be packaged in nanocarriers such as liposomes or other nanoparticles having a diameter around 100 nm [27]. The surface of the nanocarriers should be modified by conjugation of BBB selective biomolecules (i.e. insulin, glucose, and transferrin) [30].

1.3.Liposomes

Liposomes were first described by the British physician Alec D. Bangham in the early 60's [31]. He stated that in aqueous environment phospholipids spontaneously form a bilayered spherical structure due to presence of both water soluble and water insoluble ends [31]. Water insoluble ends are hidden from aqueous environment and form a lipid phase in circumference of the spherical shape as shown in Figure 1.6. It is possible to encapsulate both water soluble and insoluble compounds in liposomes. The water soluble therapeutics are encapsulated in the aqueous core whereas the water insoluble ones are encapsulated in the lipid phase [32]. Liposomes were firstly studied by the physiologists and biophysicists to investigate ionic flow through cell membranes and phase behavior of the phospholipids [33]. They have been as delivery systems of drugs, genes, cosmetics, and nutrients by many researchers since early 90's [33].

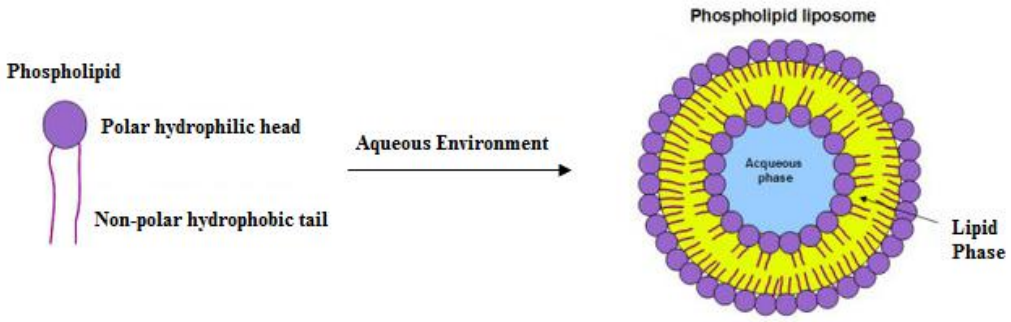

Figure 1.6. Formation of a liposome from phospholipids in the aqueous environment (modified from http://www.springerimages.com)

1.3.1. Types of Liposomes

Liposomes are composed of natural phospholipids, which make them biocompatible and biodegradable [34]. They are biologically inert and have low intrinsic toxicity [34]. The liposomes are classified according to lipid composition and surface modifications. There are mainly three types of liposomes: conventional liposomes, long circulating liposomes, and targeted liposomes (Figure 1.7) [35].

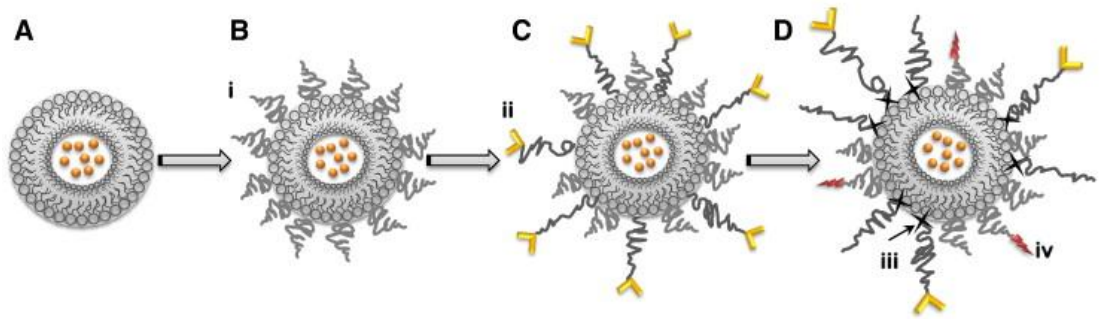

Figure 1.7. Types of liposomes

(a) conventional liposome

(b) long-circulating liposomes coated with a polymer such as (i) polyethylene glycol (PEG)

(c) antibody-targeted long-circulating liposome with (ii) monoclonal antibodies (mAbs) attached to the long-chain PEG

(d) stimulus-sensitive immuno-targeted liposome with mAbs attached to the long-chain PEG via (iii) hidden cell penetrating peptides (CPPs) (iv) conjugated to the short-chain PEG [35]

1.3.1.1.Conventional Liposomes

The conventional liposomes are composed of phospholipids and cholesterol; to encapsulate biomolecules for protecting them from degradation (Figure 1.7) [35]. They are composed of saturated or unsaturated phospholipids. The liposomes composed of saturated phospholipids are more stable as the saturated lipids are packed closely together [36]. Addition of cholesterol increases the packing of the

phospholipids in the lipid bilayer by decreasing the phospholipid transfer to the plasma proteins [37]. Addition of cholesterol also affects the release behavior of the liposomes since the encapsulated molecules are released upon binding to plasma proteins (i.e. high density and low density proteins) [37].

1.3.1.2.Long Circulating Liposomes

The long circulating liposomes are formed by surface modification of the conventional liposomes with hydrophilic polymers (Figure 1.7) [35]. They are generated to resolve some drawbacks of the conventional liposomes. The long circulating liposomes are more effective in preventing aggregation of the liposomes and the removal by the mononuclear phagocyte system (MPS) [38]. In polymer coating, polyethylene glycol (PEG) of various chain lengths has been commonly used owing to low toxicity, low immunogenicity, low antigenicity, and high water solubility [39]. PEG is a polymer of ethylene oxide that has a chemically inert backbone and hydroxyl groups available for derivatization [40]. Various PEG derivatives are commercially available that are covalently bound to proteins, phospholipids, functional groups, and even fluorescent probes [40]. The PEGylated liposomes (also known as stealth liposomes) increase the stability and circulation times of the liposomes by reducing the reticuloendothelial uptake and macrophage encapture, called as steric stabilization [35].

1.3.1.3.Targeted Liposomes

The targeted liposomes are prepared via attachment of certain biomolecules onto the liposome surface in order to target the disease site and enable cellular uptake of the liposome [35]. The targeting moieties are either adsorbed onto the liposome surface or covalently bound to lipids or PEG chains on the surface (Figure 1.7) [35]. Covalently bound targeting moieties have higher binding efficiency on the liposomes and higher binding affinity to the target site. The targeted moieties adsorbed on the liposomes have lower binding affinity due to steric hindrance caused by high density PEG molecules [41].

Actively targeted liposomes contain certain targeting moieties such as peptides, proteins, oligosaccharides, and monoclonal antibodies [42]. Monoclonal antibodies (mAb) are the most widely used targeting moieties [42]. In order to increase the conjugation efficiency, the monoclonal antibodies are divided into smaller fragments via reducing agents or enzymatic degradation by preserving the antigen binding function of the antibody [42]. In general, the targeting moieties are conjugated to the lipids or PEG chains via amine modification, disulfide modification, carbohydrate modification, or noncovalent modification [43].

1.3.2. Preparation of Liposomes

The liposomes can be prepared with different size (small, intermediate, or large) and lamellarity (uni-lamellar, or multi-lamellar) by the different liposome preparation methods [44]. Uni-lamellar vesicles have one lipid bilayer and a large aqueous core to entrap the water-soluble drugs [44].

Uni-lamellar vesicles vary in size. Small unilamellar vesicles (SUVs) have diameter less than 100 nm whereas large unilamellar vesicles (LUVs) have diameter higher than 100 nm (Figure 1.8) [44]. Multilamellar vesicles (MLVs) have 5-25 lipid bilayer and plenty of lipid phases to entrap the lipid-soluble drugs. MLVs are 500-10,000 nm in diameter (Figure 1.8) [45]. The liposomes having diameter higher than 10,000 nm are called as Giant liposomes [45].

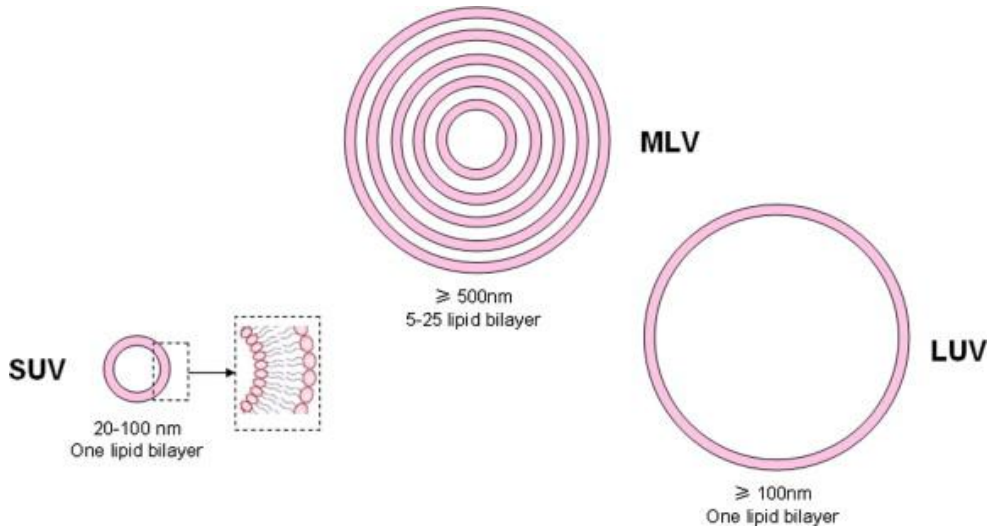

Figure 1.8. Main classification of liposomes based on size and structure [51]

Liposomes can be prepared by various methods (Figure 1.9) to achieve desired properties for the intended application. The simplest and the most widely used method is the thin film hydration method [46]. The characteristics of the liposomes such as size, polydispersity, lamellarity, and surface charge are optimized by controlling the experimental parameters during liposome preparation [46].

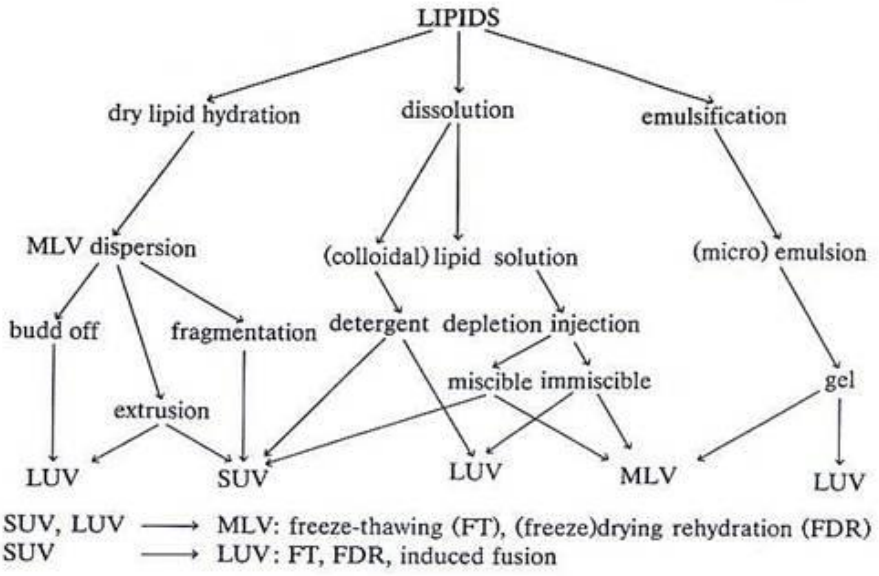

Figure 1.9. Liposome preparation methods [modified from http://www.biotec.boku.ac.at]

1.3.3. Liposomes as Delivery Systems

Liposomal delivery systems have various application areas including drug and vaccine delivery, cosmetics, and food industry [47]. They can be easily and conventionally prepared with good biocompatibility and biodegradability [47]. The liposomal delivery systems have many advantages over conventional drug formulations with site-specific targeting. In liposomal formulations, the bioavailability of the encapsulated bioactive molecule is increased with sustained release and increased circulation time in the body. The sustained controlled release of

the bioactive molecules has higher treatment efficiency with lessen side effects. Targeted delivery systems have advantage of improved intracellular therapeutics delivery with lower systemic toxicity [48, 49].

Liposomal delivery systems are most commonly used in delivery of therapeutics for better therapeutic efficacy and safety over conventional therapeutic formulations [47]. Delivery of various bioactive agents such as therapeutic drugs (i.e. doxorubicin, daunorubicin, amphotericin B, verteporphin, and vincristine), hormones (i.e. growth hormone, parathyroid hormone, and testosterol), and enzymes (i.e. elastase and beta glucosidase) have been performed by liposomal delivery systems [50-52]. Liposomal drug products marketed and in-clinical trials are listed in Table 1.2 and Table 1.3 respectively. Most of the liposomal drug formulations are approved for intravenous application since oral application has potential of liposome breakdown upon exposure to bile salts [52].

In cosmetics, the liposomes have been used since 1987 by Dior's Capture and L'oreals Niosome and Nactosomes (skin regenerating creams) [53]. There are several liposomal cosmetic products on market including skin creams, sunscreens, dentrifrices, shampoos, skin-lightening lotions, and perfumes having good penetrating the various skin layers [53, 54]. There are various liposomal vaccine delivery systems (i.e. Hepatitis-A, Hepatitis-B, diphtheria, tetanus, and influenza vaccines) in advanced phases of clinical development [55]. The liposomal delivery systems are also utilized in food industry for delivery of pesticides, enzymes, and nutritional supplement (i.e. liposomal vitamins, minerals, antioxidants, and herbal extracts for oral administration) [56-58].

Table 1.2. Liposomal products on the market [52]

Product name	Route of injection	Drug	Particle type/size	Drug form /Storage time	Approved indication
Ambisome	Intravenous	Amphotericin B	Liposome	Powder/ 36 months	Sever fungal infections
Dauno Xome	Intravenous	Daunorubicin	Liposome	Emulsion/ 12 months	Blood tumors
Depocyt	Spinal	Cytarabine	Liposome	Suspension /18 months	Neoplastic meningitis and lymphomatous meningitis
DepoDur	Epidural	Morphine sulfate	Liposome	Suspension /24 months	Pain management
Doxil	Intravenous	Doxorubicin	PEGylated liposome	Suspension /20 months	Kaposi's sarcoma, Ovarian/breast cancer
Epaxal	Intramuscular	Inactivated hepatitis A virus (strain RG-SB)	Liposome	Suspension /36 months	Hepatitis A
Inflexal V	Intramuscular	Inactivated hemaglutinine of Influenza virus strains A and B	Liposome	Suspension /12 months	Influenza
Lipo-dox	Intravenous	Doxorubicin	PEGylated liposome	Suspension /36 months	Kaposi's sarcoma, ovarian/breast cancer
Myocet	Intravenous	Doxorubicin	Liposome	Powder/ 18 months	Combination therapy with cyclophosphamide in metastatic breast cancer
Visudyne	Intravenous	Verteporfin	Liposome	Powder/ 48 months	Age-related molecular degeneration, pathologic myopia, ocular histoplasmosis

Table 1.3. Liposomal products in advanced clinical studies [52]

Product name	Route of injection	Drug	Approved indication	Trial phase
Arikace	Portable aerosol delivery	Amikacin	Lung infection	Phase III
Aroplatin	Intrapleural	Cisplatin analog (L-NDDP)	Metastatic colorectal carcinoma	Phase II
Atragen	Intravenous	Tretinoin	Acute promyelocytic leukemia, hormone-refractory prostate cancer	Phase II
EndoTAG-1 (powder/24 months)	Intravenous	Paclitaxel	Anti-angiogenic properties, breast and pancreatic caner	Phase II
INX-0125	Intravenous	Vinorelbine	Advanced solid tumors	Phase I
INX-0076	Intravenous	Topotecan	Advanced solid tumors	Phase I
LEM-ETU	Intravenous	Mitoxantrone	Leukemia, breast, stomach, liver, ovarian cancers	Phase I
LEP-ETU (powder/12 months)	Intravenous	Paclitaxel	Ovarian, breast, and lung cancers	Phase I/II
LE-SN38	Intravenous	SN-38, active metabolite of irinotecan	Metastatic colorectal cancer	Phase I/II
Lipoplatin (suspension/36 months)	Intravenous	Cisplatin	Pancreatic, head and neck cancer, mesothelioma, breast, gastric, and non-squamous non-small-cell lung cancer	Phase III
Liposomal Grb-2	Intravenous	*Grb2* antisense oligodeoxynucleotide	Acute myeloid, chronic, myelogenous, and acute lymphoblastic leukemia	Phase I
Liposome-annamycin (powder)	Intravenous	Annamycin	Acute lymphocytic leukemia	Phase I/II
Liprostin	Intravenous	Prostaglandin E1	Peripheral vascular disease	Phase II/III
Marqibo	Intravenous	Vincristine	Metastatic malignant uveal melanoma	Phase III
Nyotran	Intravenous	Nystatin	Systemic fungal infections	Phase I/II
OSI-211	Intravenous	Lurtotecan	Ovarian, head, and neck cancer	Phase II
S-CKD602	Intravenous	Camptothecin analog	Recurrent or progressive carcinoma of the uterine cervix	Phase I/II
SPI-077	Intravenous	Cisplatin	Head and neck and lung cancer	Phase I/II
Stimuvax	Subcutaneous	BLP25 lipopeptide (MUC1-targeted peptide)	Cancer vaccine for multiple myeloma developed encephalitis	Phase III
ThermoDox	Intravenous	Doxorubicin	Non-resectable hepatocellular carcinoma	Phase III
T4N5 liposome lotion	Topical	Bacteriophage T4 endonuclease 5	Xeroderma pigmentosum	Phase III

1.3.4. *In vivo* Properties of Liposomes

1.3.4.1.Route of Administration, Stability, and Biodistribution

The liposomes are administered to body through various routes including oral, nasal, intravenous, and dermal according to the intended application [59]. The liposomes designed as nutritional supplement (i.e. liposomal vitamins, minerals, antioxidants, and herbal extracts) are taken orally [56-58]. The liposomes designed for other applications should be taken by other routes, different from oral route since the intestinal system breakdowns the liposomes with bile salts and intestinal lipases [52]. The liposomal cosmetic formulations (i.e. skin products) are designed to be administrated by dermal route for good penetrating ability of the liposomes through various skin layers [53, 54]. The liposomal delivery systems designed for respiratory system infections are given to the patients through nasal route [60-62]. The liposomal size must be well adjusted before nasal application since the deposition of the liposomes in the respiratory tract is size-dependent [63]. In nasal delivery of the liposomes, very big liposomes are avoided as they can be retained in the throat and swallowed [63].

Most of the liposomal drug formulations are approved for intravenous application to bypass the gastrointestinal system, called as first-pass effect [64]. When intravenously administered, the conventional liposomes can be easily captured by the MPS and removed from the bloodstream [64]. This situation is advantageous in delivery of antiparasitic and antimicrobial drugs for the treatment of the infections in MPS [64]. If the target site is beyond the MPS, the conventional liposomal are not sufficient and more efficient liposomal systems are required. The surfaces of the liposomes are modified with polymers such as polyethylene glycol (PEG), polyacrylamide, polyvinylalcohol, and polyvinylpyrolidine to yield more bioavailability in the bloodstream when administrated intravenously [65]. In polymer coating, PEG is most commonly used in preparation of long circulating (stealth) liposomes [66]. PEGylated liposomes have higher biodistribution and half-life as PEGylation decreases the interaction between the liposomes and plasma proteins with its entangled structure [66]. The PEGylation ratio is optimized in order to yield

efficient steric stabilization while keeping cellular binding of the liposomes. A study revealed that low degree of PEGylation had higher binding affinity than higher degrees of PEGylation up to 5% of phospholipids [67].

The conventional liposomes can passively target the tissues and organs having discontinuous endothelium such as spleen, liver, and bone marrow [68]. The PEGylated liposomes are effective in tumor targeting via the enhanced permeability and retention effect (EPR), meaning passive targeting to the tumor site [69]. The tumors have increased microvascular permeability through highly permeable microvessels with discontinuous epithelium [69]. The liposomes pass through microvessels of tumors and stay locked in the interstitial fluid compartment due to lack of lymphatic drainage as shown in Figure 1.10 [69].

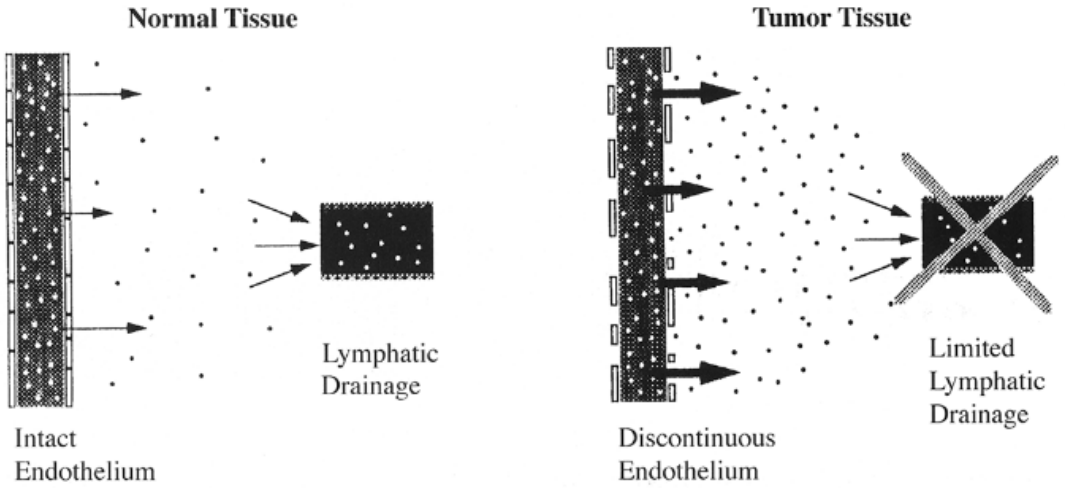

Figure 1.10. Accumulation of the long-circulating liposomes in tumors via enhanced permeability and retention (EPR) effect [69]

The biodistribution of the liposomes are affected by the physicochemical properties of the liposomes such as lipid composition, bilayer rigidity and fluidity, packing of the lipid bilayer, size, surface charge, pH sensitivity, hydrophobicity, and presence of targeting moiety [70]. *In vivo* half-life and biodistribution characteristics of the

liposomes are relevant to the structural stability and bioavailability of the liposome in the bloodstream [70].

Lipid composition is one of the most important parameters in structural stability and biodistribution and release characteristics of the liposomes. In liposome preparation, synthetic/natural saturated and unsaturated phospholipids are used according to the intended application [71]. Saturated phospholipids are chemically more stable than the unsaturated phospholipids since they are more resistant to oxidation and hydrolysis [72]. Saturated phospholipids are preferable in liposome preparation having closely packed structure [36]. In order to increase the chemical stability of the liposomes, presence of heavy metals and oxygen should be avoided to prevent oxidation [73].

Use of antioxidants is recommended to prevent phospholipid oxidation and to increase bioavailability [73]. The amount of liposome at systemic circulation and target organ gets increased after addition of antioxidants with protective antioxidizing effect in aqueous media [73]. Antioxidants prevent oxidative effects of free radicals by removing the free radical intermediates being oxidizing themselves [83]. In literature addition of antioxidant is recommended not only for improving stability of liposomes but also for delivery of the antioxidant to the cells [84]. Glutathione (GSH) is the major endogenous antioxidant synthesized in the body, directly involved in the neutralization of free radicals and reactive oxygen compounds [85]. Studies revealed that incorporation of GSH have improved chemical and physical stability of liposomes [86-88]. Liposomal GSH is also revealed promising for the treatment of degenerative diseases (such as Alzheimer's Disease, Parkinson's Disease, Multiple Sclerosis, Cancer, Diabetes, and Heart Disease) by preventing oxidative stress and maintaining cell functioning [88].

In phospholipid selection, phase transition temperature of the phospholipid should be considered since the liposomes are prepared above this temperature to yield bilayer spherical structure [74]. Each phospholipid has a characteristic phase transition temperature where the closely ordered hydrocarbon chains having gel phase turn into

randomly oriented hydrocarbon chains having disordered liquid crystalline phase [75]. The phospholipids with longer hydrocarbon chain length have higher phase transition temperatures due to intermolecular forces between the hydrocarbons [75]. The type of the encapsulated biomolecule is also important in selection of the phospholipids in order to preserve the chemical structure and biological activity of the biomolecule during preparation of the liposomes. If the proteins or growth factors are encapsulated into the liposomes, the phospholipids having phase transition temperature near the body temperature should be selected considering the decomposition of the proteins or growth factors above body temperature [76].

Liposomes are incorporated with cholesterol in order to yield membrane fluidity, elasticity, and permeability [77]. Addition of cholesterol creates stabilizing effect by filling the gaps between the phospholipids [77]. Bioavailability of the liposomes increases with the decrease in the phospholipid transfer to the plasma proteins. Egg or wool grease cholesterol can be used in liposome preparation [78]. Wool grease cholesterol is not preferred in the liposomes designed for humans due to animal derived contamination issues [78].

Size and the surface charge of the liposomes affect the liposome uptake by the mononuclear phagocyte system (MPS), spleen, and liver [79]. A study revealed that very big ($d>300$ nm) and very small ($d<70$ nm) liposomes are captured and removed from the bloodstream [79]. The medium-sized liposomes have increased bioavailability in the body [79]. Charged liposomes are used for specific applications. Negatively and positively charged phospholipids are used in the preparation of anionic (negatively charged) and cationic (positively charged) liposome preparations, respectively [80]. In order to encapsulate DNA (negatively charged), cationic liposomes are preferred to increase loading efficiency [80]. Negatively charged liposomes are revealed to have shorter half-life in bloodstream than the neutral liposomes whereas positively charged liposomes have the shortest half-life and are quickly removed from blood stream [80]. Size and surface charge of the liposomes are modified and optimized to increase the bioavailability and effectiveness of the liposomes.

1.3.4.2.Liposome-cell Interaction

Liposomes interact with the cells in different ways as shown in Figure 1.11. The liposomes can be adsorbed onto the cell surface specifically or non-specifically (Figure 1.11, a and c) and release their contents to the cell cytoplasm [78]. The liposomes can fuse with the cell membrane (Figure 1.11, b) and release their content into the cell cytoplasm [78]. The liposome can be taken into the cell by endocytosis (Figure 1.11, d) and later into the lysosome (Figure 1.11, e) and release their content into the cyctoplasm [78]. In bloodstream, the macrophages bind to the liposomes by endocytosis [81]. The macrophages cannot recognize the liposomes themselves but can recognize opsonins (i.e. serum proteins) bound to the liposomes [81]. The liposomes recognized by the macrophages are then removed from the bloodstream [81].

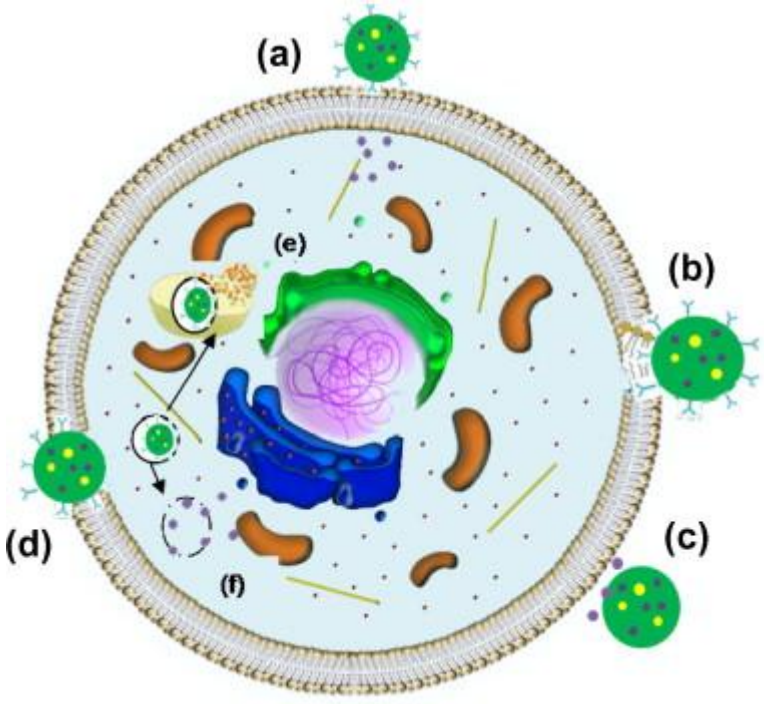

Figure 1.11. Liposome-cell interactions (a) Specific adsorption (b) Fusion (c) Non-specific adsorption (d) Specific or non-specific endocytosis by the cell membrane (e) Endocytosis of the liposome by the lysosome (f) drug release into the cell cytoplasm [78]

1.3.5. Liposomal Targeting of the Brain

Localized and controlled delivery of drugs at their desired site of action is preferred because it reduces toxicity and increases treatment efficiency [41]. Conventional drug delivery systems to brain are ineffective to cross BBB. Brain targeted drug delivery systems should be developed in order to increase the therapeutic efficiency of the drugs at the disease site with lowered side effects of the drug [48, 49].

Liposomes are suitable carrier systems for brain drug delivery owing to their lipophilic nature [82]. The brain has transcytosis capacity of specific molecules as explained in Section 1.1.2. The liposomal formulations are optimized for them to be transported via one of the BBB transporter systems while retaining the biological activity of the bioactive agent. The surfaces of the liposomes are modified with BBB selective molecules to enable BBB transport.

In literature the liposomes are reported to be transported to enter the brain endothelial cells via receptor mediated endocytosis or adsorptive-mediated endocytosis [159]. Cationic liposomes are reported to be transported through the BBB via adsorptive-mediated trancytosis. Cationic liposomes bind to the negatively charged endothelial cell membranes by non-specific electrostatic interactions [160]. Liposome brain targeting using adsorptive-mediated endocytosis is generally accomplished by using cationized human serum albumin (cHSA) [161]. However, adsorptive-mediated endocytosis is not desirable for brain delivery since this process is also present to a large extent in liver and kidneys resulting in decrease in brain specificity [162]. Furthermore, the cationic liposomes are not preferable due to aggregate formation due to cationic charge in the circulation [161] and quick removal from blood stream [80]. The liposomes more specifically enter the brain via receptor-mediated endocytosis. Brain specific ligand conjugated liposomes bind to the receptors which are specifically expressed on the brain endothelial cells. Later the liposomes are endocytosed and transported through the endothelial cell towards the other side of the cell. The liposomes are ultimately exocytosed at the other side of the cell membrane [163]. In literature the liposomes are targeted to the brain using receptor-

mediated endocytosis approach with conjugation of specific molecules such as transferrin [164], monoclonal antibody OX26 [165], and glucose [166]. In literature various studies revealed that dextrins are also promising for brain targeting using receptor-mediated endocytosis [167-169]. Among dextrins, maltodextrin is conventionally present in a novel class of Alzheimer Disease medication called Memantine to increase brain transport [170].

1.4.Aim of the Study

Parkinson's disease is a progressive and permanent brain disorder. Medications are used to control the disease symptoms such as tremor, brandykinesia, and rigidity. Levodopa is the most commonly used drug in Parkinson's disease treatment. The Levodopa is given to the patients with high doses since most of the drug is metabolized in the body before reaching to the brain. High Levodopa doses result in drug side effects in the body (dyskinesias, nausea, vomiting, and hypotension) and the medication becomes ineffective after a while. It is not available yet to find any brain targeted drug formulation in the pharmaceutical market and in the clinical trials to cure Parkinson's Disease. It is already clear that development of a brain targeted drug delivery systems for treatment of neurodegenerative diseases has high importance. Current study was designed on development of a brain-targeted liposomal formulation for the most important Parkinsonian drug: Levodopa.

Liposomes are biocompatible, biodegradable, non-immunogenic, and non-toxic drug carrying systems. They are widely and effectively used for drug targeting to the disease site. In previous studies the liposomes were targeted to the brain with certain targeting molecules such as glucose, amino acids, and transferrin. In this study, maltodextrin was selected as targeting molecule because of brain's high nutrient requirement for sugars. In literature various studies revealed that dextrins are promising for brain targeting using receptor-mediated endocytosis [167-169]. Maltodextrin was conjugated to the long chain PEG molecule instead of liposome surface in order to yield more conjugation efficiency. This study is novel for

maltodextrin conjugated liposomes as a brain targeted Levodopa delivery system for the first time.

The liposomes were prepared at different temperatures with different lipid compositions. The liposomes were PEGylated in order to increase the bioavailability of the liposomes by reducing the reticuloendothelial uptake and macrophage encapture. The liposomes were loaded with Levodopa or Levodopa and GSH. Antioxidant was incorporated to improve liposome stability and drug bioavailability as the antioxidant was encapsulated in the aqueous phase of the liposomes. Liposomal GSH is revealed promising for the treatment of the Parkinson's Disease, by preventing oxidative stress and maintaining cell functioning [89]. This study is novel to bring Levodopa and GSH in the same liposomal formulation. Drug and antioxidant loadings and release profiles of the liposomes were investigated. Size and surface charge of the liposomes were modified and optimized to increase the bioavailability and effectiveness of the liposomes. The liposomes were produced in sizes to be administrated intravenously (D: 100-150 nm). Intravenously administered liposomal Levodopa could be more effective for increased bioavailability and less drug side effects. This brain targeted liposomal delivery system would bring a novel approach for Parkinson's Disease therapy.

In *in vitro* cell culture studies, the liposomes were tested for toxicity on 3T3 and SH-SY5Y cells to minimize cellular toxicity and to adjust liposome concentration in doses. 3T3 cell line was used as standand fibroblact cell line for cytotoxicity [171] and SH-SY5Y cell line was specifically used in brain cytotoxicity experiments as a neuronal cell model with the similar biochemical characteristics to human dopaminergic neurons [172]. The liposomes were tested for their transport efficiency through Blood-Brain Barrier (BBB) Parallel Artificial Membrane Permeability Assay (PAMPA-BBB). In order to determine targeting ability of the designed targeted liposomal formulation, they were also tested for binding to Madin-Darby Canine Kidney (MDCK) cells that are mimicking the BBB functional structure with sugar receptors [90, 91]. This brain targeted liposomal delivery system will bring a novel approach for the delivery of Levodopa to brain with decreased drug side effects.

CHAPTER 2

MATERIALS AND METHODS

2.1.Materials

PC (1,2-dipalmitoyl-*sn*-glycero-3-phosphocholine, 16:00) (DPPC), 1,2-distearoyl-*sn*-glycero-3-phosphoethanolamine-N-[amino(polyethylene glycol)-2000] (ammonium salt) (DSPE-PEG(2000) Amine), L-α-Phosphatidylethanolamine-N-(lissamine Rhodamine B sulfonyl) (Ammonium Salt) (Egg-Transphosphatidylated, Chicken), Mini-extruder set, filter supports, Nucleopore Track-Etch Membranes (800, 400, 100 nm) were purchased from Avanti Polar Lipids, Inc. (USA). 1,2-Distearoyl-sn-glycero-3-Phosphoethanolamine-N-[Methoxy (Polyethylene Glycol)2000 (18:00 mPEG(2000)-DSPE) was provided by Lipoid (Germany). Levodopa and maltodextrin (Roquette, France) were gifts from Abdi Ibrahim Pharmaceutical, Inc. (Istanbul, Turkey). Cholesterol, L-Glutathione reduced, dialysis sacks, benzoylated dialysis tubing, uranyl acetate dehydrate, chloroform (HPLC grade), N,N-dicyclohexylcarbodiimide (DCC), N-hydroxysuccinimide (NHS), isopropyl alcohol, sodium hydroxide, monochloroacetic acid were purchased from Sigma Aldrich Chem. Co. (USA). Sephadex G-75, PD-10 Disposable Columns were purchased from GE Healthcare (UK). Glutathione Assay Kit was obtained from Cayman Chemical Company (USA). Iron(III) chloride hexahydrate, ethanol (HPLC grade), ammonium thiocyanate were purchased from Merck (Germany). Formvar-Carbon Film on 300 square mesh Copper Grids were obtained from Electron Microscopy Sciences (USA).

3T3 fibroblast cell line (Anl Swiss albino mouse fibroblast) for *in vitro* cytotoxycity studies was obtained from Foot-and-Mouth Disease Institute of Ministry of Agriculture and Rural Affairs of Turkey. SH-SY5Y cell line (Neuronal tumor cell line with human neuroblastoma cell) for *in vitro* cytotoxicity studies and MDCK (Madin-Darby Canine Kidney) cell line for cellular association studies were gift from

Abdi Ibrahim Pharmaceuticals Inc. (Istanbul, Turkey).Dulbecco's modified Eagle's medium (DMEM) with high glucose (4.5 g/l) and L-glutamine, fetal bovine serum (FBS), Penicillin/Streptavidin and Trypsin EDTA were purchased from Biochrom AG (Germany). L-Glutamine and HAM's nutrient mixture F-12 with L-Glutamine was obtained from Sigma Aldrich Chem. Co. (USA). Dimethyl sulphoxide (molecular biology grade) (DMSO) was the product of AppliChem Co. (Germany). MTT reagent (3-(4,5-Dimethylthiazol-2-yl)-2,5-Diphenyltetrazolium Bromide) was purchased from Invitrogen (USA). Cell culture plastic-wares were obtained from Orange Scientific (Germany). Polyethersulfone syringe membrane (0.2 μm pore size) was purchased from Minisart (Germany). Blood-brain Barrier (BBB) Parallel Artificial Membrane Permeability Assay (PAMPA-BBB) (Pion Inc., USA) was obtained from Abdi Ibrahim Pharmaceuticals Inc. (Istanbul, Turkey).

2.2.Methods

2.2.1. Preparation of Liposomes

The multilamellar vesicles (MLVs) were prepared by lipid film hydration method. The lipids (Figure 2.1) were dissolved in chloroform (2 ml) in polypropylene (PP) tubes at different molar ratios (Table 2.1). In cellular association experiments, the liposomes were prepared with Lissamine-Rhodamine labeled lipid at 0.5 mole % of total lipid mixture. The chloroform was then removed under nitrogen gas stream to form a lipid film. Remaining chloroform was removed in vacuum oven overnight (Nüve EV 018, Turkey). The lipid film was stored at 4^{o}C after flushing with nitrogen gas. The lipid film was hydrated with 1 ml phosphate buffer solution (PB, 0.1 M, pH 7.4) containing Levodopa (5 mg) or Levodopa(5 mg) and Glutathione (0.012 or 0.006 mg) by heating at 38-44^{o}C and vortex mixing (CAT VM3, France) in 2 minute cycles for 60 minutes.

Table 2.1. Composition of Lipid Films

Liposome Type	Liposome	DPPC (μmol)	Cho (μmol)	DSPE-mPEG (2000) (μmol)	DSPE-PEG (2000) amine (μmol)	DSPE-PEG-malto-dextrin (μmol)
Conventional Liposome	DPPC:Cho (8:2)	32	8	-	-	-
	DPPC:Cho (7:3)	28	12	-	-	-
	DPPC:Cho (6:4)	24	16	-	-	-
Stealth Liposome	2% PEG/LUV	28	12	0.55	-	-
	4% PEG/LUV	28	12	1.10	-	-
Targeted Liposome	0.35% MD-4% PEG/LUV	28	12	-	0.55	0.55
	0.7% MD-4% PEG/LUV	28	12	-	-	1.10

Large unilamellar vesicles (LUVs) were prepared from the multilamellar vesicles (MLVs) by extrusion method. The MLVs were extruded with mini-extruder set at 38-44^{o}C starting from 800 nm polycarbonate membrane (Avanti Polar Lipids, USA). Liposome suspension was passed through 800, 400, and 100 nm membranes 5 times, 5 times and 11 times, respectively. The final liposomes were passed through Sephadex G-75 size exclusion chromatography by using PD-10 disposable column (GE Healthcare, USA) to separate the unincorporated lipids and unentrapped drug. The elution buffer was PB solution (0.1 M, pH 7.4). The liposomal fractions were collected into polypropylene (PP) tubes and absorbance at 410 nm was measuredby microplate spectrophotometer (GMI Biotech 3550, USA) to detect LUV fractions. The loaded LUVs were pooled in a new vessel for further studies.

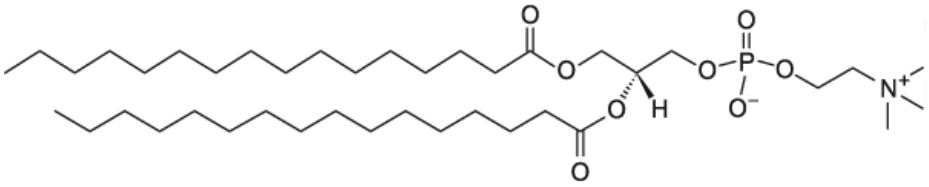

DPPC

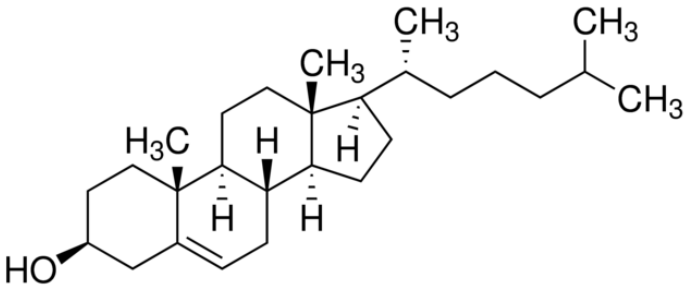

Cholesterol

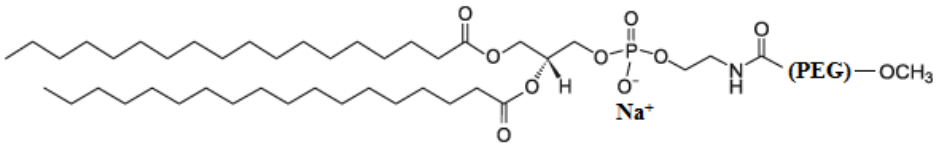

DSPE-mPEG(2000) (Na^+ salt)

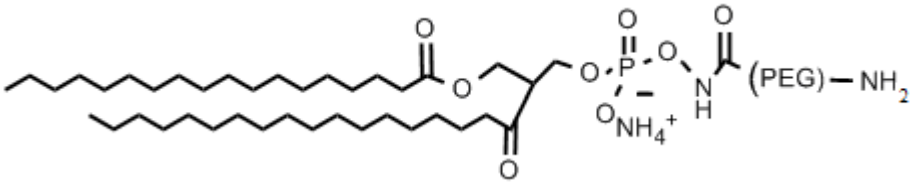

DSPE-PEG(2000)Amine (Ammonium salt)

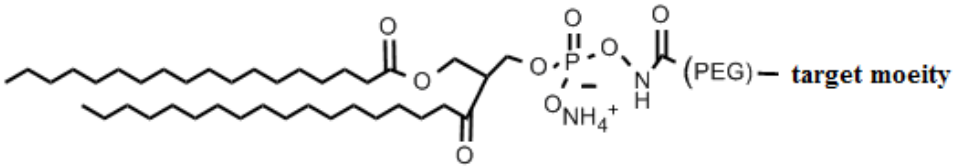

DSPE-PEG-target moiety

Figure2.1. Chemical structures of DPPC, Cholesterol, DSPE-mPEG(2000), DSPE-PEG(2000)Amine, and DSPE-PEG(2000)-target moiety

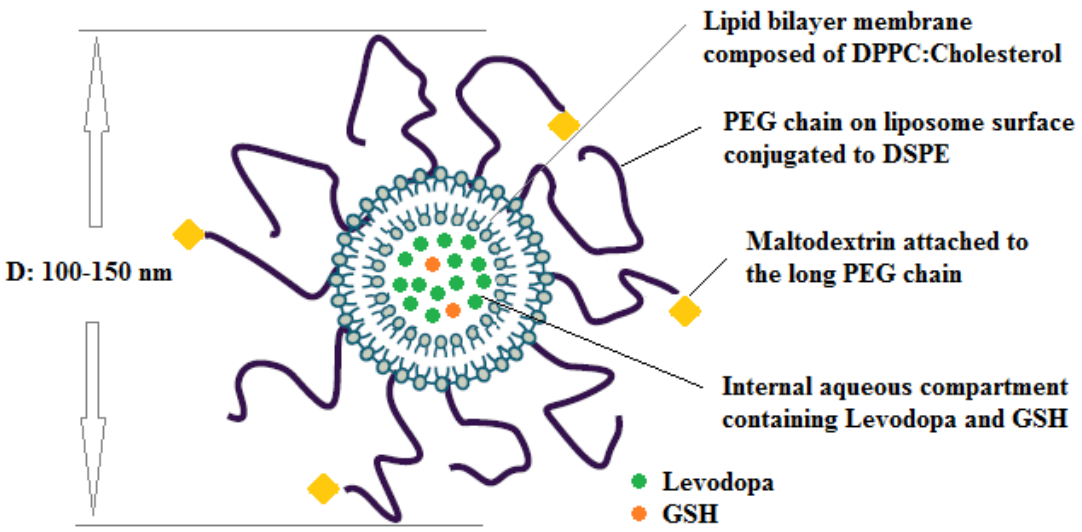

Figure 2.2. Schematic illustration of maltodextrin conjugated PEGylated liposomes designed for the delivery of Levodopa and Glutathione to brain in this study [Modified from www.azonano.com]

2.2.2. Conjugation of Maltodextrin to DSPE-PEG(2000)Amine

Maltodextrin and DSPE-PEG(2000)Amine molecules were conjugated via carbodiimide chemistry. Before conjugation, some of the hydroxyl groups (-OH) of the maltodextrin were converted to carboxymethyl groups (-CH_2COOH) in order to yield carboxylic acid groups (-COOH) for carbodiimide conjugation. Carboxylic acid group containing maltodextrin was later reacted with DSPE-PEG(2000)Amine via carbodiimide chemistry.

2.2.2.1.Carboxymethylation of Maltodextrin

Maltodextrin (0.2 g) and sodium hydroxide (0.046 g) were mixed in isopropanol:water (4:1 v/v) mixture in a two-neck round-bottom flask using a condenser and magnetic stirrer. The mixture was allowed to react at 50^{o}C for 1 h. Then, monochloroacetic acid (0.7 g) in isopropanol (0.93 ml) was added and the

mixture was allowed to react for additional 4 h at 50^{o}C. The reaction was stopped by adding ethanol solution (70%, 10 ml). The solid precipitate was obtained by evaporating the solvents in laminar flow cabinet followed by freeze-drying.

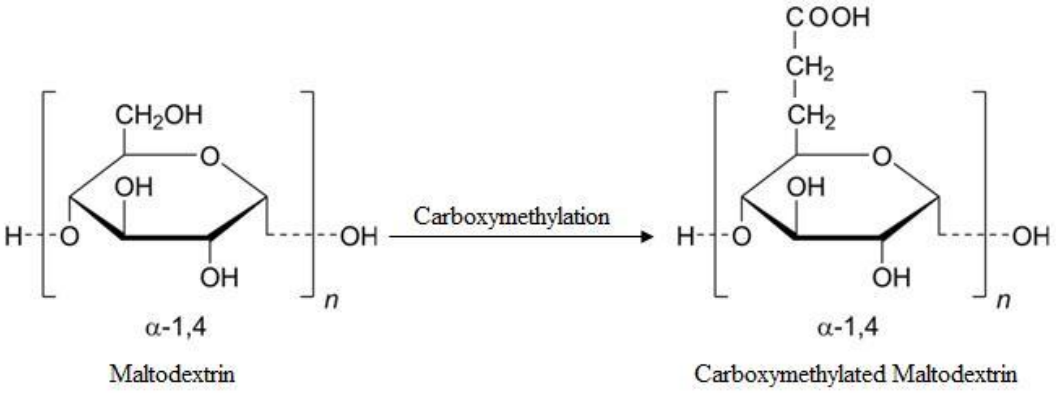

Figure 2.3. Carboxymethylation of maltodextrin

2.2.2.2.Determination of Maltodextrin Carboxymethylation Efficiency

The change in chemical structure of maltodextrin was analyzed by Attenuated Total Reflectance Fourier Transform Infrared Spectroscopy. ATR-FTIR spectra of unreacted maltodextrin and carboxymethylated-maltodextrin were obtained using Fourier Transform Infrared and Raman Spectrometer (ATR-FTIR, Bruker IFS 66/S, Middle East Technical University Central Laboratory) at mid infrared (MIR) spectrum range (4000-400 cm^{-1}). Each sample was scanned 32 times during analysis.

Carboxymethylation efficiency (CM.Ef.) was calculated from the decrease in the hydroxyl bond of maltodextrin by using the wavenumber (cm^{-1}) versus transmittance (%) spectrum. The area under the hydroxyl bond peak for unreacted maltodextrin and carboxymethylated maltodextrin were calculated using OMNIC Spectra software (Thermo Fisher Scientific, USA) and the carboxymethylation efficiency was calculated according to the following formula:

$$\text{CM. Ef.} = \frac{\text{Area (unreacted maltodextrin)} - \text{Area (carboxymethylated-maltodextrin)}}{\text{Area (unreacted maltodextrin)}} \text{ x100\% [92]}$$

2.2.2.3.Conjugation of Carboxymethylated-Maltodextrin to DSPE-PEG(2000)Amine

Carboxymethylated-maltodextrin (0.74 g) was dissolved in acetone (100 ml) and then, N,N-dicyclohexylcarbodiimide (DCC)(0.28 g) and N-hydroxysuccinimide (NHS) (0.17 g) were added. The mixture was allowed to react for 22h at room temperature. The acetone was removed under nitrogen gas stream in laminar flow cabinet. The activated maltodextrin was mixed with DSPE-PEG(2000)Amine (0.052 g) and dissolved in DMSO solution (20 ml, 96%). The mixture was allowed to react for 24h at room temperature. The reaction medium was put into dialysis tubing (2000 MWCO) and dialyzed against distilled water for 24h. The water was refreshed every six hours. The remaining solution in the dialysis tubing was centrifuged at 14,000 rpm at 4^{o}C for 10 minutes (Sigma 3-30K, Germany). The conjugated lipid pellet was dried under nitrogen gas stream in laminar flow cabinet and dried in vacuum oven overnight (Nüve EV 018, Turkey). The conjugated lipid was dissolved in acetone and stored at 4^{o}C under nitrogen gas.

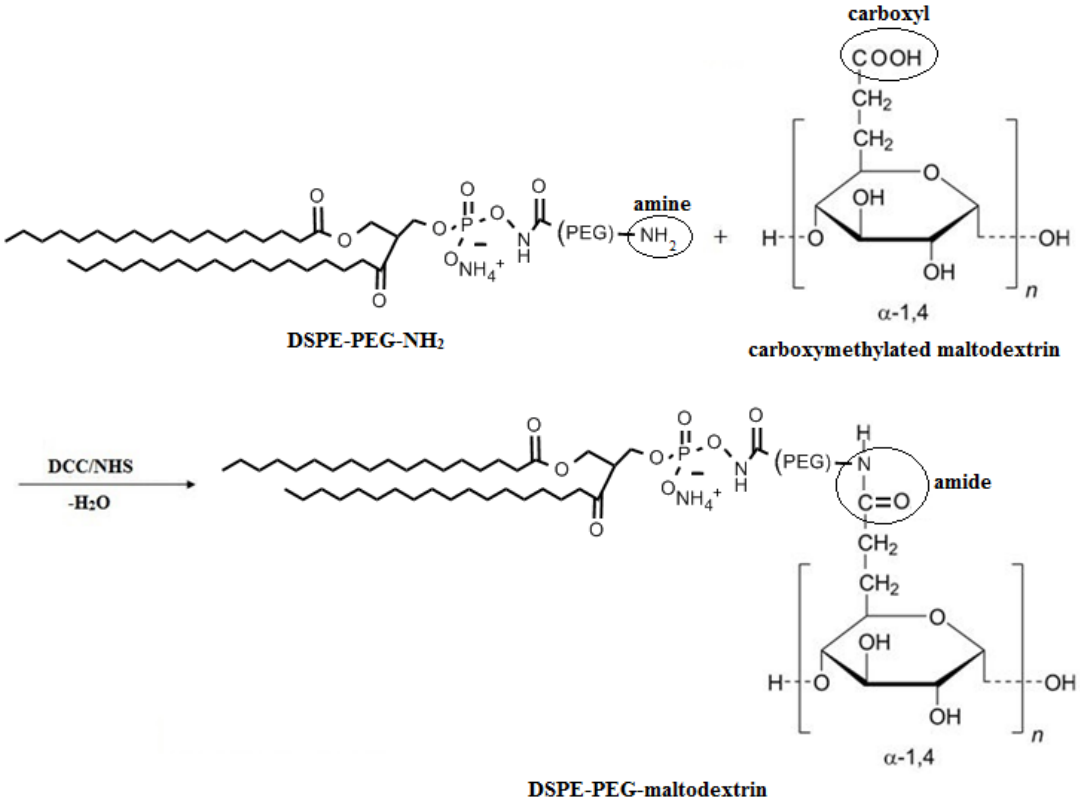

Figure 2.4. Conjugation of DSPE-PEG(2000)Amine and carboxymethylated maltodextrin

2.2.2.4.Determination of Maltodextrin Conjugation Efficiency

The maltodextrin conjugation efficiency to DSPE-PEG(2000)Amine was analyzed by Attenuated Total Reflectance Fourier Transform Infrared Spectroscopy. ATR-FTIR spectra of physical mixture of DSPE-PEG(2000)Amine and carboxymethylated-maltodextrinand reaction product DSPE-PEG-maltodextrin were performed using Fourier Transform Infrared and Raman Spectrometer and (ATR-FTIR, Bruker IFS 66/S, Middle East Technical University Central Laboratory) at mid infrared (MIR) spectrum range (4000-400 cm^{-1}). Each sample was scanned 32 times during analysis.

Conjugation efficiency (Conj. Eff.) was calculated from the decrease in the amine bond by using the wavenumber (cm^{-1}) versus transmittance (%) spectrum. The area under the amine bond peak was calculated using OMNIC Spectra software (Thermo Fisher Scientific, USA) and the conjugation efficiency was calculated according to following formula:

$$\text{Conj. Eff.} = \frac{\text{Area (physical mixture)} - \text{Area (reaction product)}}{\text{Area (physical mixture)}} \times 100\% \quad [93]$$

2.2.3. Quantification of Levodopa

The amount of Levodopa was determined with the Fluorescence Spectrometry (Turner Biosystems Modulus Fluorometer, UV Kit, USA) by using disposable methacrylate cuvettes. Levodopa concentrations in the pooled LUVs and release samples were calculated from Levodopa calibration curve constructed (range: 0-100 µg/ml) in PB (0.1 M, pH 7.4) where PB was used as blank and subtracted from the sample.

2.2.4. Quantification of Glutathione

The amount of Glutathione (GSH) was determined by ELISA(Enzyme-linked Immunosorbent Assay) kit (Glutathione Assay Kit, Cayman, USA) using the enzymatic recycling method, using glutathione reductase (Figure 2.5). GSH is easily oxidized to the Glutathione disulfide (GSSG).Since glutathione reductase is used in this assay, both GSH and GSSG are measured and the assay gives total amount of glutathione (Figure 2.5, a).The sulfhydryl group of GSH reacts with DTNB (5,5'-dithio-bis-2-(nitrobenzoic acid) and produces 5-thio-2-nitrobenzoic acid (TNB).The mixed disulfide, GSTNB (between GSH and TNB) that is similtaneously produced, is reduced by glutathione reductase to recycle the GSH and produce more TNB (Figure 2.5, b).The rate of TNB production is directly proportional to the concentration of GSH in the sample.

The total amount of GSH in the sample is obtained by measuring the absorbance of TNB at 405-414 nm. Glutathione amount in the poolled LUVs and release samples were calculated from the standard curve (range: 0-16 μM) which was run at each time simultaneously with the samples.

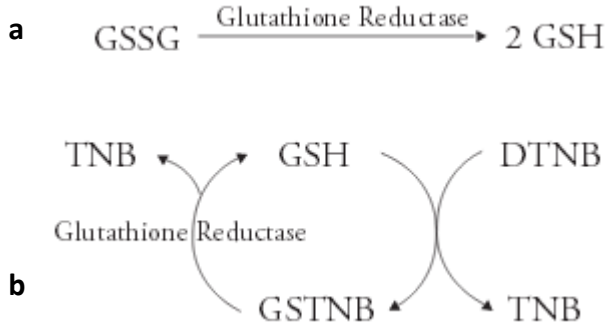

Figure 2.5. Enzymatic recycling of GSH

2.2.5. Quantification of Phospholipids (DPPC)

The amount of DPPC was determined by UV-Visible Spectrophotometer (Hitachi U-2800A, Japan) using the previously defined colorimetric method, which was based on a complex formation between the phospholipids and ferrothiocyanate [91]. The liposomes were dried in vacuum oven overnight (Nüve EV 018, Turkey). The dry phospholipid residue was dissolved in 2 ml chloroform and 1 ml thiocyanate reagent. Then they were vortex mixed (CAT VM3, France) for 1 minute and centrifuged (Hettich EBA 20, UK) at 2000 rpm for 5 minutes. After centrifugation, the lower (chloroform) phase was removed and its absorbance was read at 488 nm. The amount of DPPC was quantified according to DPPC calibration curve constructed (range: 10-100 μg/ml). Chloroform was used as blank.

2.2.6. Characterization of Liposomes

2.2.6.1.Particle Size Measurement

The particle size distribution of the LUVs was determined by Dynamic Light Scattering Method. The average hydrodynamic diameter of the freshly prepared LUVs was measured after 1:10 dilution with PB solution (0.1 M, pH 7.4) using particle sizer (Malvern Mastersizer 2000) at Middle East Technical University Central Laboratory.

2.2.6.2.Surface Charge Measurement

The surface charge of the LUVs was determined by Zeta Potential Method. The surface charge of the freshly prepared LUVs was measured after 1:2 dilution with PB solution (0.1 M, pH 7.4) with Malvern Nano ZS90 at Middle East Technical University Central Laboratory.

2.2.6.3.Morphological Characterization

The morphological characterization of the liposomes was performed by High Contrast Transmission Electron Microscopy (TEM) (FEI Technai G2 Spirit BioTwin CTEM, Middle East Technical University Central Laboratory) at 80 kV in bright field imaging mode. Uranyl acetate solution was used as coloring agent. The LUVs (100 µl) were placed onto Copper Grids (Formvar-Carbon Film on 300 square mesh Copper Grids) after 1:50 dilution with PB solution (0.1 M, pH 7.4) and they were dyed with 2% (g/ml) uranyl acetate solution. The morphological characterization of the stained LUVs was performed under High Contrast Transmission Electron Microscopy (TEM).

2.2.6.4.Drug Encapsulation Efficiency and Percent Drug Loading

The amount of Levodopa was calculated as described in Section 2.2.3 and percent drug encapsulation efficiency (% EE) was calculated according to following equation:

$$\% \text{ EE} = \frac{\text{mgLevodopa in LUVs}}{\text{mg Levodopa initially added}} \text{ x } 100 \%$$

The amount of DPPC was calculated as described in Section 2.2.5 and percent drug loading was calculated according to following equation:

$$\% \text{ drug loading} = \frac{\text{mg Levodopa in LUVs}}{\text{mg DPPC in LUVs}} \text{ x } 100 \%$$

2.2.6.5.Levodopa and Glutathione Release Studies

In vitro release experiments were performed in a previously constituted experimental setup, which mimics the *in vivo* conditions with the set parameters such as medium composition, temperature and pH. The LUVs (1 ml) were put into dialysis sacks (Molecular weight cut off: 12000 Da) and placed in 15 ml polypropylene (PP) tubes containing 10 ml release medium (0.1 M PB, pH 7.4). The release media was continuously and mildly shaken in the water bath (NÜVE ST 402, Turkey) at 37^{o}C. The release samples were taken after 6, 24 and 48 hours in order to quantitate the released amount of Levodopa and Glutathione as described in Section 2.2.3 and 2.2.4, respectively.

2.2.7. Stability of Liposomes

The stability of the liposomes was investigated by Dynamic Light Scattering Method (Malvern Nano ZS90, Middle East Technical University Central Laboratory) and Zeta Potential Method (Malvern Nano ZS90, Middle East Technical University Central Laboratory). The liposomes were stored at 4^{o}C and 25^{o}C for six months. Particle size and zeta potential measurements were performed monthly. After 6 months of incubation, the liposomes were tested for drug encapsulation. The liposomes were centrifuged at 25,000 rpm for 20 minutes at 4^{o}C (Sigma 3-30K, Germany) to separate released drug from drug loaded liposomes. The released amount of Levodopa was calculated from supernatant liquid as described in Section 2.2.3.

2.2.8. Cell Culture

2.2.8.1.Cell Culture Conditions

3T3 and MDCK cells were routinely cultured in Dulbecco's modified Eagle's medium (DMEM high glucose-glutamine) supplemented with fetal bovine serum (FBS, 10 %, v/v) and penicillin-streptomycin (1 %, v/v) at 37^{o}C under humidified atmosphere of 5 % CO_2 – 95 % air in incubator (5215, SHEL LAB, USA). The medium was refreshed every two days. When the cells reached at least 80-90 % confluency, they were passaged using trypsin-EDTA (0.25 % in PBS).

SH-SY5Y cells were routinely cultured in 1:1 mixture of Dulbecco's modified Eagle's medium (DMEM high glucose-glutamine) and HAM's nutrient mixture F-12 with L-Glutamine supplemented with fetal bovine serum (FBS, 10 %, v/v) and penicillin-streptomycin (1 %, v/v) at 37^{o}C under humidified atmosphere of 5 % CO_2 – 95 % air in incubator (5215, SHEL LAB, USA). The medium was refreshed every two days. When the cells reached at least 80-90% confluency, they were passaged using trypsin-EDTA (0.25 % in PBS).

2.2.8.2.Cell Viability and Toxicity Assay

The cytotoxicity effect of pure Levodopa and liposomes were tested on 3T3 and SH-SY5Y cells by MTT assay. 3T3 cells and SH-SY5Y cells were seeded at an initial density of $6x10^4$ cells/well and $2x10^5$ cells/well in 24-well plates, respectively and allowed to attach for 24 hours. After 24 hours, the medium was removed and fresh cell culture media (containing either drug solution (0, 20, 40, 60, 80, 100 μM Levodopa with and without 0.06 μM GSH) or liposome solution (empty liposome or 100 μM Levodopa with and without 0.06 μM GSH containing liposome) were added.After 24 and 48 hours, the media were removed and the wells were washed with PBS (0.01 M, pH 7.4). 500 μL MTT test solution was then added and the cells were incubated in dark for 4 hours. After 4 hours, test solutions were removed and the cells were lysed with DMSO (500 μL/well) with shaking at 200 rpm for 15 minutes in dark. The optical densities were measured at 570 nm using microplate spectrophotometer (GMI Biotech 3550, USA). Each experimental group was studied in quaternary replicates in a plate with three technical replicates (n=3). *In vitro* liposome groups used in cytotoxicity experiments are listed in Table 2.2.

The cells were imaged by Phase Contrast Inverted Microscope (Nikon Eclipse TS100, USA) at the beginning of the MTT assay. Percent cellular viability values were calculated according to following equation where Absorbance (c=0) is the absorbance of the control group containing no drug or liposome and Absorbance (c) is the absorbance of an experimental group containing a known concentration of drug or liposome solution.

$$\text{Percent Cellular Viability} = \frac{\text{Absorbance (c)}}{\text{Absorbance (c=0)}} \text{ x } 100\%$$

Table 2.2. Liposome groups studied in *in vitro* cytotoxicity experiments

Group no	**Liposome**
1	No liposome added (Control)
2	Empty PEGylated liposome (4% PEG/LUV)
3	Empty targeted liposome (0.7% MD-4% PEG/LUV)
4	Levodopa loaded PEGylated liposome (LD-4% PEG/LUV)
5	Levodopa and GSH loaded PEGylated liposome (LD-GSH-4% PEG/LUV)
6	Levodopa loaded targeted liposome (LD-0.7% MD-4% PEG/LUV)
7	Levodopa and GSH loaded targeted liposome (LD-GSH-0.7% MD-4% PEG/LUV)

2.2.8.3.*In vitro* Blood-Brain Barrier (BBB) Transport Assay

In vitro Blood-brain Barrier (BBB) transport experiments were performed using BBB Parallel Artificial Membrane Permeability Assay (PAMPA-BBB), which mimics the properties of the brain lipid membranes. The artificial membranes between donor and acceptor compartments were formed by adding lipid solution (10 μL/well in 96-well plates) to each compartment. The wells of the acceptor plate were filled with phosphate buffer solution (PB, 0.1 M, pH 7.4) (200 μL/well in 96-well plates). The donor plate was placed on the acceptor plate and the wells of the donor plate were filled with either drug solution (0.75 mg/ml Levodopa) or liposome solution (0.75 mg/ml Levodopa containing liposome) (200 μL/well in 96-well plates) as shown in Figure 2.6. The system was incubated at 37^{o}C in dark for 48 hours. The aliquots of the acceptor phase were analyzed after 6, 9, 24, and 48 hours in order to obtain the transported amount of Levodopa as described in Section 2.2.3. *In vitro*

experimental groups used in BBB transport assay are listed in Table 2.3. Each experimental group was studied with triple replicates (n=3). Percent drug passage (%drug passage) and Percent lipid passage (%lipid passage) values were calculated according to following equations:

$$\%\text{drug passage} = \frac{\text{mg Levodopa in acceptor compartment}}{\text{mg Levodopa initially added to donor compartment}} \text{ x100\%}$$

$$\%\text{lipid passage} = 100 - \frac{\text{mg DPPC remained in donor compartment after 48h incubation}}{\text{mg DPPC initially added to donor compartment}} \text{ x } 100\%$$

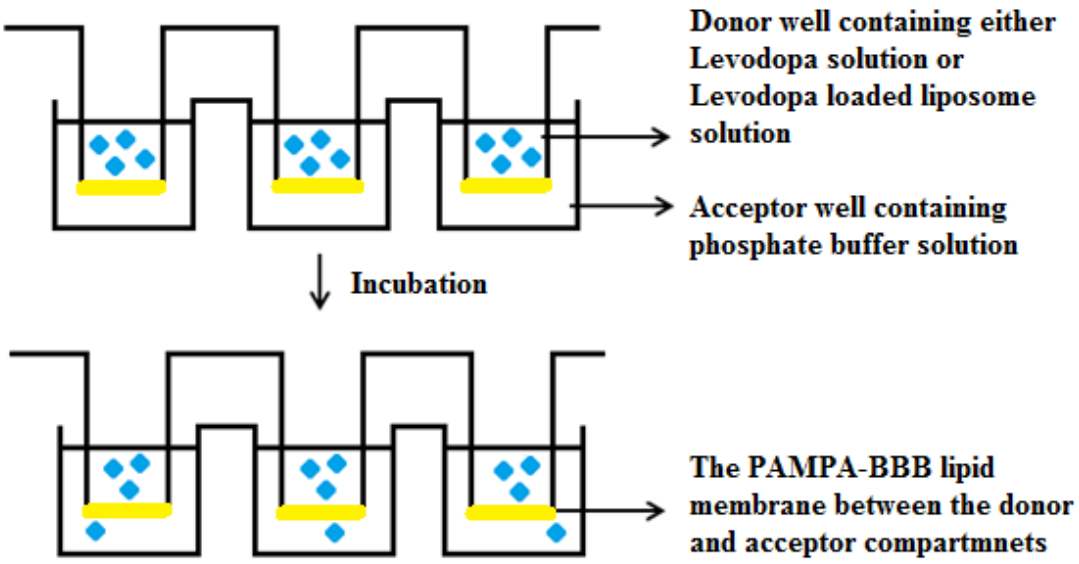

Figure 2.6. Schematic illustration of *in vitro* Blood-Brain Barrier (BBB) transport assay using BBB Parallel Artificial Membrane Permeability Assay (PAMPA-BBB) model

Table 2.3. Experimental groups studied in Blood-Brain Barrier (BBB) Transport Assay

Group no	Groups
1	Levodopa solution
2	Levodopa loaded PEGylated liposome (LD-4% PEG/LUV)
3	Levodopa and GSH loaded PEGylated liposome (LD-GSH-4% PEG/LUV)
4	Levodopa loaded targeted liposome (LD-0.35% MD-4% PEG/LUV)
5	Levodopa and GSH loaded targeted liposome (LD-GSH-0.35% MD-4% PEG/LUV)
6	Levodopa loaded targeted liposome (LD-0.7% MD-4% PEG/LUV)
7	Levodopa and GSH loaded targeted liposome (LD-GSH-0.7% MD-4% PEG/LUV)

2.2.8.4.Cellular Association of Liposomes

Drug and antioxidant loaded stealth and targeted liposomal formulations (i.e. 4% PEG/LUV and 0.7% MD-4% PEG/LUV, respectively) were evaluated for cellular surface binding to MDCK cells by Laser Scanning Confocal Microscopy (LSCM). MDCK cells were seeded at an initial density of $3x10^5$ cells/well on glass coverslips in 6-well plates and allowed to attach for 2 days. After 48 hours, the medium was removed and fresh cell culture media containing Lissamine-Rhodamine labeled liposomes having 500 μM total lipid concentration were added and incubated in dark. After 3 and 6 hours incubation, the media containing labeled liposomes were removed and the cells were washed with PBS (0.01 M, pH 7.4). The glass coverslips were gently removed from the plates and mounted to glass slide. The lam-lamella system was immobilized at the edges by sticking. The cellular binding of the labeled

liposomes was imaged in Laser Scanning Confocal Microscopy (LSCM) using Plan-Neofluar 40x/1.3 Oil DIC objective (Zeiss LSM 510, Middle East Technical University Central Laboratory, Molecular Biology and Biotechnology Research Center). Excitation and emission wavelengths were set to 560 and 583 nm, respectively.

In cellular association experiment, untreated MDCK cells were used as negative control group. The fluorescence intensity around the cells was measured using an image processing programcalled Image J and corrected fluorescence (CF) values were calculated according to following formula where mean fluorescence is integrated fluorescence intensity per unit area.

CF = Mean fluorescence of selected region – Mean fluorescence of background [94]

The Corrected Fluorescence (CF) values were calculated from the mean fluorescence intensity of the regions around the cells by subtracting the background mean fluorescence intensity. Each experimental group was studied with triple replicates (n=3), i.e., three different liposome-cell associated region were studied in the same LSCM image.

2.2.9. Statistical Analysis

In comparing the groups for a single parameter, One-way Analysis of Variance (ANOVA) test was done with Tukey's Multiple Comparison Test for the post-hoc pairwise comparisons (SPSS-22 Software Programme, SPPS Inc., USA). Differences were considered significant for $p < 0.05$.

CHAPTER 3

RESULTS AND DISCUSSION

Liposomes as drug carriers are preferred due to high drug loading capacity and low cytotoxicity [95]. In this study Levodopa was loaded into liposomes by lipid film hydration method. Liposomes were composed of phospholipid and cholesterol which are readily present in cell membrane composition [96]. The liposomes were prepared within 38-44^{o}C temperature range during hydration and extrusion steps in order to protect bioactivity of the Levodopa. Levodopa is an amino acid (i.e. L-tyrosine) derived biomolecule and loses its activity above 45^{o}C [97]. PC (1,2-dipalmitoyl-sn-glycero-3-phosphocholine, 16:00) (DPPC) and cholesterol were preferred due to their moderate phase transition temperatures of 41^{o}C and 40^{o}C, respectively. LUVs were prepared with different molar ratios as listed in Table 2.1.

In size exclusion chromatography (SEC), drug encapsulated LUVs were separated from unencapsulated drug and unincorporated lipids according to turbidity of the collected fractions. Figure 3.1 shows the turbidity and fluorescence readings of liposomal fractions and fluorescence reading of a free drug solution through size exclusion column. According to this figure, free drug is observed after 8th fraction, thus, drug loaded liposomes were collected through the fractions 3 to 7 to avoid unencapsulated drug.

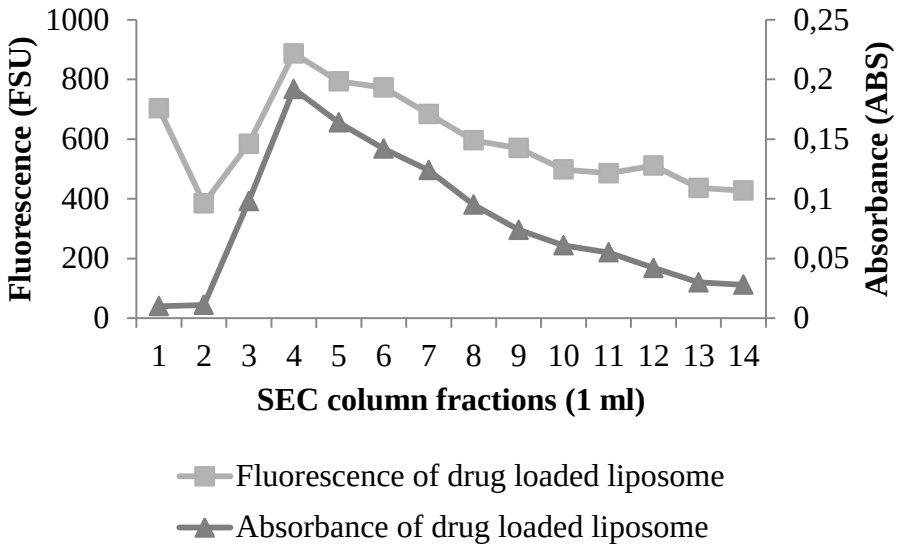

Figure 3.1.A representative chromatogram showing turbidity readings of Levodopa loaded LUVs by UV spectrophotometry and fluorescence readings by fluorescence spectrometry

3.1.Characterization of Conventional Liposomes

3.1.1. Effects of Hydration Temperature and Lipid Composition

In initial optimization studies, the LUVs were prepared with three different molar lipid compositions (DPPC:Cho 8:2, 7:3, and 6:4) at four different temperatures (38, 40, 42 and 44^{o}C) The liposomes were evaluated in terms of size distribution, morphology, drug encapsulation efficiency, percent lipid recovery, percent drug loading, and *in vitro* drug release profiles.

3.1.1.1.Particle Size Distribution and Morphology

Liposomes were aimed to be produced in sizes suitable for intravenous administration in order to increase their circulation time in bloodstream. In literature, it is stated that liposomes in 100-150 nm range can be given intravenously and they can have high bioavailability since they can bypass gastrointestinal system [98]. Liposomes were prepared by extrusion through 100 nm pore sized polycarbonate

membrane. The number of passes through the extruder system was optimized to have the liposomes between 100 and 150 nm size.

Particle size distribution of the liposomes was obtained by Dynamic Light Scattering (DLS) method with laser diffraction principle. Hydrodynamic diameter of the liposomes in aqueous form was determined by Mie Theory. The diameter obtained by this technique refers to a sphere having the same translational diffusion coefficient as the liposome being measured [99].

Table 3.1 shows the size distribution results of Levodopa loaded conventional LUVs prepared at 44^{o}C. It is seen that all liposomal formulations had similar particle size distribution with low PdI values. The mean hydrodynamic diameters of the liposomes were in the desired particle size range (D: 100-150 nm) having monodisperse size distribution (PdI $\leq$ 0.1). This shows that changing lipid composition does not reveal a significant effect on particle size distribution of conventional liposomes.

Table 3.1. Size distribution results of L-Dopa loaded LUVs prepared at 44^{o}C

Liposome Compositions (molar ratios)	**z-average diameter (nm)**	**Peak diameter (nm)**	**Width (nm)**	**PdI**
DPPC:Cho 8:2	117.7	110.0	27.14	0.018
DPPC:Cho 7:3	123.9	116.7	28.06	0.018
DPPC:Cho 6:4	138.1	129.3	41.39	0.109

Figure 3.2 shows the representative DLS results of size distribution for Levodopa loaded LUVs (DPPC:Cho 8:2, DPPC:Cho 7:3, and DPPC:Cho 6:4) prepared at 44^{o}C by exclusion through 100 nm polycarbonate membrane. All of the liposomes had unimodal size distribution with quite narrow range. Figure 3.3 shows TEM image of Levodopa loaded DPPC:Cho (7:3 m:m) liposomes prepared at 44^{o}C. Liposomes had unilamellar morphology with mean diameter between 100 and 150 nm in accordance with size distribution results. No aggregation was observed in the TEM images.

a)

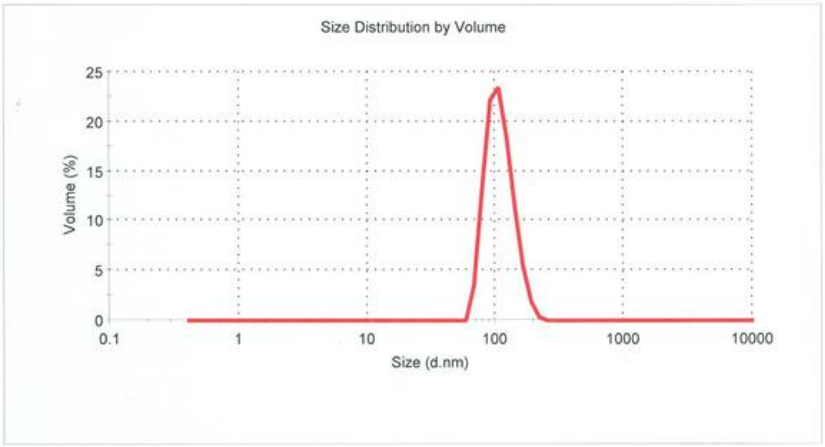

b)

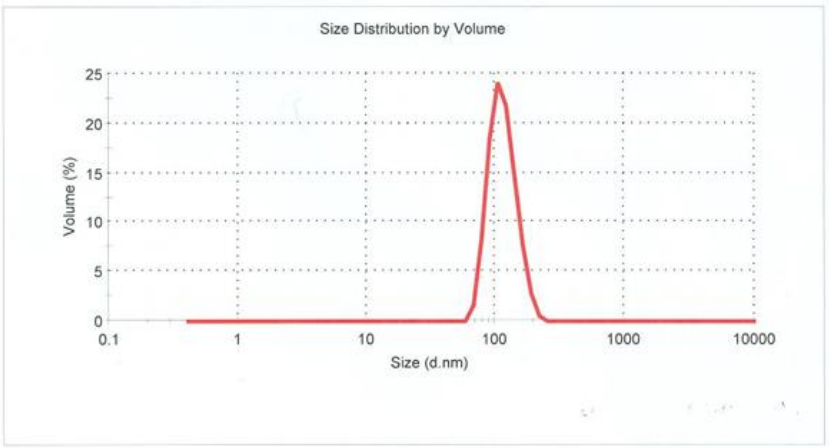

c)

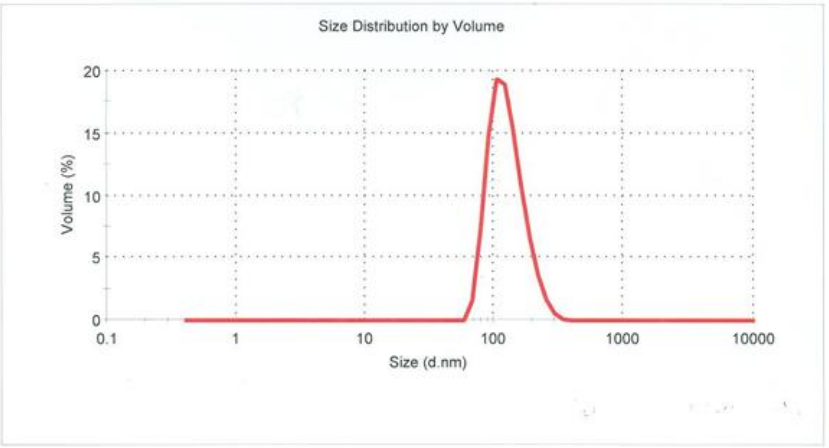

Figure 3.2. Representative DLS results of size distribution for Levodopa loaded LUVs (**a.** DPPC:Cho 8:2 **b.** DPPC:Cho 7:3 **c.** DPPC:Cho 6:4) prepared at 44^{o}C by exclusion through 100 nm polycarbonate membrane

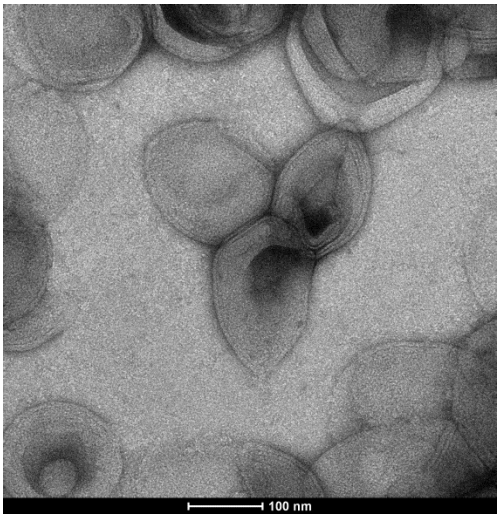

Figure 3.3.TEM image of Levodopa loaded DPPC:Cho (7:3) liposomes prepared at 44^{o}C

3.1.1.2.Drug Encapsulation Efficiency, Percent Lipid Recovery, and Percent Drug Loading

The conventional LUVs were tested for drug encapsulation efficiency (% drug EE), lipid recovery, and drug loading. Levodopa encapsulation efficiency values ranged between 50% and 80%. Lipid recovery values were between 40% and 57%. Percent loading values ranged between 22% and 45%. Lower percent lipid recovery and loading values resulted from liposome preparation at low temperatures. Temperatures were retained between 38^{o}C and 44^{o}C in order to maintain bioactivity of the Levodopa. Among the conventional liposome groups, DPPC:Cho (7:3 m:m) prepared at 40^{o}C had the highest drug encapsulation efficiency (79.83 ± 0.95 %) and percent drug loading (45.16 ± 0.70 %). So, this condition was chosen for further studies. In literature a study revealed 1.36% Levodopa loading in egg yolk phosphotidylcholine:cholesterol (EPC:Cho) (7:3) liposomes prepared by sonication method [100]. First reason for this wide difference is the difference in initial loading used. Their initial loading was four times lower than this study. Preparation of liposomes by sonication method is another reason for decrease in drug loading; sonication method resulted in smaller liposomes with diameter in 60-100 nm (SUVs) and SUVs had smaller inner aqueous volume for drug encapsulation.

Table 3.2. Comparison of drug encapsulation efficiencies (% drug EE), percent lipid recoveries, and percent drug loadings of L-Dopa loaded conventional LUVs prepared at difeerent temperatures (n=3)

Liposome Preparation Temperature	Liposome Compositions (molar ratios)	% drug EE	% Lipid Recovery	% Drug Loading
38^{o}C	DPPC:Cho 8:2	60.38 ± 1.88	40.76 ± 0.15	31.95 ± 2.10
	DPPC:Cho 7:3	63.72 ± 4.18	42.27 ± 0.16	37.68 ± 2.35
	DPPC:Cho 6:4	61.95 ± 1.32	48.62 ± 0.69	35.79 ± 0.25
40^{o}C	DPPC:Cho 8:2	62.09 ± 1.17	41.99 ± 0.63	31.60 ± 1.08
	DPPC:Cho 7:3	**79.83 ± 0.95**	**43.54 ± 0.15**	**45.16 ± 0.70**
	DPPC:Cho 6:4	75.37 ± 4.49	51.18 ± 0.18	41.84 ± 2.36
42^{o}C	DPPC:Cho 8:2	50.68 ± 0.62	48.32 ± 0.19	22.03 ± 0.18
	DPPC:Cho 7:3	53.01 ± 3.67	50.10 ± 0.30	25.68 ± 1.32
	DPPC:Cho 6:4	50.04 ± 3.12	57.60 ± 0.22	24.82 ± 0.98
44^{o}C	DPPC:Cho 8:2	69.24 ± 3.67	42.67 ± 0.14	34.97 ± 1.73
	DPPC:Cho 7:3	60.44 ± 0.02	40.51 ± 0.14	37.30 ± 0.14
	DPPC:Cho 6:4	66.30 ± 3.64	49.46 ± 0.19	37.65 ± 1.93

3.1.1.3.*In vitro* Release Profiles

The conventional LUVs were evaluated based on *in vitro* release profiles. Figure 3.4 shows comparison of cumulative percent Levodopa release from DPPC:Cho (8:2, 7:3, and 6:4 m:m) liposomes prepared at 38^{o}C, 40^{o}C, 42^{o}C, and 44^{o}C. Controlled drug release from liposomes is desired to improve bioavailability of the drug in bloodstream. Figure 3.3 reveals that liposomes did show a small burst release at 4h. At each temperature, the DPPC:Cho 8:2 ratio group had the fastest and DPPC:Cho 7:3 group had the slowest cumulative drug release. Cholesterol inclusion of 30 mole % of the total lipid content decreased the cumulative amount of Levodopa released within 48 hours. Inclusion of cholesterol increases the rigidity of the bilayer and

decreases the permeability of liposomes; thereby decreasing the release rate [6]. However, increasing the cholesterol concentration above 55% was reported to disrupt the regular structure of the liposomal membrane resulting in the change in release profile [102, 103].

Among liposomal groups, the liposomes prepared at 38^{o}C and 40^{o}C had slower drug release profiles (Figure 3.4). Among the LUVs, the liposome DPPC:Cho 7:3 prepared at 40^{o}C had the slowest cumulative drug release (29.99 ± 0.81 % and 44.98 ± 1.63 % at 24h and 48h, respectively) despite having highest drug encapsulation efficiency (79.83 ± 0.95 %). In literature the studies revealed that the liposomes reached to the brain following 12 hours [104] and 8 hours [105] after given by oral and intravenous routes, respectively. This means that the liposomes developed in this study can be either given orally or intravenously as most of the drug still retained within the liposomes after 8 or 12 hours. However, intravenous administration was favorable over oral administration due to increased plasma liposome concentration which leads to increased bioavailability.

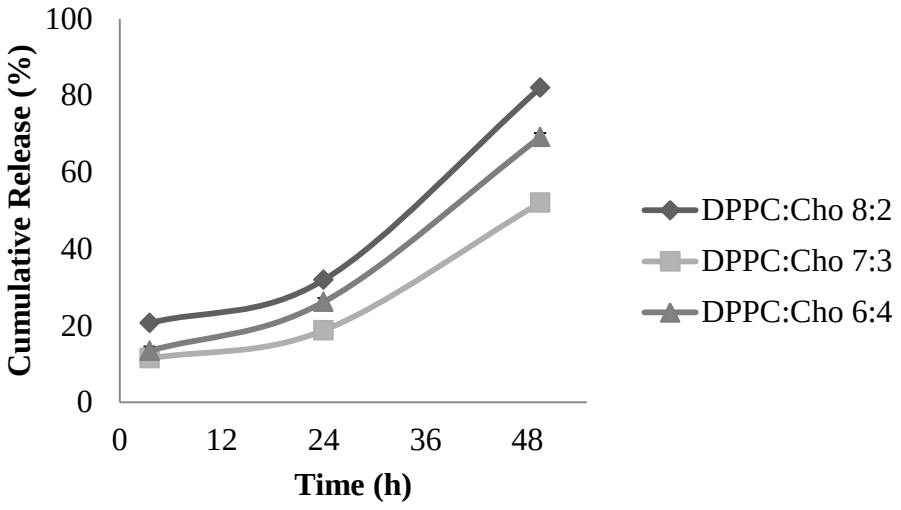

a)

Figure 3.4. Effect of liposome preparation temperature on the release of Levodopa from DPPC:Cho (8:2, 7:3, and 6:4 m:m) liposomes prepared at **a)** T = 38^{o}C **b)** T = 40^{o}C **c)** T = 42^{o}C **d)** T = 44^{o}C (n=3)

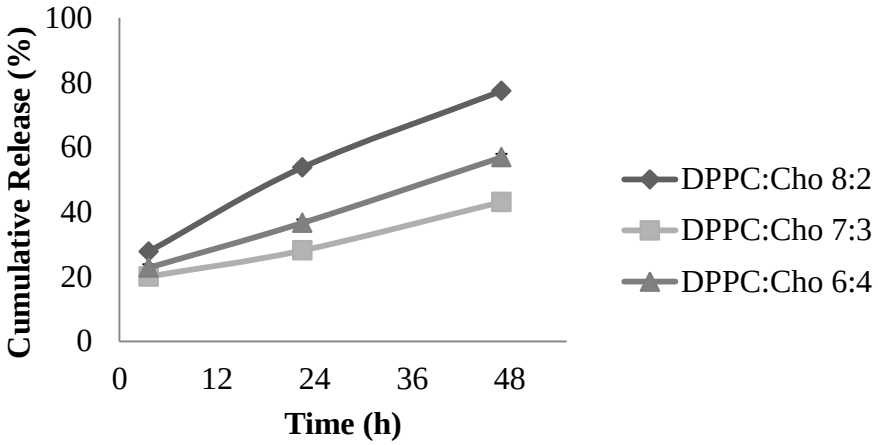

b)

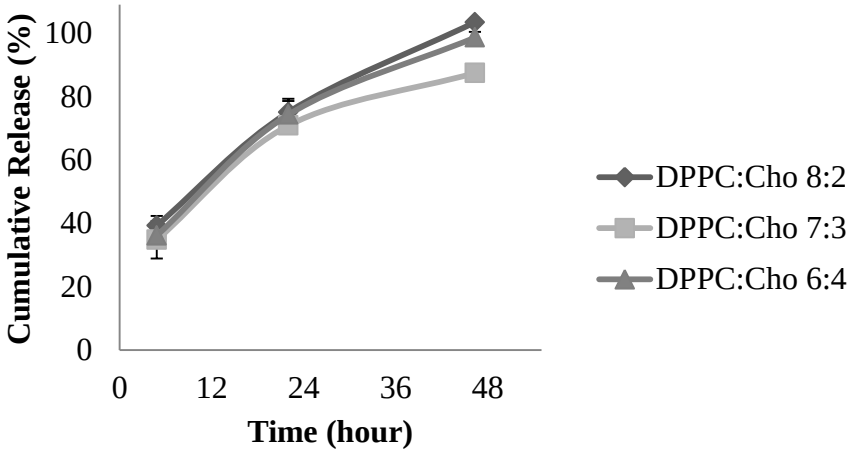

c)

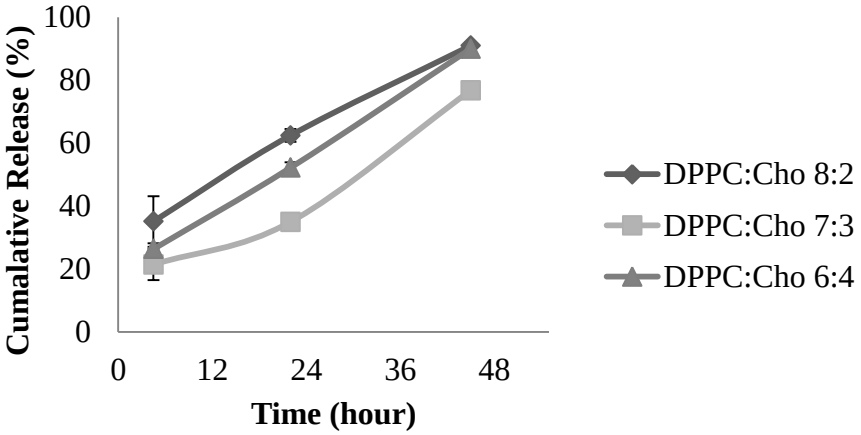

d)

Figure 3.4.(continued)

3.2. Characterization of Stealth Liposomes

Stealth liposomes were prepared with PEG coating of the conventional DPPC:Cho liposomes. In literature PEGylated liposomes are reported to be more stable with prolonged blood circulation [106]. PEGylated liposomes are revealed to have low potential to be captured by the Reticuloendothelial system (RES) cells [107]. High degree of PEGylation may destabilize the integrity of the lipid bilayer which causes difficulty in cellular binding and intracellular drug delivery [108]. Low degree of PEGylation may result in rapid removal of the liposomes from the blood stream by the RES cells. Therefore, degree of PEGylation is very important for liposomal drug carriers. A study revealed that the liposomes with PEGylation degree lower than 5% of phospholipids had higher binding affinity than the higher degree of PEGylation [67].

In this study PEGylation was achieved by addition of 18:00 DSPE-mPEG(2000) into lipid film with two different ratios (2 and 4 mole percentage of DPPC) as listed in Table 2.1.The stealth liposomes were prepared with PEGylation of DPPC:Cho (7:3) liposomes prepared at 40^{o}C. They were evaluated in terms of size distribution, surface charge, morphology, drug encapsulation efficiency, percent lipid recovery, percent drug loading, and *in vitro* drug release profiles.

3.2.1. Particle Size Distribution, Surface Charge, and Morphology

Size distribution of the PEGylated liposomes was obtained by DLS analysis. PEGylated liposomes had slightly higher hydrodynamic diameter than the conventional liposome (DPPC:Cho; 7:3) (i.e. 123.9 nm) due to hydrophilic nature of the PEG molecule. However, they had size distribution in the desired range (D: 100-150 nm) with monodisperse distribution (PdI $\leq$ 0.1). The zeta potential values of the PEGylated liposomes were similar and slightly lower than neutrality indicating the stability of the PEGylated liposomes. In literature it was shown PEGylation up to a certain level of render liposome surfaces more hydrophilic and neutralize it for increased cellular binding [108].

Figure 3.5 shows the representative size distribution of the levodopa loaded PEGylated liposomes obtained by DLS analysis. It is seen that PEGylated liposomes had unimodal size distribution with narrow range. TEM micrographs of the PEGylated liposomes (Figure 3.6) showed that the liposomes had spherical morphology and unilamellar structures. The size of the stealth liposomes was compatible with the size distribution results (D: 100-150 nm).

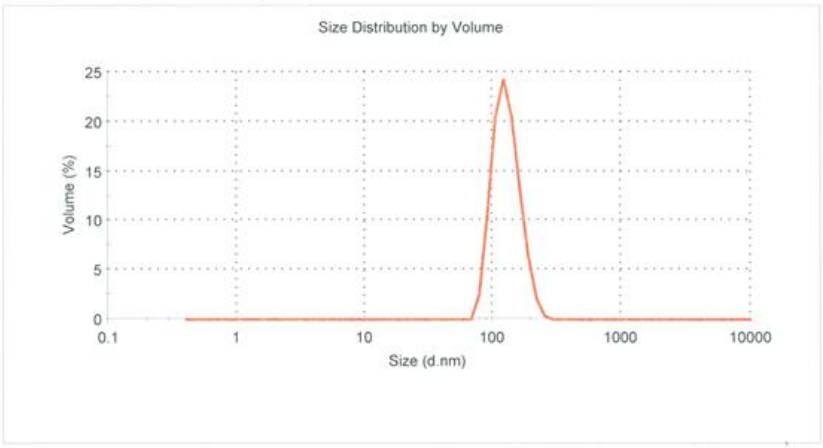

a)

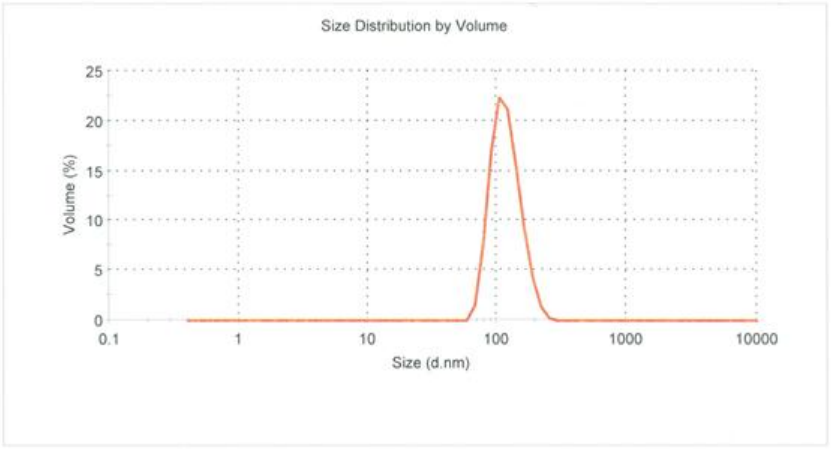

b)

Figure 3.5. Representative DLS results of size distribution for levodopa loaded LUVs **a)** 2% PEG/LUV **b)** 4% PEG/LUV prepared at 40^{o}C by exctrusion through 100 nm polycarbonate membrane

Table 3.3. Size distribution and zeta potential results of the Levodopa loaded PEGylated LUVs

Liposome	z-average diameter (nm)	Peak diameter (nm)	Width (nm)	PdI	Zeta Potential (mV)
2% PEG/LUV	137.0	131.0	31.50	0.035	-7.76
4% PEG/LUV	129.2	120.9	31.68	0.030	- 5.94

a) 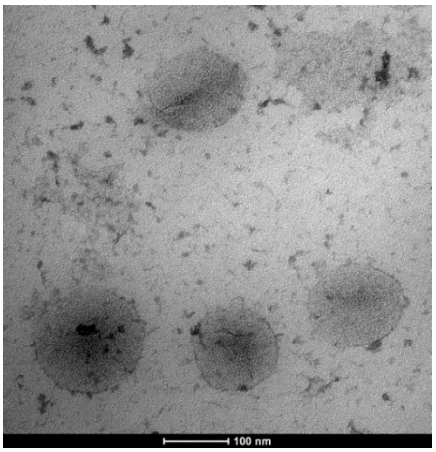

b) 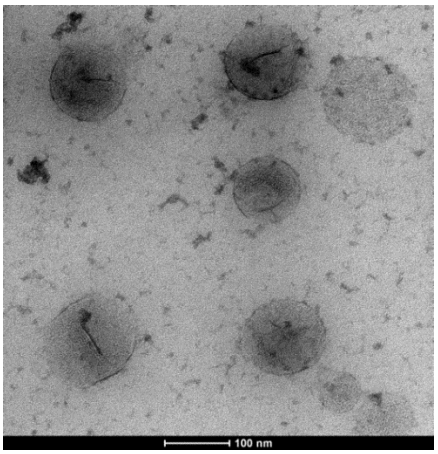

Figure 3.6.TEM images of levodopa loaded **a)** 2% PEG/LUV **b)** 4% PEG/LUV

3.2.2. Lipid Recovery, Drug Encapsulation Efficiency, and Loading

Drug encapsulation efficiency, percent lipid recovery, and percent drug loading values of the PEGylated liposomes are listed in Table 3.4. Different PEGylation degrees did not result in any significant difference in terms of drug encapsulation efficiency, lipid recovery, and drug loading. However, as the degree of PEGylation increased, there was a slight decrease in drug encapsulation efficiency (from 79.83 ± 0.95 %) and slight increase in lipid recovery (from 43.54 ± 0.15 %) when compared with conventional liposome DPPC:Cho 7:3 (m:m). The decrease in drug encapsulation efficiency was resulted from PEGylation; PEGylated liposomes had smaller internal volume for drug encapsulation due to PEG coating of the liposomes.

The increase in lipid recovery was resulted from enhanced stability of the PEGylated liposomes; in literature PEGylated liposomes were revealed more stable than conventional liposomes [109].

Table 3.4. Comparison of drug encapsulation efficiency (% drug EE), percent lipid recovery, and percent drug loading of Levodopa loaded PEGylated liposomes prepared at 40^{o}C (n=3)

Liposome	% drug EE	% Lipid Recovery	% Drug Loading
2% PEG/LUV	71.60 ± 0.65	47.77 ± 0.37	36.92 ± 0.33
4% PEG/LUV	74.57 ± 1.04	49.05 ± 0.18	38.01 ± 0.63

3.2.3. *In vitro* Release Profiles

The cumulative percent drug release of the conventional liposome (DPPC:Cho 7:3) and PEGylated liposomes (2% and 4% PEGylated DPPC:Cho 7:3) are shown in Figure 3.7. The liposomes had similar cumulative drug release profiles. They showed similar burst drug release with conventional liposomes; only 18-20 % of total levodopa was released in the first 4 hours. However, drug release slowed down when liposomes were PEGylated and also when PEGylation degree was increased from 2% to 4%. For higher bioavailability in bloodstream, 4% PEGylated liposome (DPPC:Cho 7:3) was found optimal with slowest drug release for 24h and 48h periods (25% and 36% cumulative drug release, respectively).

The results revealed that PEGylated liposomes were more stable with slower drug release. The decrease in drug release rate might have resulted from difficulty in drug release through entanglement of the drug molecules in PEG chains covering the liposome surfaces. In literature, PEGylated liposomes were shown to have prolonged drug release avoiding adverse effects and fluctuations in plasma drug concentration

[110]. In many studies, PEGylated liposomes were indicated to have slower drug release profile than conventional liposomes [111-114].

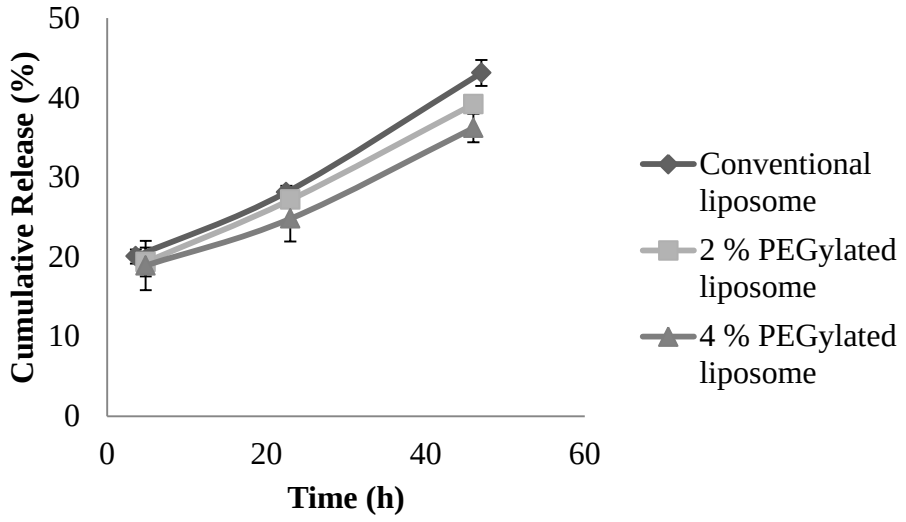

Figure 3.7. Comparison of *in vitro* drug release of Levodopa loaded LUVs and PEGylated liposomes prepared at 40^{o}C (n=3)

3.3. Characterization of Targeted Liposomes

Targeted liposomes were prepared via covalent conjugation of maltodextrin to the end of PEG chains attached to DSPE lipid in lipid bilayer membrane of the liposomes. In order to conjugate maltodextrin molecules to the PEG molecules, firstly maltodextrin was carboxylmethylated to yield carboxyl groups. Thereafter carboxyl groups of the maltodextrin (-COOH) and amine groups of the PEG lipid (-NH_2) reacted via carbodiimide chemistry. Targeted liposomes were prepared with maltodextrin conjugated PEG lipids by inserting the conjugated lipid during lipid film preparation step.

3.3.1. Evaluation of Conjugation of Maltodextrin to DSPE-PEG(2000)

3.3.1.1. Carboxymethylation of Maltodextrin

Prior to conjugation of maltodextrin to PEG lipid, maltodextrin was firstly carboxylmethylated as described in Section 2.2.2.1. In carboxymethylation reaction, some of the hydroxyl groups (-OH) of the maltodextrin were converted to carboxylmethyl groups (-CH_2-COOH) as shown in Figure 2.3. Figure 3.8 represents the FTIR spectra of the unreacted maltodextrin and carboxylmethylated maltodextrin. The reduced intensity at hydroxyl bond (3200-3550 cm^{-1}) band and intensity formation at carboxyl bond (1649-1780 cm^{-1}) band proved the carboxymethylation of maltodextrin. In IR spectrum of the carboxylmethylated maltodextrin, the increase in intensity at 1400 and 1600 cm^{-1} were attributed to symmetrical and asymmetrical vibrations, respectively due to incorporation of carboxylmethyl groups into the maltodextrin molecule [115].

Carboxymethylation efficiency was calculated as 62.68% from FTIR spectrum of the maltodextrin (Figure 3.8) by using the intensity decrease in between 3200 and 3550 cm^{-1}, representing OH stretching in hydroxyl bond. In literature carboxymethylation efficiency values ranged between 50 and 80 percent according to reaction parameters such as alcohol type in the reaction medium, volume and concentration of sodium hydroxide and alcohol solution, amount of chloroacetic acid, reaction temperature, and reaction time [115-118]. A study revealed that carboxymethylation efficiency is the highest in isopropyl alcohol solution among methyl, ethyl, propyl, isopropyl, butyl, sec-butyl, and tert-butyl alcohol solutions keeping the other reaction conditions same [116]. Thus, isopropyl alcohol was used in reaction medium. In carboxymethylation reaction, sodium hydroxide is used as a strong base to increase nucleophilicity of the free hydroxide groups (-OH) by deprotonating them; thereafter activated hydroxyl groups are converted to carboxylmethyl groups reacting with chloroacetic acid; thus volume and concentration of the sodium hydroxide and chloroacetic acid are very important [115]. In this study, amount of sodium hydroxide, chloroacetic acid and isopropyl alcohol were adapted from a previously conducted study with high carboxymethylation efficiency [93] as explained in

Section 2.2.2.1. The reaction was carried out at 50°C for 4 hours as mostly done in literature for higher carboxymethylation efficiency [115-118].

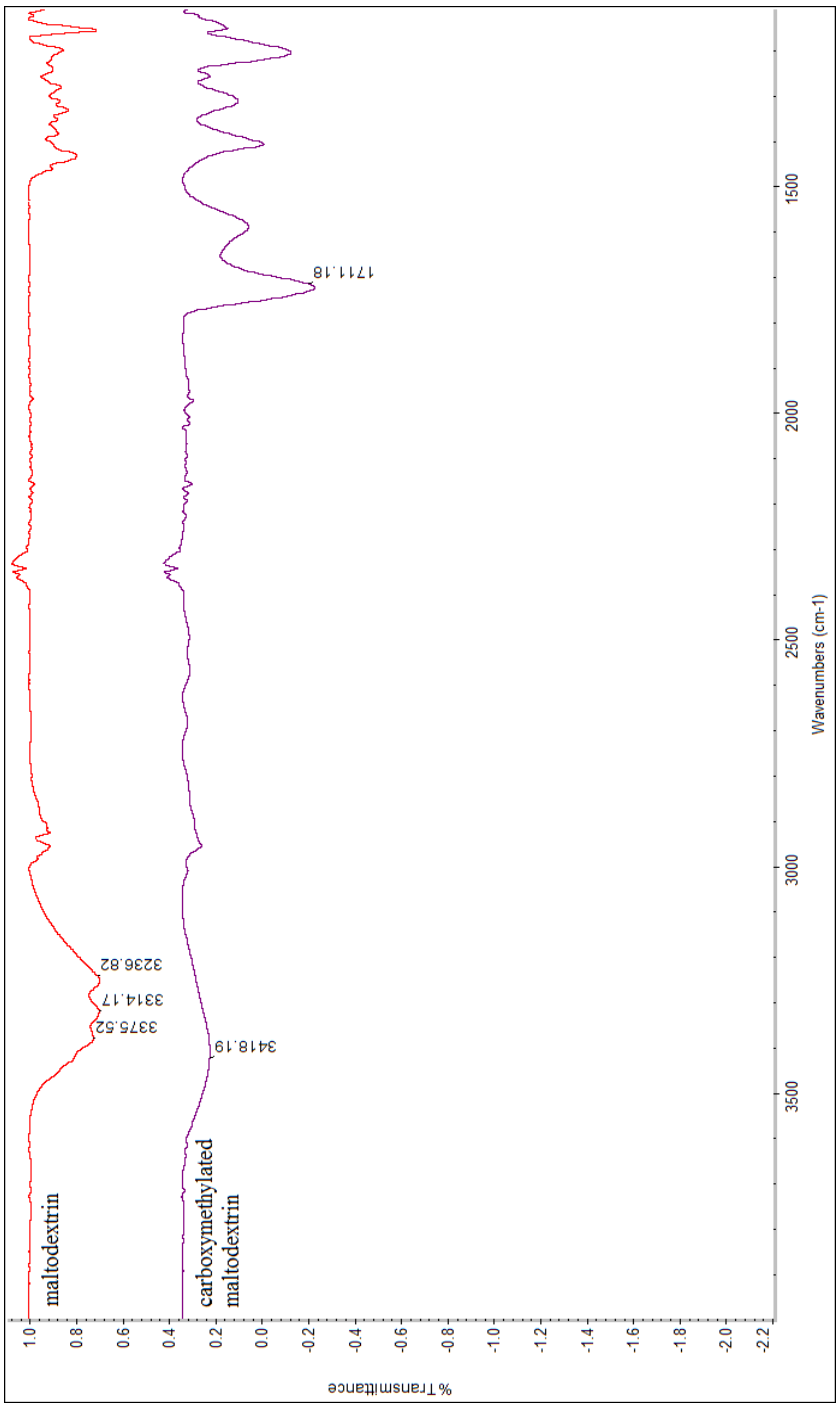

Figure 3.8.ATR-FTIR spectra of maltodextrin and carboxylmethylated maltodextrin (3200-3550 cm^{-1}: hydroxyl bond (-OH), 1649-1780 cm^{-1}: carboxyl bond (-COOH))

3.3.1.2. Conjugation of Carboxylmethylated Maltodextrin and DSPE-PEG(2000)

Maltodextrin and DSPE-PEG(2000)amine were conjugated using carbodiimide chemistry after carboxymethylation of the maltodextrin; carboxyl groups of the maltodextrin (-COOH) and amine groups of the PEG lipid (-NH_2) were reacted as shown in Figure 2.4. In this conjugation, the carboxyl groups of the maltodextrin were initially activated by N,N-dicyclohexylcarbodiimide (DCC) and N-hydroxysuccinimide (NHS). Thereafter the activated maltodextrin reacted with nitrogen nucleophiles of the PEG lipid to form stable amide bonds. In order to confirm the conjugation, FTIR analysis was performed. Figure 3.9 shows the FTIR spectra of physical mixture and reaction product of the maltodextrin and DSPE-PEG(2000)Amine. The decreased intensity at amine bond (3180-3500 cm^{-1}) and carboxyl bond (1649-1780 cm^{-1}) bands and the intensity increase at amide bond (1600-1640 cm^{-1}) band confirmed the conjugation of the maltodextrin and PEGylated lipids.

Conjugation efficiency was calculated from the decrease in amine bond peak between 3180 and 3500 cm^{-1}, representing N-H strecting, considering the peak for the same amount of lipids used in the analysis. The conjugation efficiency was found as 44.76% revealing that almost half of the PEG lipids were conjugated to targeting moiety. In literature conjugation efficiency of the studies conducted with carbodiimide chemistry ranged between 32% and 79% depending on the reaction conditions [119-122].

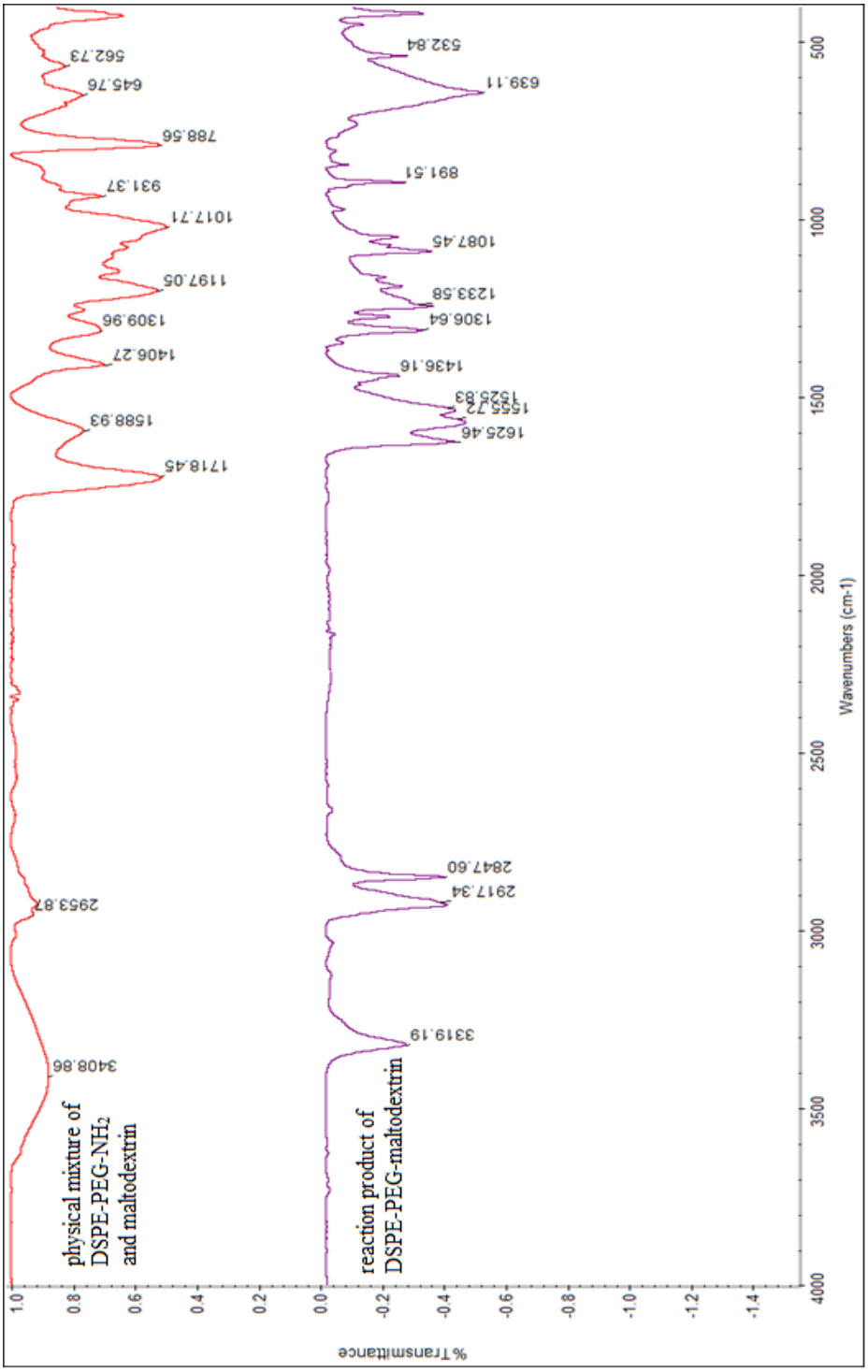

Figure 3.9.ATR-FTIR spectra of physical mixture of DSPE-PEG(2000)Amine & carboxylmethylated maltodextrin and reaction product DSPE-PEG-maltodextrin (3180-3500 cm^{-1}: amine bond ($-NH_2$), 1649-1780 cm^{-1}: carboxyl bond (-COOH), and 1600-1640 cm^{-1}: amide bond (N- C=O))

Activation of the carboxyl groups by DCC and NHS is the most important parameter for conjugation efficiency of carbodiimide chemistry. DCC and NHS are the carbodiimides commonly used for the activation of the carboxylic acids for the subsequent coupling with the amine nucleophiles. In carbodiimide chemistry, the carboxyl groups are firstly activated by DCC and then NHS is coupled to the acid to produce immediate reaction [123]. Carboxyl group (-COOH) to carbodiimide (DCC/NHS) ratio is quite important for efficient activation; however, excess carbodiimide addition is avoided due to difficulty in removal at the end of the reaction. In literature, carboxyl group to carbodiimide ratio was studied between 1:0.5 and 1:1.5 [119-122], thus in this study carboxylic acid to DCC/NHS ratio was adjusted to 1:0.5. The conjugation efficiency is also dependent on solvent type used in reaction medium; in studies organic solvents with low dielectric constants such as dimethylformamide, dichloromethane, chloroform or DMSO were preferred to minimize side reactions [119-122]; thus, in this study DMSO was used during conjugation.

3.3.2. Drug Loaded Targeted Liposomes

Targeted liposomes were prepared with different mole percentage of maltodextrin conjugated PEGylated liposomal formulation. Two different targeted liposomal formulations with different maltodextrin ratio (0.7 and 0.35 mole percentage of DPPC) were prepared as described in Section 2.2.1 (i.e. LD-0.35% MD-4% PEG/LUV and LD-0.7% MD-4% PEG/LUV). The targeted liposomal groups were prepared in a way that each targeted liposome had 4% PEGylation. LD-0.7% MD-4% PEG/LUV was prepared directly using the conjugated lipid DSPE-PEG-maltodextrin whereas LD-0.35% MD-4% PEG/LUV was prepared by diluting the conjugated lipid with DSPE-mPEG(2000) maintaining 4% PEG ratio.

The drug loaded targeted liposomes were evaluated based on size distribution, surface charge, morphology, drug encapsulation efficiency, percent lipid recovery, percent drug loading, and *in vitro* drug release profiles.

3.3.2.1. Particle Size Distribution, Surface Charge, and Morphology

Size distributions of the drug loaded targeted liposomes were obtained by DLS analysis. The targeted liposomes had similar hydrodynamic diameter with the nontargeted 4% PEGylated liposome (i.e. 129.2 nm) revealing that addition of maltodextrin did not affect the liposome size. They also had mean size in the desired range (D: 100-150 nm) with monodisperse distribution (PdI $\leq$ 0.1) as shown in Table 3.5.

The zeta potential values of the targeted liposomes were higher than nontargeted 4% PEGylated liposome (i.e. - 5.94 mV) and the zeta potential values were increasing with increasing maltodextrin ratio. The zeta potential values of the LD-0.35% MD-4% PEG/LUV and LD-0.7% MD-4% PEG/LUV were respectively -3.92 and 0.971 mV suggesting that addition of maltodextrin resulted in more neutral surface charge. In literature neutral liposomal were revealed to have higher half-life in bloodstream than negatively charged liposomes as explained in Section 1.3.4.1 [80]. Therefore, in this study targeted liposomes are more promising to have higher bioavailability with more neutral surface charge and LD-0.7% MD-4% PEG/LUV is thought to be the most effective one with neutral charge.

Table 3.5. Size distribution and zeta potential results of Levodopa loaded targeted liposomes

Liposome	**z-average diameter (nm)**	**Peak diameter (nm)**	**Width (nm)**	**PDI**	**Zeta Potential (mV)**
LD-0.35% MD-4% PEG/LUV	130.8	121.1	35.12	0.054	-3.92
LD-0.7% MD-4% PEG/LUV	124.8	120.4	26.48	0.049	0.971

Figure 3.10 shows the representative size distribution of the Levodopa loaded targeted liposomes obtained by DLS analysis. It is seen that targeted liposomes had unimodal size distribution with narrow range. TEM micrographs (Figure 3.11) of the drug loaded targeted liposomes revealed that the liposomes had spherical morphology and unilamellar structures with mean diameter between 100 and 150 nm in accordance with the size distribution results.

a)

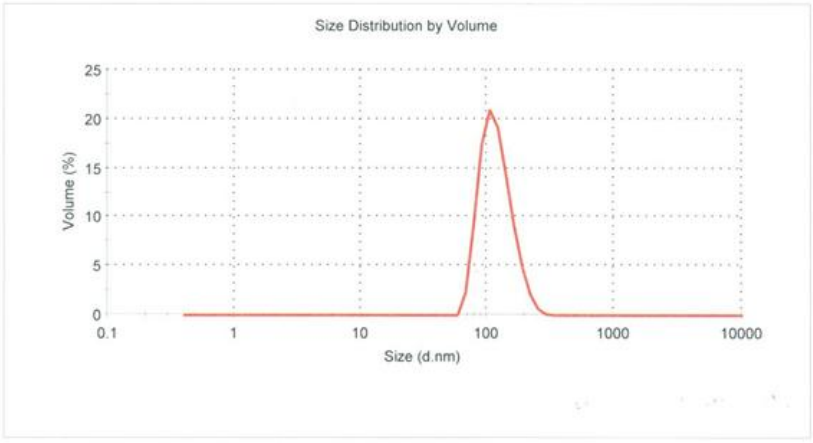

b)

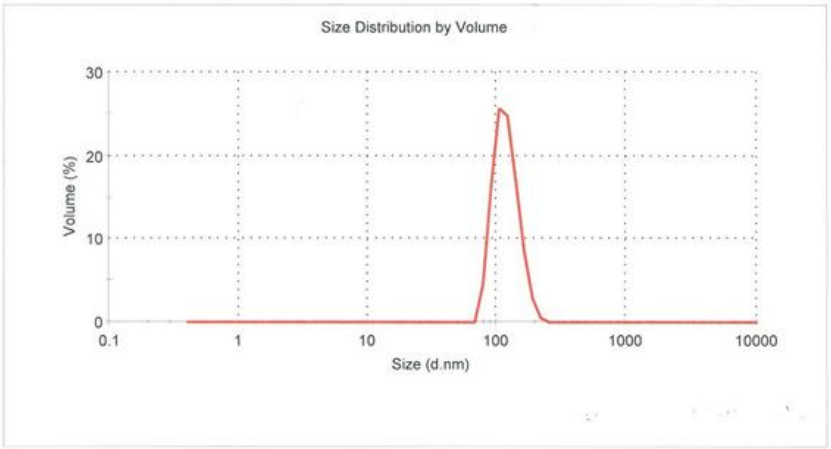

Figure 3.10. Representative DLS results of size distribution for Levodopa loaded targeted liposomes **a)** LD-0.35% MD-4% PEG/LUV **b)** LD-0.7% MD-4% PEG/LUV prepared at 40^{o}C by exclusion through 100 nm polycarbonate membrane

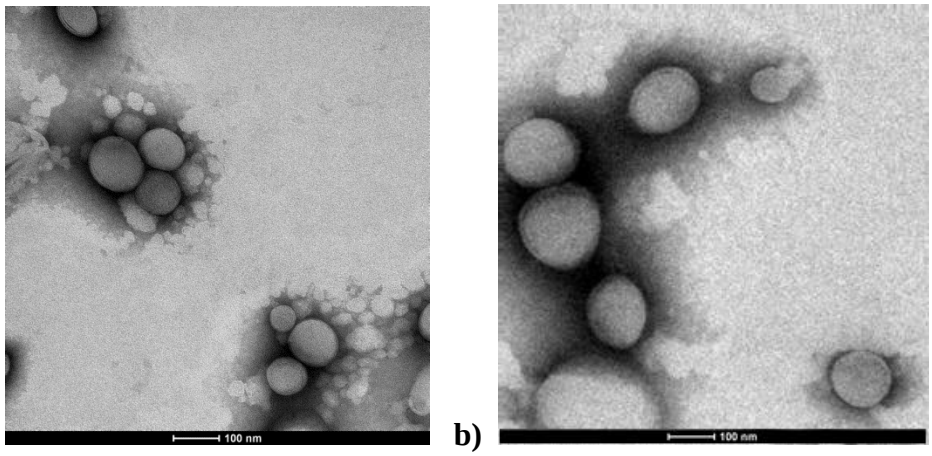

Figure 3.11.TEM images of Levodopa loaded targeted liposomes **a)** LD-0.35% MD-4% PEG/LUV **b)** LD-0.7% MD-4% PEG/LUV

3.3.2.2. Lipid Recovery, Drug Encapsulation Efficiency, and Loading

Drug encapsulation efficiency and loading values of the LD-0.7% MD-4% PEG/LUV were quite higher (92.47 ± 2.70 % and 44.25 ± 0.33 %, respectively) than the nontargeted 4% PEGylated liposome (74.57 ± 1.04% and 38.01 ± 0.63%, respectively) and LD-0.35% MD-4% PEG/LUV (71.38 ± 0.21% and 33.68 ± 0.49%, respectively). On the other hand, different maltodextrin conjugation ratios did not result in any significant difference in terms of lipid recovery; about 52% lipid recovery was attained in both drug loaded targeted liposomal formulations. However, the lipid recovery values were slightly higher than nontargeted 4% PEGylated drug loaded liposome (49.05 ± 0.18% versus 52%) revealing that conjugation of maltodextrin to PEGylated lipid slightly increased the lipid recovery.

Table 3.6. Comparison of encapsulation efficiency (% drug EE), percent lipid recovery, and percent drug loading of Levodopa loaded targeted liposomes prepared at 40^{o}C (n=3)

Liposome	%EE	%Lipid Recovery	%Drug Loading
LD-0.35% MD-4% PEG/LUV	71.38 ± 0.21	52.46 ± 0.19	33.68 ± 0.49
LD-0.7% MD-4% PEG/LUV	92.47 ± 2.70	52.24 ± 0.19	44.25 ± 0.33

3.3.2.3. *In vitro* Release Profiles

The cumulative drug release from the targeted liposomes were similar to each other and to the nontargeted 4% PEGylated liposome (Figure 3.12) revealing that addition of the targeting molecule had no significant effect on *in vitro* drug release. At the end of 24h and 48h, LD-0.7% MD-4% PEG/LUV had 24% and 36% cumulative drug release, respectively. In Parkinson's disease therapy, controlled release of the Levodopa is desired for increased bioavailability and decreased drug side effects. Since most of the liposomes will be either eliminated from the circulation or targeted within first 24h, it is aimed to have small amounts of drug release during this period. Accordingly, the results showed about 75% of the Levodopa remained in liposomes and suggested a sustained Levodopa release at the target site. Brain targeted drug carriers are intended for the delivery of the therapeutics to increase brain transition with decreased drug side effects [14]. So, with the successive targeting of the liposomes most of the Levodopa will be carried to the brain and small amounts released during this period will have less negative effects at the other sites.

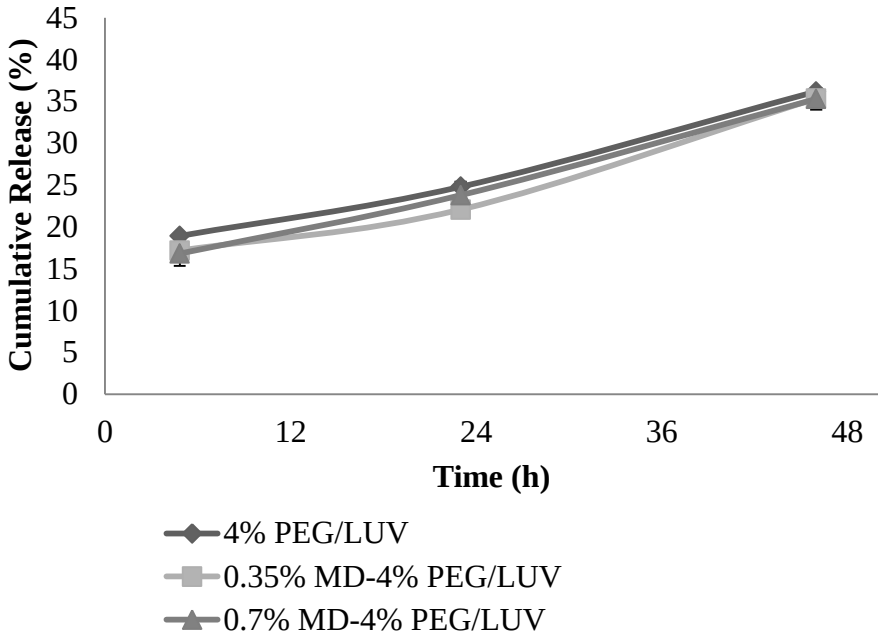

Figure 3.12. Comparison of *in vitro* release of Levodopa from nontargeted 4%PEGylated and targeted liposomes prepared at 40^{o}C (n=3)

3.3.3. Drug and Antioxidant Loaded Targeted Liposomes

Drug and antioxidant (Glutathione, GSH) loaded targeted liposomes were prepared with the optimal targeted drug loaded liposomal formulation (i.e. LD-0.7% MD-4% PEG/LUV) by two different amounts of initial GSH loading (20 and 40 μM). The liposomes were evaluated in terms of size, drug encapsulation efficiency, lipid recovery, drug loading, and *in vitro* drug release.

3.3.3.1. Particle Size Distribution and Morphology

Drug and antioxidant dual loaded targeted liposomes had similar size distribution with the nontargeted liposomes (D: 100-150 nm) and it showed a monodisperse distribution (PdI $\leq$ 0.1) as shown in Table 3.7. These results are quite reasonable as the dual loaded targeted liposomal formulations were prepared with the same lipid-polymer and maltodextrin composition.

Table 3.7. Size distribution results of Levodopa and GSH loaded targeted liposomes

Liposome	Initial GSH Loading (µM)	z-average diameter (nm)	Peak diameter (nm)	Width (nm)	PDI
LD-GHS-0.7% MD-4% PEG/LUV	20	129.4	119.7	33.92	0.045
	40	128.9	119.1	35.49	0.070

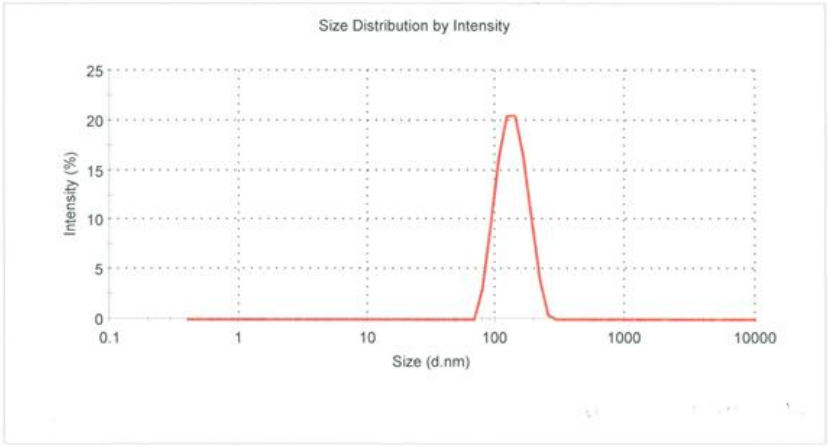

a)

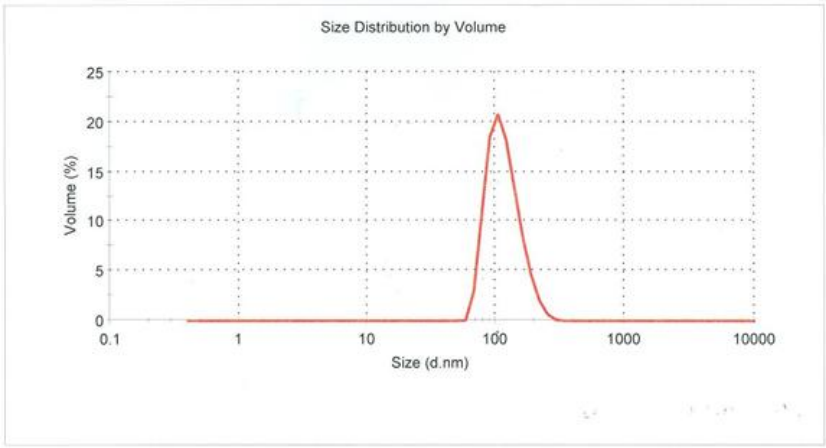

b)

Figure 3.13. Representative DLS result of size distribution for Levodopa and GSH loaded targeted liposomes **a)** 20 µM GSH **b)** 40 µM GSH loaded

3.3.3.2. Lipid Recovery, Drug Encapsulation Efficiency, and Drug Loading

Drug encapsulation efficiency, percent lipid recovery, and percent drug loading values of the drug and antioxidant loaded targeted liposomes are listed in Table 3.8. GSH encapsulation efficacy values were quite high; 82.95% and 86.98% for 20 and 40 μM initial GSH amounts, respectively. Levodopa encapsulation efficiency and loading values of the drug and antioxidant loaded liposomes were found lower (Table 3.8) than LD-0.7% MD-4% PEG/LUV (92.47 ± 2.70% and 44.25 ± 0.33%, respectively). The decrease in the drug encapsulation efficiency and loading may be due to dual encapsulation of Levodopa and GSH in the aqueous phase of the liposomes. Lipid recovery values were similar to each other and to the LD-0.7% MD-4% PEG/LUV (52.22%) revealing that addition of the antioxidant did not affect the lipid recovery of the targeted liposomes.

Table 3.8. Comparison of GSH and drug encapsulation efficiency (% drug EE), percent lipid recovery, and percent Levodopa loading of targeted liposomes (n=3)

Liposome	**Initial GSH Loading (μM)**	**%GSH EE**	**%Levodopa EE**	**%Lipid Recovery**	**%Levodopa Loading**
LD-GHS-0.7% MD-4% PEG/LUV	20	82.95 ± 1.99	72.88 ± 0.60	50.13 ± 0.17	36.34 ± 0.17
	40	86.98 ± 3.28	83.76 ± 2.57	51.16 ± 0.17	40.93 ± 1.39

3.3.3.3. *In vitro* Release Profiles

In vitro release profiles of Levodopa and GSH from dual loaded targeted liposomes are shown in Figures 3.14 and 3.15, respectively. Release profiles of Levodopa and GSH were similar with a small burst release at 4h. Figure 3.14 reveals controlled release of Levodopa; 20% and 33% cumulative drug release was obtained at 24h and 48h, respectively. Figure 3.16 shows cumulative GSH release from dual loaded LD-GHS-0.7% MD-4% PEG/LUV. Initially 40 μM GSH loaded targeted liposome had slower GSH release when compared with initially 20 μM GSH loaded liposomal formulation; after 24h and 48h, 26% and 50% of the GSH was released from the initially 40 μM GSH loaded liposomal formulation, respectively. Controlled and slow GSH release was desired to maintain both Levodopa and liposome stability and also to deliver this antioxidant to the brain. Controlled release of Levodopa is a promising approach in Parkinson's disease therapy to increase Levodopa concentration in brain by increasing its stability. Besides that, in literature, neurodegenerative diseases were associated with the oxidative damage on neurons due to the deficiency of antioxidants [124]. Thus, brain delivery of GSH is also thought to have additional benefit on neuronal cells and hence, on treatment efficacy.

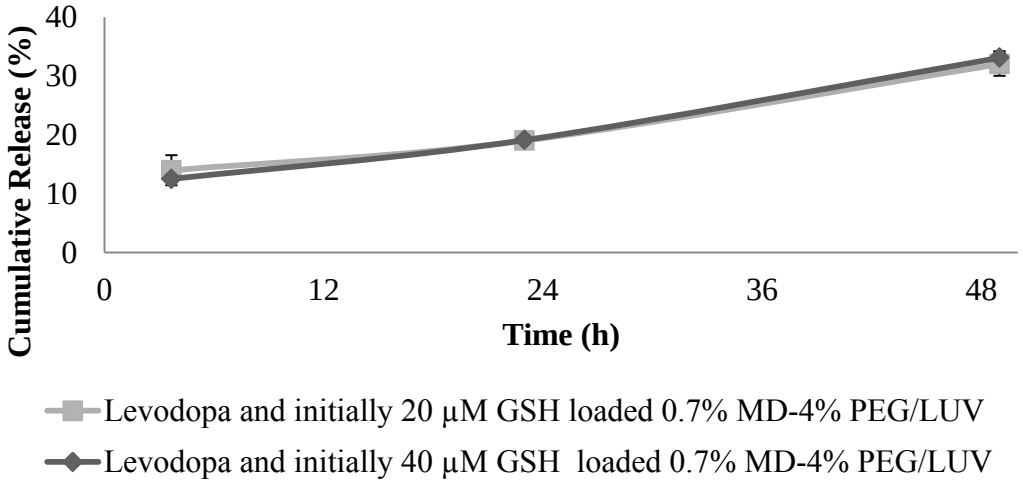

Figure 3.14. Comparison of *in vitro* Levodopa release of Levodopa and GSH loaded targeted liposomes (LD-GHS-0.7% MD-4% PEG/LUV) (n=3)

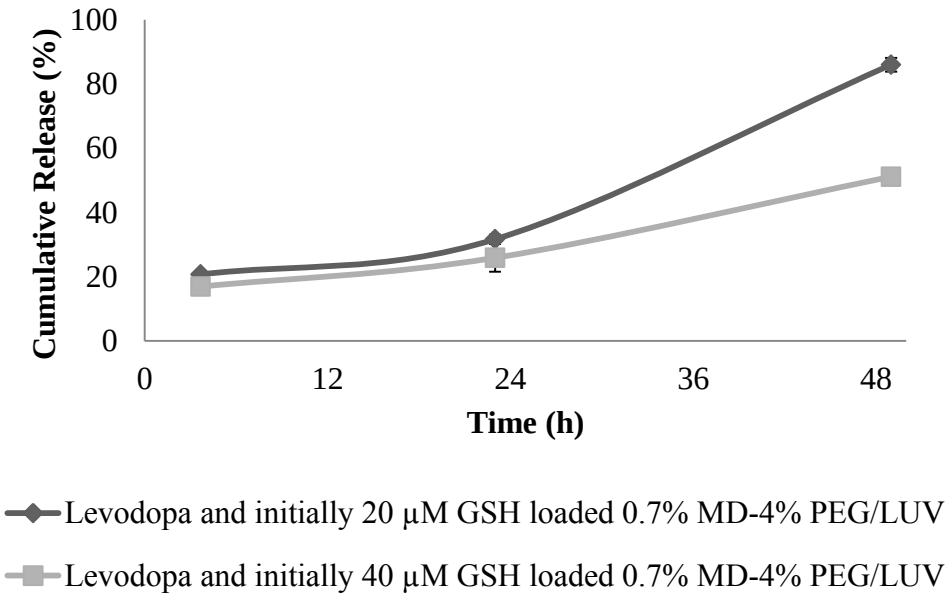

Figure 3.15. Comparison of *in vitro* GSH release of Levodopa and GSH loaded targeted liposomes (LD-GHS-0.7% MD-4% PEG/LUV) (n=3)

Figures 3.16, 3.17, and 3.18 show comparison of *in vitro* drug release profiles of the conventional liposome (DPPC:Cho 7:3), stealth liposome (4%PEG/LUV), drug loaded targeted liposome (LD-0.7% MD-4% PEG/LUV) and drug and antioxidant loaded targeted liposome (LD-GHS-0.7% MD-4% PEG/LUV). It is seen that conventional liposomal formulation had the fastest *in vitro* drug release profile among all experimental groups in terms of cumulative percent and cumulative amount of Levodopa release. PEGylated and targeted liposomal formulations had similar cumulative percent and cumulative amount of Levodopa release. These results suggested that PEGylation, addition of targeting molecule and addition of GSH did not affect the Levodopa release profiles of the liposomes.

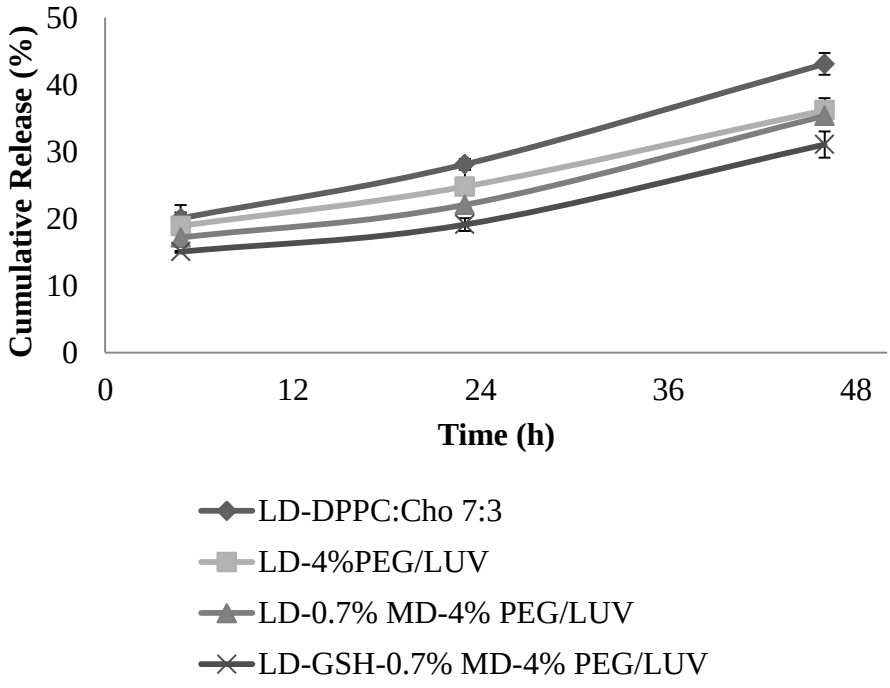

Figure 3.16. Comparison of *in vitro* cumulative Levodopa release (%) of conventional liposomes (DPPC:Cho 7:3), stealth liposomes (4% PEG/LUV), Levodopa loaded targeted liposomes (LD-0.7% MD-4% PEG/LUV) and Levodopa and GSH (initially 40 μM) loaded targeted liposomes (LD-GHS-0.7% MD-4% PEG/LUV) (n=3)

In Parkinson's disease treatment, each patient follows a specific medical treatment program according to degree of the disease. The drug doses are adjusted according to disability of the patient considering the ability to tolerate the medication [5]. In literature a study investigated the clinical effects of intravenously administered Levodopa at different doses on 125 patients. It is revealed that 600 ng/ml steady-state Levodopa concentration was well tolerated minimizing side effects [125]. At higher dose protocols (i.e. resulting in 2169 and 1200 ng/ml plasma concentration) the volunteers had unacceptably frequent side effects. The liposomal Levodopa formulations developed in this study have high Levodopa loading and *in vitro* Levodopa release profiles (Figures 3.17 and 3.18). However, these findings were obtained from *in vitro* conditions. The Levodopa concentration would be lower when

administered to body on a large scale in the same way the GSH concentration would also lower. In literature, a study investigated the plasma concentration of GSH on 148 patients in relation to sex and aging. The adult population between 18 and 73 years old had similar plasma GSH concentration; males had 3.47 ± 1.09 μM and females had 3.29 ± 0.98μM plasma GSH concentration [126].

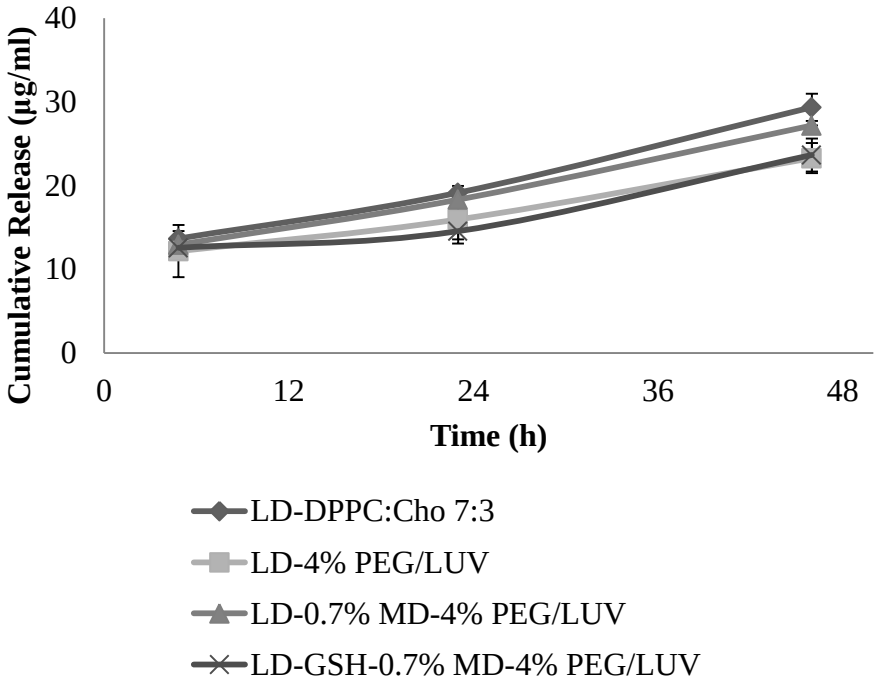

Figure 3.17. Comparison of *in vitro* cumulative Levodopa release (μg/ml) of conventional liposome (DPPC:Cho 7:3), stealth liposome (4% PEG/LUV), Levodopa loaded targeted liposome (LD-0.7% MD-4% PEG/LUV) and Levodopa and GSH (initially 40 μM) loaded targeted liposome (LD-GHS-0.7% MD-4% PEG/LUV) (n=3)

In literature, there is only one brain targeted Levodopa loaded liposomal study; i.e., chlorotoxin conjugated liposomes were studied for brain targeting [127]. In literature there is no maltodextrin conjugated liposomal formulation to compare the similarities or contrasts with this study. However, various carbohydrate ligands such as polysaccharides, lipo-polysaccharides, glycoproteins, and glycolipids were studied in

liposome targeting and immunization studies [128]. In brain drug targeting studies, various polysaccharides such as mannose [129-131], pullulan [132, 133], dextran [133], amylopectin [133] were conjugated to liposome surface for brain transport via receptor mediated endocytosis. Polysaccharide coated liposomes were revealed advantageous in targeting specific organs and cells with good physical and biochemical stability [128]. In this study maltodextrin conjugated Levodopa loaded liposomes had sustained drug release with increased bioavailability owing to neutral surface charge. The Levodopa and GSH loaded targeted liposomes also had sustained drug release profile with a small increase in cumulative amount of Levodopa release.

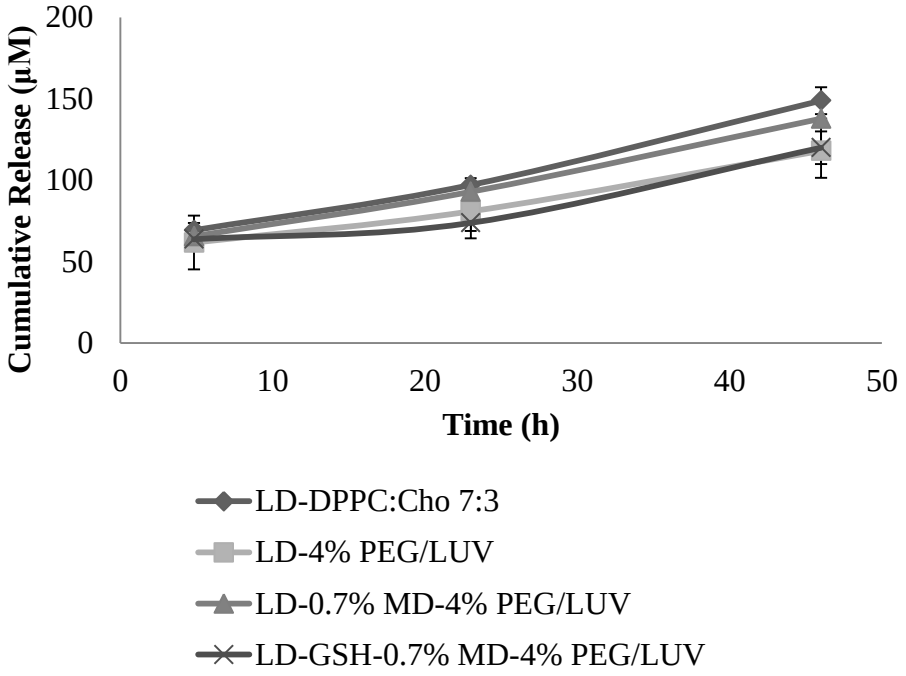

Figure 3.18. Comparison of *in vitro* cumulative Levodopa release (µM) of conventional liposome (DPPC:Cho 7:3), stealth liposome (4% PEG/LUV), Levodopa loaded targeted liposome (LD-0.7% MD-4% PEG/LUV) and Levodopa and GSH (initially 40 µM) loaded targeted liposome (LD-GHS-0.7% MD-4% PEG/LUV) (n=3)

3.4. Cell Culture Studies

Cell culture studies were done with both 3T3 and SH-SY5Y cells to evaluate the cytotoxicity of the liposomal formulations and the used drug concentrations on fibroblast and neuronal type cells. In literature 3T3 cell line is commonly used for *in vitro* cyctotoxicity experiments as a standard fibroblast cell line [171]. SH-SY5Y cell line is specifically used for *in vitro* brain cytotoxicity experiments as a model neuronal cell line with the similar biochemical characteristics to human dopaminergic neurons [172]. In cellular association studies MDCK cells were used to investigate cellular binding of the liposomal formulations. In literature MDCK cell line is commonly used for *in vitro* assays predicting *in vivo* characteristics of the BBB [173]. Figure 3.19 shows the micrograph of the 3T3 and SH-SY5Y cells at the beginning of the MTT assay and the micrograph of the MDCK cells at the beginning of the cellular association experiment. It is seen that the 3T3 cells has fibroblast-like, SH-SY5Y cells has neuron-like, and MDCK cells has epithelial-like morphology. The cells were viable and confluent to be able to perform the assay.

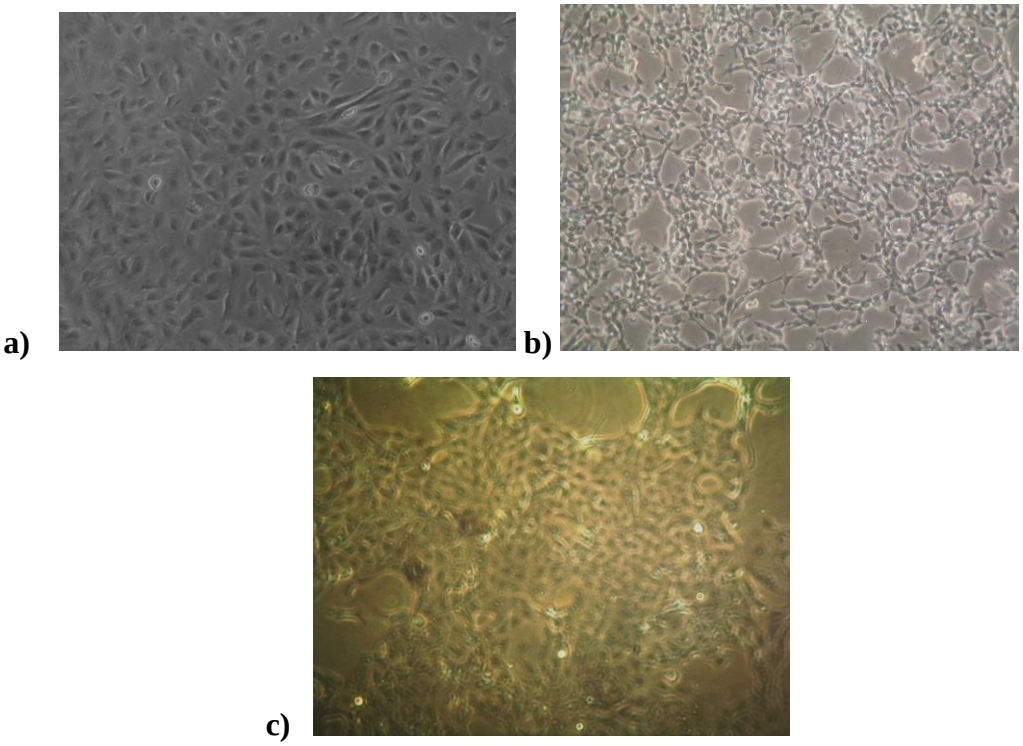

Figure 3.19. Phase contrast micrographs of **a)** 3T3 and **b)** SH-SY5Y **c)** MDCK cells (x20)

3.4.1. Cellular Toxicity of Pure Levodopa

At first, the cytotoxic effect of free Levodopa at concentrations (0, 20, 40, 60, 80, and 100 μM Levodopa) was tested on 3T3 and SH-SY5Y cell lines by MTT assay. In the second part of the experiment, the cells were incubated with different concentrations of Levodopa (0, 20, 40, 60, 80 and 100 μM Levodopa) together with 0.06 μM reduced glutathione (GSH) in order to observe the protective effect of this antioxidant. The cells were incubated with the drug solutions for 24 and 48 hours separately in order to evaluate the cytotoxicity for adjustment of the drug dosages in liposomal formulations.

Figure 3.20 and Figure 3.21 show relative viabilities of the 3T3 cells (with respect to control) after 24h and 48h treatment with Levodopa or Levodopa and GSH, respectively. The cells were less viable after 48h incubation compared to 24h incubation at all drug concentrations. Percent viability of 3T3 cells decreased as drug concentration increased. These findings suggest that increasing drug concentration and incubation time give rise to cellular toxicity. However, the cells were quite viable even after addition of the highest concentrated drug solution; after 24 and 48 hours incubation with 100 μM Levodopa, cellular viabilities of the 3T3 cells were 86.66 ± 3.70 % and 82.60 ± 5.35 %, respectively.

Cellular viability values were higher with addition of GSH than only Levodopa treated ones. After 24 and 48 hours incubation with 100 μM Levodopa and 0.06 μM GSH, cellular viabilities of the 3T3 cells were 94.70 ± 5.09 % and 93.14 ± 2.81 %, respectively. Addition of antioxidant had a protective effect on cells by reducing the cytotoxic effect of the drug solution and thus, increased cellular viabilities considerably.

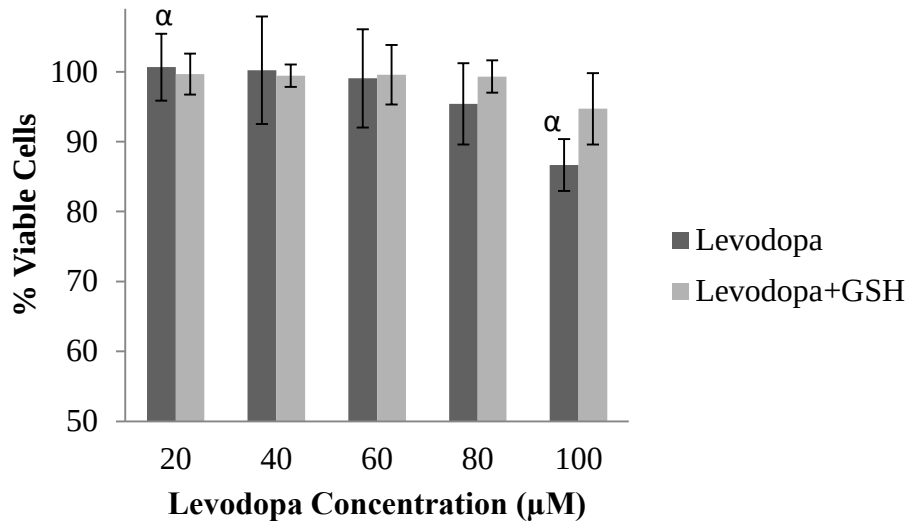

Figure 3.20. Cellular Viability of 3T3 cells after 24h treatment with Levodopa (at different concentrations) or Levodopa and GSH (0.06 µM) (n=3)

α: statistically significant difference between different dosage groups ($p<0.05$)

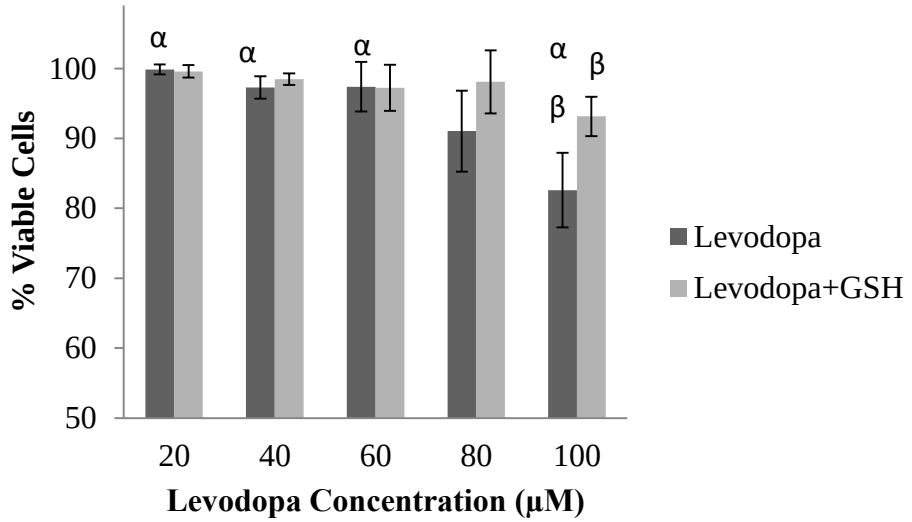

Figure 3.21. Cellular viability of 3T3 cells after 48h treatment with Levodopa (at different concentrations) or Levodopa and GSH (0.06 µM) (n=3)

α: statistically significant difference between 100 µM Levodopa and other groups

β: statistically significant difference between 100 µM Levodopa and 100 µM Levodopa and GSH ($p<0.05$)

Figures 3.22 and 3.23 show relative viabilities of SH-SY5Y cells (with respect to control) after 24h and 48h treatment with Levodopa or Levodopa and GSH, respectively. Viabilities of the cells decreased with increasing time of incubation. Viabilities of the SH-SY5Y cells after 24 and 48h incubation with the highest drug concentration (100 μM Levodopa) were 92.71 ± 2.69% and 85.84 ± 3.93%, respectively. However, viability values increased with addition of GSH; after 24 and 48 hours incubation with 100 μM Levodopa and 0.06 μM GSH, they were 99.82 ± 2.58% and 92.85 ± 1.27%, respectively. Addition of GSH increased viabilities of SH-SY5Y cells for both incubation periods.

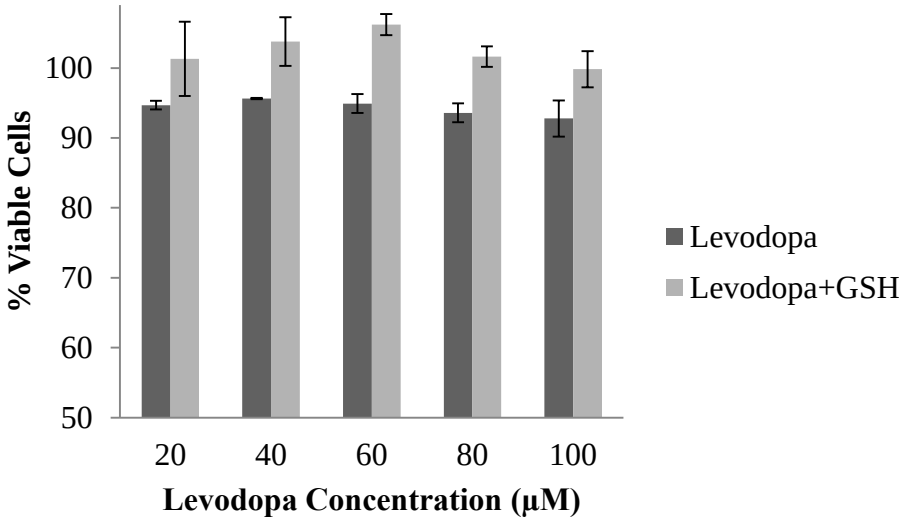

Figure 3.22. Cellular viability of the SH-SY5Y cells after 24h treatment with Levodopa (at different concentrations) or Levodopa and GSH (0.06 μM) (n=3)

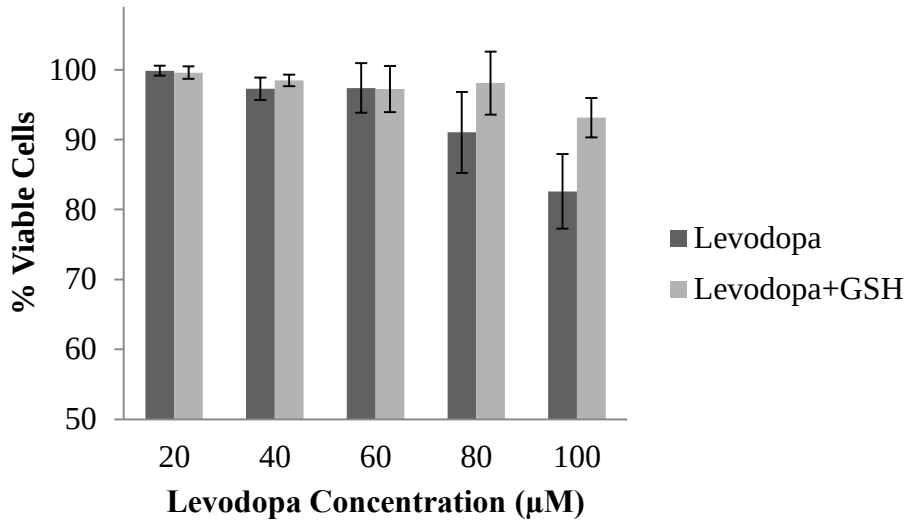

Figure 3.23. Cellular viability of SH-SY5Y cells after 48h treatment with Levodopa (at different concentrations) or Levodopa and GSH (0.06 µM) (n=3)

In vitro drug cytotoxicity experiments revealed that cellular viabilities of the 3T3 and SH-SY5Y cells decreased with increasing treatment time and Levodopa concentration in agreement with literature [134, 135]. The decrease in cellular viability at high Levodopa concentrations was due to auto-oxidation of the cells by quinone formation [136]. However, the cellular toxicity of Levodopa is considered to be moderate up to 100 µM [135]. The results of this study were parallel with the literature; both cell lines were quite viable at all drug concentrations for both 24h and 48h incubations.

The effect of antioxidant addition to the drug solution on both cell lines was also investigated in the current study. Antioxidant addition resulted with higher cellular viability. In literature it is reported that oxidative stress is one of the most important reasons of cell death leading to apoptosis and necrosis [137]. The antioxidants were shown to protect cells from Levodopa toxicity *in vitro* [138]. The antioxidants prevent oxidative reactions either by preventing the formation of oxidative reactive species or by removing them before they can damage the vital components of the cells [139]. GSH is the major endogenous antioxidant readily produced by the cells, having role in neutralization of free radicals and reactive oxygen compounds and maintaining exogenous antioxidants such as vitamin C and E in their active forms

[139]. GSH protects cells from oxidation as reducing agent with the thiol group in its cysteine moiety leading to increase in cell viability [140]. In this study the cellular viabilities of the both cell lines considerably increased after addition of the GSH to Levodopa.

3.4.2. Cellular Toxicity of Levodopa Loaded Liposomes

3T3 and SH-SY5Y cells were incubated with empty and Levodopa loaded liposomes for 24 and 48h separately in order to observe the cytotoxic effects of the liposomal formulations. Liposomes were diluted to yield 100 μM Levodopa or 100 μM Levodopa and 0.06 μM GSH concentrations in each experimental group owing to good cellular viabilities at these concentrations (Section 3.5.1). The empty liposomes were diluted in order to obtain an equivalent lipid concentration of loaded liposomes.

Figure 3.24 and 3.25 show the cellular viability of 3T3 and SH-SY5Y cells incubated with liposomes, respectively after 24h and 48h incubations. A numerical decrease in the viability of both cell lines was observed upon 48 hours of incubations for all liposomal formulations. 3T3 cells had slightly higher viability when incubated with empty liposomes than loaded liposomes at the same incubation periods. This suggests that release of the drug had some negative effect on the viability of these cells as empty and loaded liposomes had equivalent lipid concentration. Yet, all the viability values were above 90% suggesting very low level of toxicity. On the other hand, SH-SY5Y cells had similar cellular viability for empty and loaded liposomes at the same incubation periods.

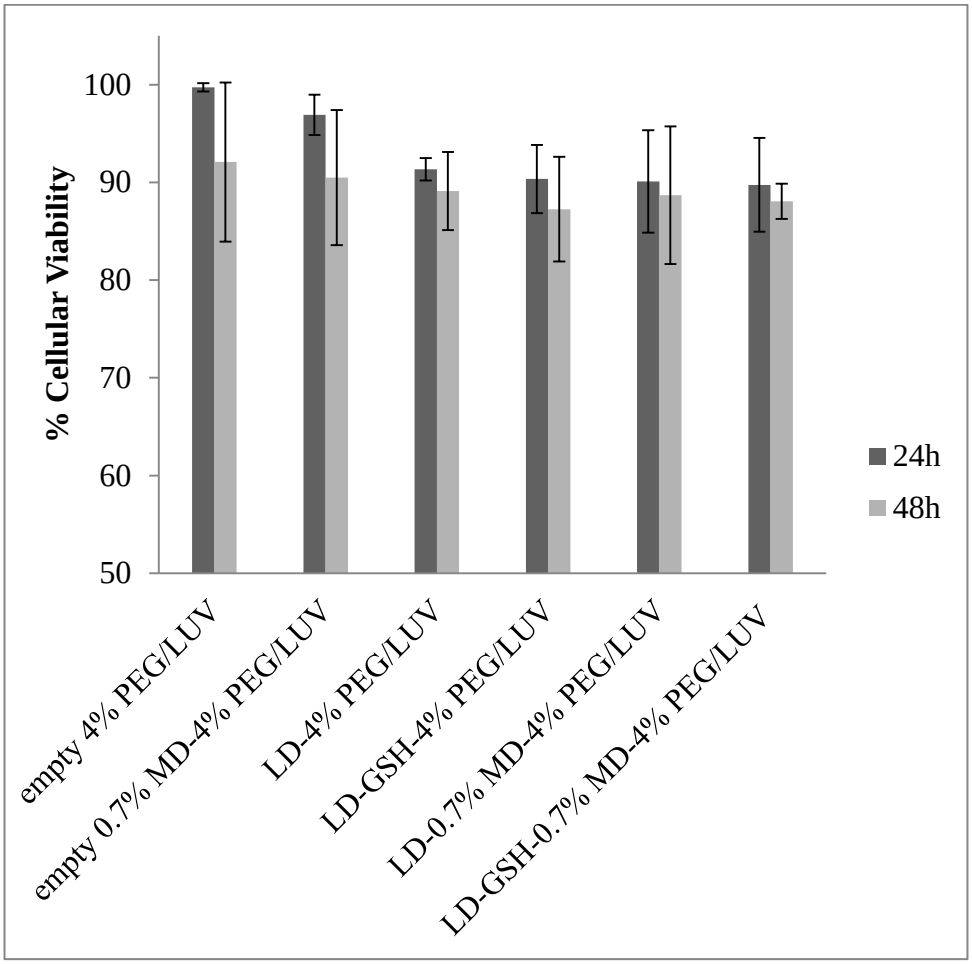

Figure 3.24. Cellular viability of 3T3 cells after 24h and 48h treatment with liposomes (n=3)

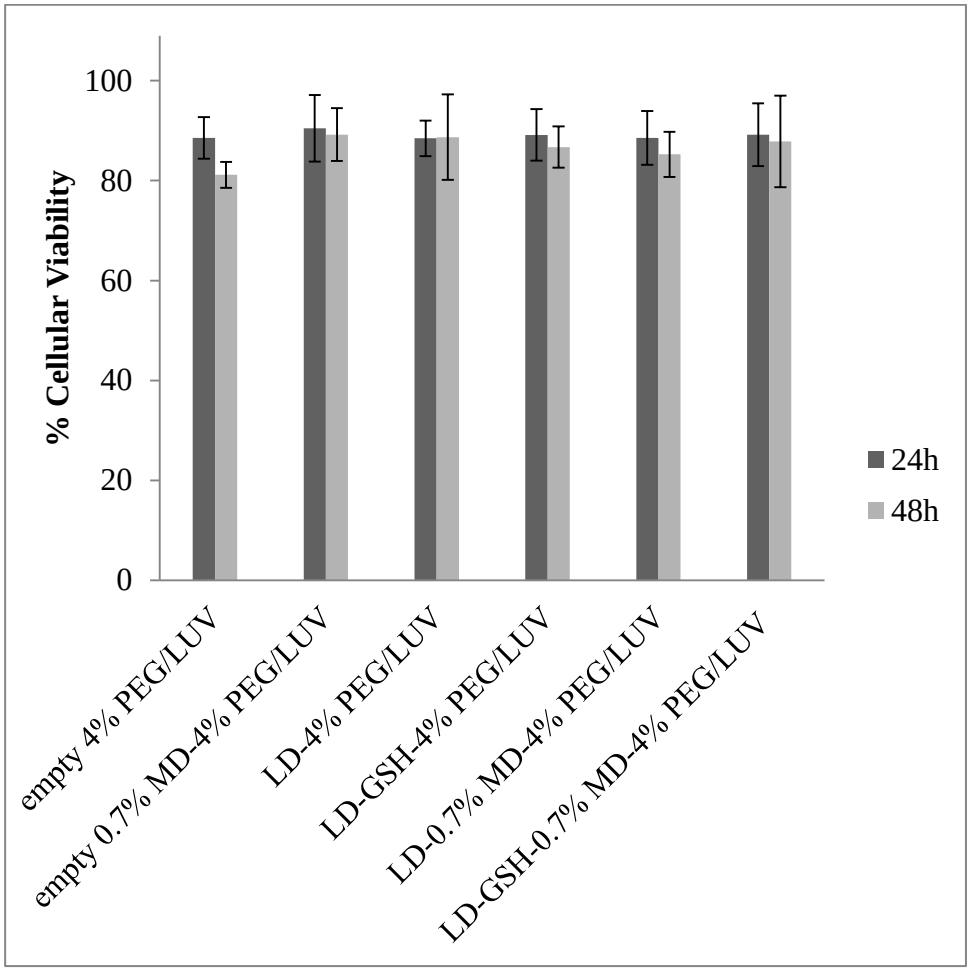

Figure 3.25. Cellular viability of the SH-SY5Y cells after 24h and 48h treatment with liposomes (n=3)

In vitro cytotoxicity experiments revealed that the cellular viabilities of the 3T3 and SH-SY5Y cells decreased with time and concentration. Cellular viability values of the SH-SY5Y cells were slightly lower than 3T3 cells for the same liposome groups at the same incubation period. The less viability of human neuroblastoma (SH-SY5Y) cells was also observed in other studies due to sensitivity of this cell line to oxidative stress leading to simultaneous apoptotic and necrotic cell death [141-143]. However, percent viabilities of both cell lines were quite high for all liposomal groups; after 48h incubation, viability of 3T3 and SH-SY5Y cells were higher than 87% and 81%, respectively. After 48h treatment, empty and loaded liposomes showed similar toxicity on the same cell lines. This reveals that cytotoxic effect of the drug was lowered when encapsulated inside liposomes.

Drug loaded and drug and antioxidant loaded liposomes had similar cytotoxicity on the same cell lines at the same incubation periods. Protective effect of the antioxidant on cells was not clearly observed in this experiment due to controlled release of GSH from liposomes as compared to high concentration in free form (Section 3.5.1). Therefore, the amount of released GSH was not very high (26% and 51% cumulative GSH release respectively after 24 and 48 hours incubations). However, the cells were quite viable even after 48h incubation with liposomes; after 48h, cellular viabilities of both 3T3 and SH-SY5Y cells were higher than 85%. In literature 85 % *in vitro* viability was reported safe for *in vivo* studies [144].

3.5. *In vitro* Blood-Brain Barrier Transport Studies of Liposomal Formulations

Localized and controlled drug delivery to the diseased site is desired to increase treatment efficiency via increased drug bioavailability and decreased drug side effects in the other tissues [41]. In brain drug delivery, Blood-brain barrier (BBB) is the most important challenge that should be overcome. Most of the neurotherapeutics used to treat neurodegenerative diseases cannot get into brain due to the BBB [27]. The pharmacological formulations are reformulated to be transported into the brain via one of the endogenous BBB transport systems as explained in Section 1.2.2.

Drugs are packaged into nanocarriers and their surfaces are modified by conjugation of the BBB selective biomolecules [30]. Liposomes are suitable carrier systems for brain drug delivery with their lipophilic nature, adjustable size and suitability to surface modifications [82].

In this study, maltodextrin conjugation approach was used for targeting liposomes to brain for the treatment of Parkinson's disease. Maltodextrin conjugated liposomes were designed to be delivered to brain via receptor mediated endocytosis due to brain's high energy demand. The liposomes were loaded either with drug (i.e. Levodopa) alone or with drug and antioxidant (i.e. GSH) together. Their size was optimized to increase their bioavailability and brain delivery. They were produced in sizes ranging between 100-150 nm as in the case of untargeted liposomes. In literature, brain targeted liposomes were recommended to be prepared by extrusion through polycarbonate membranes with a final pore size of 100 nm [145] as performed in this study. Here, the number of passes through the extruder system was optimized to have the liposomes between 100 and 150 nm size.

Liposomal formulations were tested for blood-brain barrier (BBB) transport efficiency using Parallel Artificial Membrane Permeability Assay (PAMPA-BBB). PAMPA is an *in vitro* passive transport model used to measure transcellular permeability. In PAMPA-BBB model, the artificial membranes composed of mixture of phospholipids with a net negative charge mimicking the properties of the brain lipid membranes were placed between donor and acceptor compartments.

Levodopa solutions and liposomal formulations were tested for BBB permeability for 48 hours in PAMPA-BBB studies. The liposomes and drug solutions were diluted in order to obtain an equivalent drug concentration. Figure 3.26 shows representative picture of the PAMPA-BBB system after 6 hours incubation with drug and liposome solutions. Here, it was recognized that the drug degraded quickly in aqueous solutions (dark colored wells in Figure 3.26) due to oxidation and temperature whereas it was stable in all liposome formulations (light colored wells). This reflects that encapsulation of the drug into liposomes increase their bioavailability with

increased stability. In literature, Levodopa was stated unstable in aqueous environment with low half-life [146].

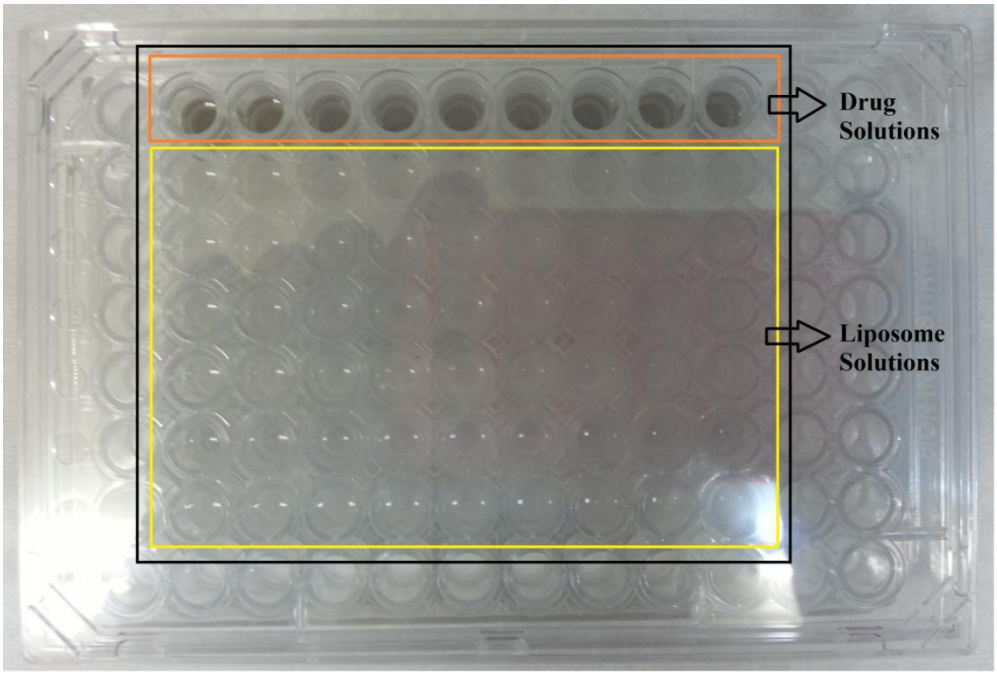

Figure 3.26. Representative picture of the PAMPA-BBB model after 6 hours of incubation with drug and drug loaded liposome formulations

Figure 3.27 shows the percent drug permeability results of PAMPA-BBB model. No significant difference was observed after 6 and 9 hours incubations ($p<0.05$). After 24 hours incubation, the most significant differences were observed between drug solution and LD-GSH-4%PEG/LUV and between drug solution and LD-0.35% MD-4% PEG/LUV ($p=0.001$). After 24 hours, drug solution, LD-GSH-4% PEG/LUV, and LD-0.35% MD-4% PEG/LUV had 5.25 ± 1.05%, 8.67 ± 0.28%, and 8.74 ± 2.22% drug delivery, respectively. After 48 hours, the most significant difference was observed between LD-4% PEG/LUV and LD-GSH-0.7% MD-4% PEG/LUV ($p=0.001$). After 48 hours, LD-4% PEG/LUV and LD-GSH-0.7% MD-4% PEG/LUV had 12.10 ± 0.18% and 17.89 ± 0.28% drug delivery, respectively.

The cumulative amount of drug passed through the model barrier increased with time for all experimental groups; after 6 hours incubation, the total amount of drug passage ranged between 2% and 4%, whereas after 48 hours incubation it ranged between 12% and 18%. After 24 and 48 hours incubations, the targeted liposomal formulations (i.e. 0.35% MD-4% PEG/LUV and 0.7% MD-4% PEG/LUV) had higher amounts of drug passage than drug solution.This reveals that incorporation of drug into liposomes not only increases the bioavailability of the drug but also enhances the passage of the drug through the BBB.

At each incubation time point, drug and antioxidant loaded liposomes had higher amounts of drug delivery than only drug loaded liposomes revealing that addition of antioxidant (i.e. GSH) increased the stability of the drug (i.e. Levodopa). After 48 hours incubation, drug and antioxidant loaded liposomal formulations, LD-GSH-0.7% MD-4% PEG/LUV, LD-GSH-0.35% MD-4% PEG/LUV and LD-GSH-0.7% MD-4% PEG/LUV had 12.85 ± 0.28%, 14.44 ± 0.15%, and 17.89 ± 0.28% drug passage, respectively. These data suggest that addition of the maltodextrin (targeting molecule) and increased maltodextrin ratio slightly enhanced the BBB penetration of the liposomes. This result is partially supporting the aim of the study, i.e., maltodextrin conjugated liposomes were designed for enhancing the brain drug delivery.

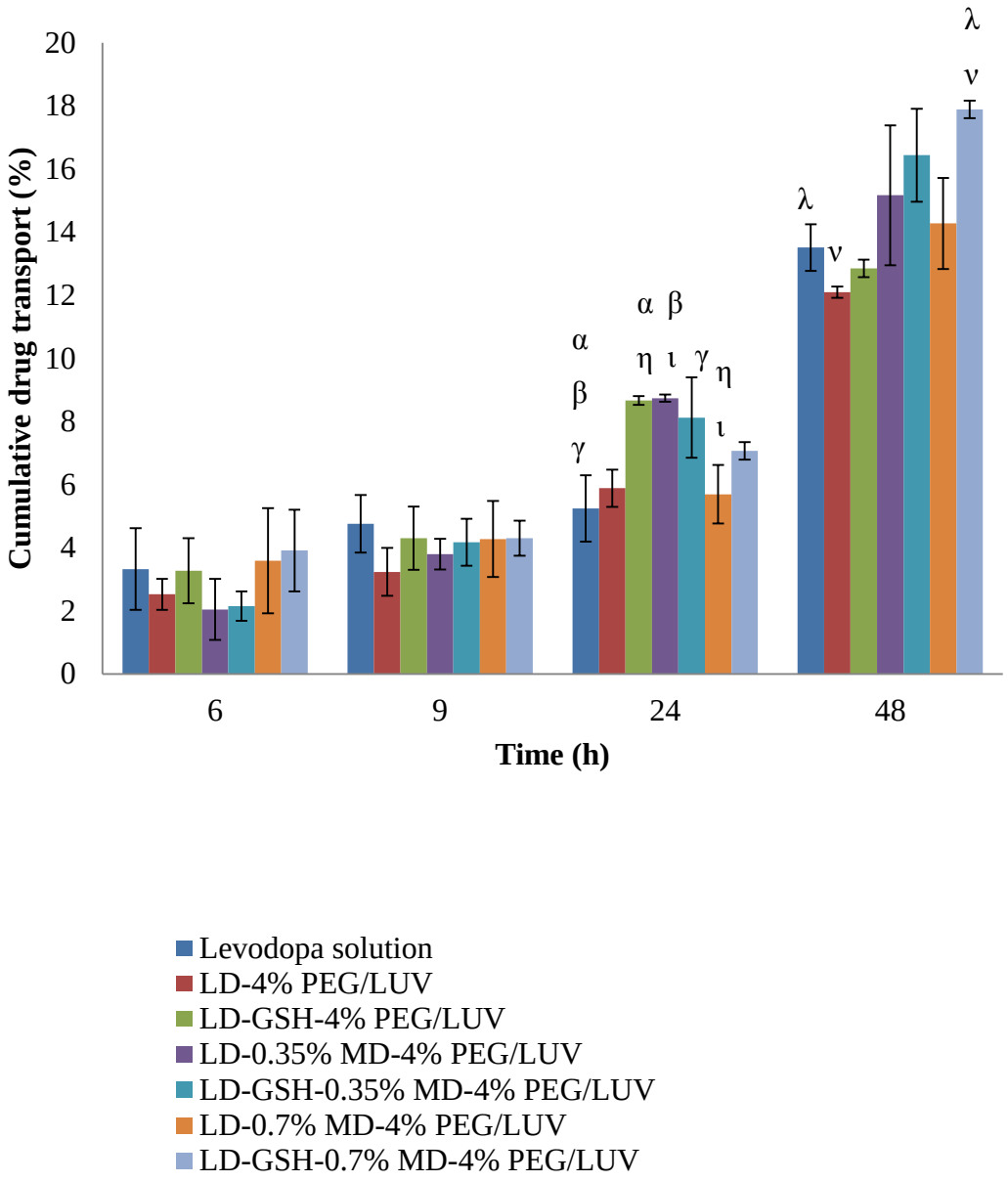

Figure 3.27. Comparison of *in vitro* passive transport of Levodopa solution and Levodopa loaded liposomal formulations through the PAMPA-BBB model (n=3)

α, β, γ, η, ι: statistically significant differences between different experimental groups after 24 hours incubation ($p<0.05$)

λ, ν: statistically significant differences between different experimental groups after 48 hours incubation ($p<0.05$)

At the end of the experiment, the liposomes at the donor wells were analyzed for phospholipid content in order to determine the liposome transport through the PAMPA-BBB system. The cumulative phospholipid delivery of the liposomal formulations after 48 hours incubation is shown in Figure 3.28. After 48 hours incubation, the most significant difference was observed between LD-4%PEG/LUV and LD-GSH-0.7% MD-4% PEG/LUV ($p=0.001$). This result might suggest that both use of GSH and maltodextrin increased liposome transport probably owing to their effect on increasing stability of the liposome formulation.

All of the liposomal formulations passed through the membrane; however the percentage of the cumulative phospholipid passage was lowest in LD-4% PEG/LUV formulation. At the beginning of the experiment and after 48 hours incubation, the donor wells were tested for percent drug loading as described in Section 2.2.6.4. Comparison of percentage of drug passage and lipid passage are listed in Table 3.9. After 48 hours incubation, the liposomal formulation LD-GSH-0.7% MD-4% PEG/LUV had cumulative drug and phospholipid delivery 17.89 ± 0.28% and 7.08 ± 0.35%, respectively. The transport of the drug in liposomes is desirable to preserve bioactivity and to increase bioavailability of the drug since it has very low plasma half-life (i.e. 0.75-1.50 hours) [148].

Table 3.9. Comparison of percent drug and lipid passage and lipid passage after 48h

Liposome	**%drug passed**	**%lipid passed**
LD-4% PEG/LUV	12.10 ± 0.18	5.11± 0.70
LD-GSH-4% PEG/LUV	12.85 ± 0.28	6.41 ± 0.36
LD-0.35% MD-4% PEG/LUV	15.17 ± 2.22	5.73 ± 0.38
LD-GSH-0.35% MD-4% PEG/LUV	16.44 ± 1.48	6.61 ± 0.36
LD-0.7% MD-4% PEG/LUV	14.28 ± 1.44	6.53 ± 0.35
LD-GSH-0.7% MD-4% PEG/LUV	17.89 ± 0.28	7.08 ± 0.36

In accordance with the Levodopa transport (Figures 3.27), Figure 3.28 also revealed that phospholipid delivery through the membrane increased with the addition the GSH revealing that addition of the antioxidant increased the bioavailability of the both drug and the phospholipid by protecting them from oxidation.

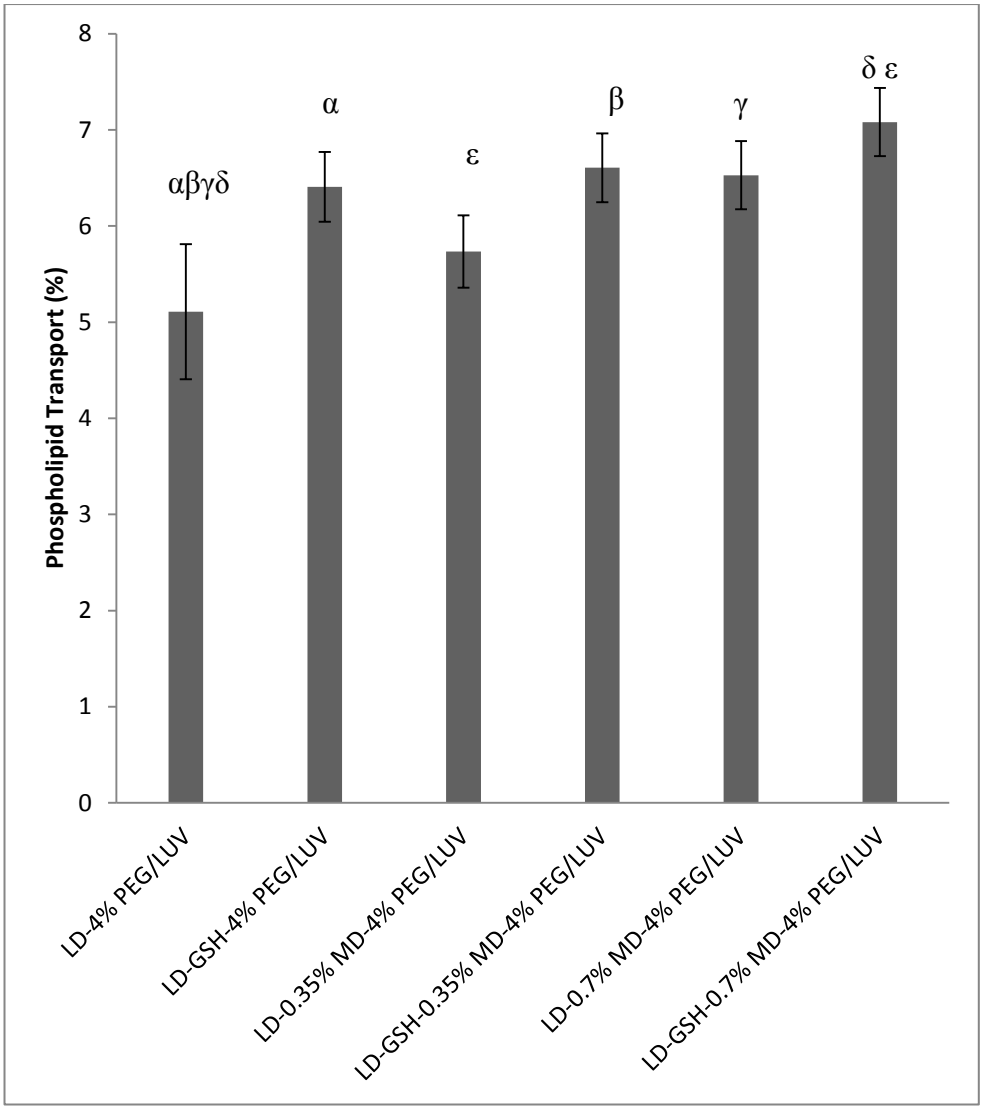

Figure 3.28. Comparison of *in vitro* passive phospholipid transport of the loaded liposomes through the PAMPA-BBB model after 48 hours incubation (n=3)

α, β, γ, δ, ε: statistically significant differences between different experimental groups after 48 hours incubation ($p<0.05$)

The PAMPA-BBB permeability assay is widely used in the pharmaceutical industry to determine BBB permeability [173]. The PAMPA-BBB model has many advantages over cellular models. Although the PAMPA-BBB is an *in vitro* passive transport model, it can predict the active BBB permeability with its well-adjusted biomimetic *in vitro-in vivo* correlation [147]. The PAMPA-BBB system is designed considering the specific parameters such as the lipid, pH, and chemical composition in order to mimic active BBB transport kinetics [147].

In literature there is no study experimenting the passive transport of the liposomes with the PAMPA-BBB model to compare the results of this study. However, the results were similar with the active transport studies conducted with *in vitro* cellular models. A study revealed that nerve growth factor (i.e. NGF) loaded PEGylated and brain targeted liposomes had higher NGF penetration on an *in vitro* BBB model composed of brain microvascular endothelial cells (i.e. BMVEC) during 20 hours incubation. After 6 and 9 hours incubations, targeted liposomes had 3 and 4.5% NGF permeability, respectively [149]. These similar findings suggest that the PAMPA-BBB model is successful in determining *in vitro* liposomal BBB permeability. Yet, it is not expected to differentiate the targeting ability of the maltodextrin conjugated liposomal formulation over untargeted groups. This is because of the fact that the targeting with maltodextrin involves special transporter molecules on membrane of endothelial cells of the BBB. Hence, the targeted group is prospected to have higher permeability in *in vivo* condition.

3.6. Cellular Association of Liposomes

In cellular association studies, the fluorescently labeled liposomes were prepared with Lissamine-Rhodamine containing phospholipid in order to visualize the liposome-cell interaction via fluorescence imaging. The MDCK cells were treated with the fluorescently labeled PEGylated and targeted liposomes for 3 and 6 hours in order to observe the cellular binding of the liposomes with respect to time. Figure 3.29 and 3.30 show the laser scanning confocal microscopy (LSCM) images of the liposomal formulations after 3 and 6 hours incubations, respectively. These LSCM

images are merged images of the fluorescence and transmission images where the brightness and contrast of the images were optimized for visualization. The negative control groups showed no fluorescence signal as they were untreated MDCK cells (Figure 3.29, a and Figure 3.30, a). The LSCM images of the cells treated with the fluorescently labeled liposomal formulations (Figure 3.29, b-c and Figure 3.30, b-c) revealed that after 6 hours incubation higher amounts of liposomes were localized around the cells. The targeted liposomes (i.e. 0.7% MD-4% PEG/LUV) had more homogenous cellular binding throughout the cell population when compared with the untargeted PEGylated liposomes (i.e. 4% PEG/LUV).

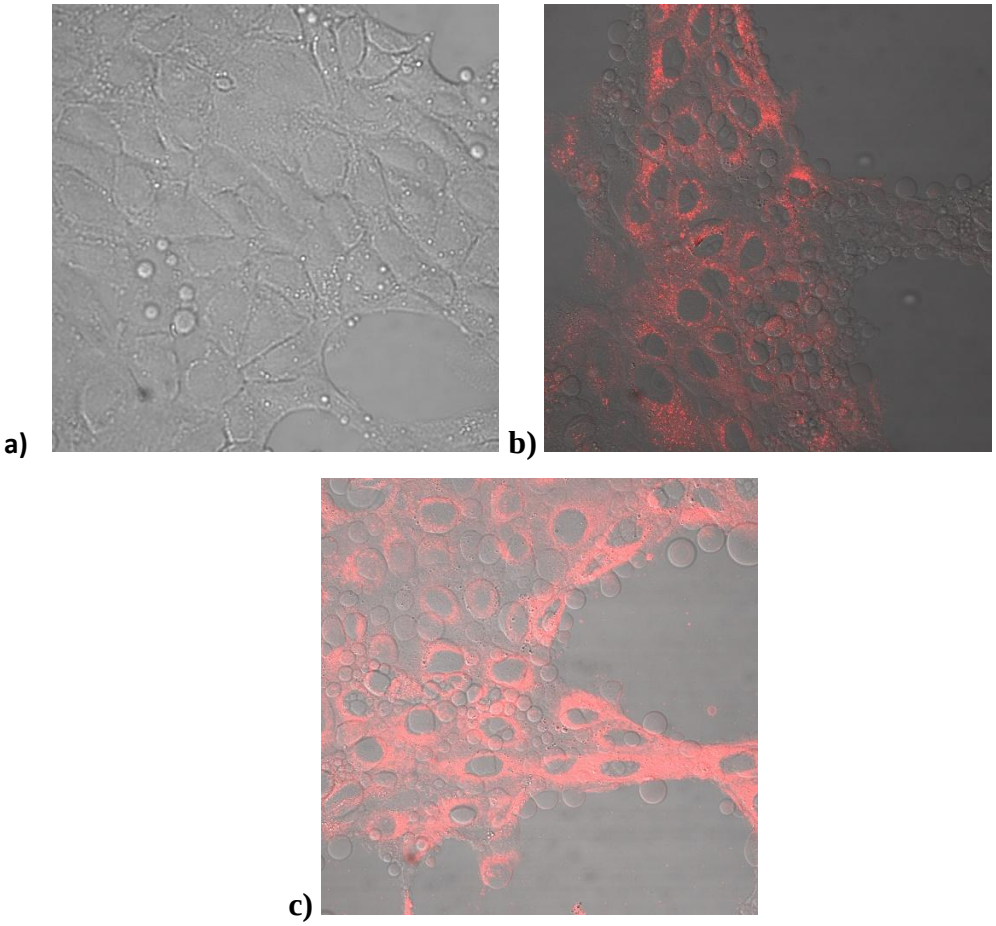

Figure 3.29. Laser Scanning Confocal Microscopy (LSCM) images of the MDCK cells associated with **a)** Negative control group **b)** Rhodamine labeled untargeted PEGylated liposome (4% PEG/LUV) **c)** Rhodamine labeled targeted liposome (0.7% MD-4% PEG/LUV) after 3 hours treatment (x40)

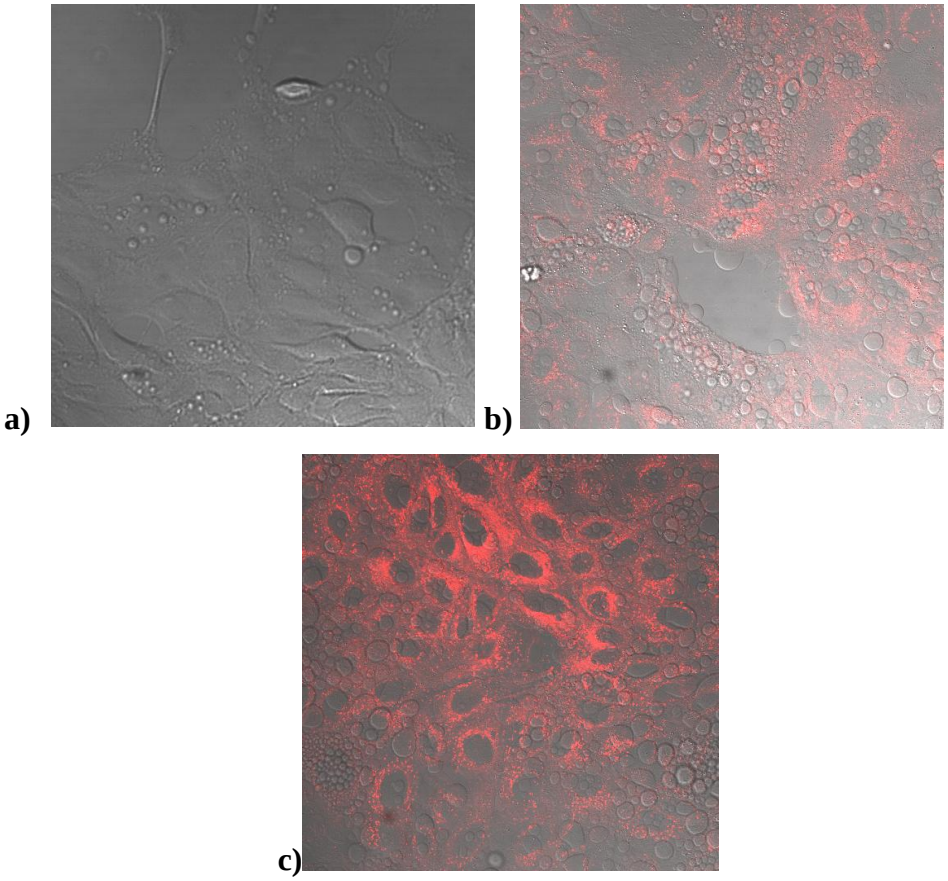

Figure 3.30. Laser Scanning Confocal Microscopy (LSCM) images of the MDCK cells associated with **a)** Negative control group **b)** Rhodamine labeled untargeted PEGylated liposome (4% PEG/LUV) **c)** Rhodamine labeled targeted liposome (0.7% MD-4% PEG/LUV) after 6 hours treatment (x40)

Figure 3.31 shows comparison of the corrected florescence intensity values due to fluorescently labeled liposomal formulations' binding to the MDCK cells with respect to time. The fluorescence intensity values due to liposome-cell binding were calculated as described in Section 2.2.8.4 using the images shown in Figure 3.29 and 3.30. Surface binding of the each liposomal formulation increased from 3 hours to 6 hours. There is a statistically significant difference for each liposomal formulations between 3 and 6 hours incubation ($p<0.05$). At each incubation period, targeted liposomes had higher cellular association yielding more fluorescence intensity around the cells. After 6 hours incubation, a statistically significant difference was

obtained between untargeted and targeted liposomal formulations. This reveals that targeted liposomal formulation (i.e. 0.7% MD-4% PEG/LUV) had higher cellular association when compared with untargeted one (i.e. 4% PEG/LUV). The result is convenient with the aim of the study; in this study brain targeted liposomal formulations were designed for brain drug delivery via receptor-mediated endocytosis. The maltodextrin conjugated targeted liposomes were aimed to binding to sugar receptors of the brain's endothelial cells and internalized.

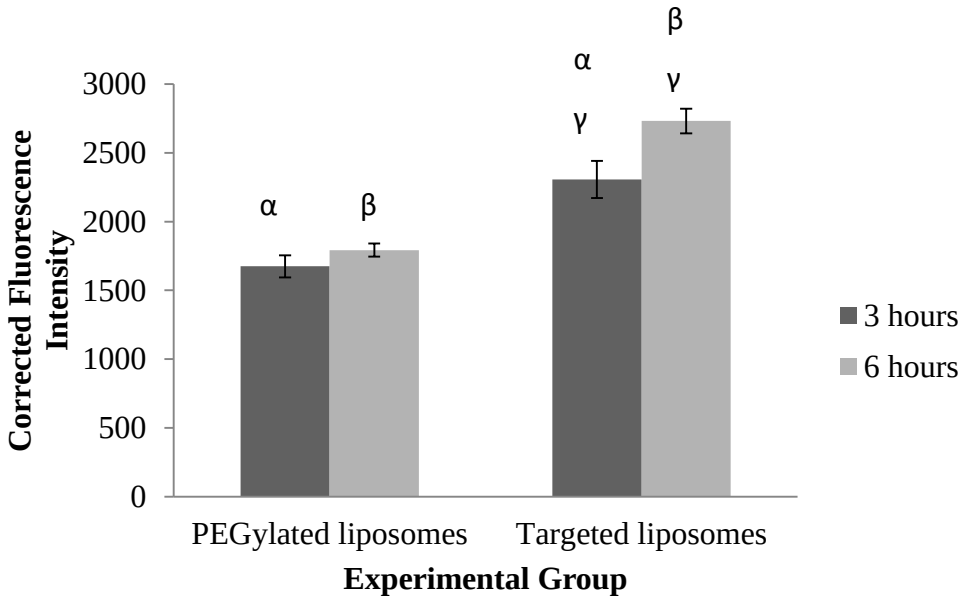

Figure 3.31. Corrected fluorescencence intensity of the MDCK cells after 3 and 6 hours treatment with untargeted (4% PEG/LUV) and targeted (0.7% MD-4% PEG/LUV) liposomal formulations (n=3)

α, β, γ: statistically significant difference between different experimental groups ($p<0.05$)

In literature various studies examined the MDCK cells in construction of *in vitro* Blood-Brain Barrier (BBB) model for BBB transport studies [150-154]. The MDCK cells are preferred for mimicking the anatomical structure of the BBB expressing tight junction proteins Clausin-1,4 and occudine, which are important to form restrictive paracellular barrier with tight junctions [155, 156]. In this study MDCK cells were preferred since they have sugar receptors in addition to BBB mimicking nature. Various studies revealed that MDCK cell line have specific Pglycoprotein receptors for glucose [89], galectin [90], and also for oligosaccharides [156]. Therefore, maltodextrin conjugated liposomes had good cellular binding to the MDCK cells. The targeted liposomal formulation 0.7% MD-4% PEG/LUV is promising for brain drug delivery via the receptor-mediated endocytosis.

3.7. Stability Studies of Liposomal Formulations

Stability is a crucial parameter not only for long circulation time in bloodstream but also for the long shelf life of the liposomes. Physical and chemical properties of the liposomes change particularly due to oxidation and hydrolysis. In this study liposomes were stored under nitrogen atmosphere as it is recommended to avoid air oxidation by creating an inert atmosphere [157]. Use of saturated phospholipids and addition of antioxidant were also reported to improve the stability of liposomes [158]. Here, a saturated phospholipid (i.e. DPPC) was used in liposomes for increasing blood stability. Besides that an antioxidant (i.e. glutathione, GSH) was used to increase Levodopa stability and treatment efficacy. These two molecules were also thought to bring stability during storage of the liposomes.

The final liposomal formulation, Levodopa and GSH loaded targeted liposome (LD-GSH-0.7% MD-4% PEG/LUV) was tested for physical and chemical stability. Freshly prepared liposomes were stored at 4^{o}C and at 25^{o}C for 6 months in aqueous form. Particle size distribution and zeta potential analysis of the liposomes were carried out monthly in order to evaluate their stability.

Average particle size of the liposomes increased with time (Table 3.10). Particle size of the liposomes stored at 4^{o}C slightly increased in the first 5 months. The sharp increase in average size and PdI reflects the aggregation of the liposomes at 4^{o}C after 5th month. On the other hand, particle size and PdI values of the liposomes stored at 25^{o}C increased faster starting from an earlier time (at 1st week). The continuous and rapid increase in size and PdI of the liposomes at 25^{o}C reflects faster destabilization of the liposomes at room temperature.

Initially, the liposomes had nearly neutral surface charge (i.e. -0.46 mV) since they were composed of neutral lipids and neutral maltodextrin molecules attached to the surface of the liposomes. However, the zeta potential values showed decreasing trend in time. The liposomes stored at 4^{o}C and 25^{o}C had similar zeta potential values at the same time points. The decrease in the zeta potential values observed with time reflects the instability of the liposomes in time. It is reported that negatively charged liposomes have lower *in vivo* half-lives and they are rapidly removed from the bloodstream [159].

Table 3.10. The particle size distribution and zeta potential values of the liposomes stored at 4^{o}C and 25^{o}C for 6 months

Month	**Liposomes at 4^{o}C**			**Liposomes at 25^{o}C**		
	z-average (nm)	**PdI**	**Zeta Potential (mV)**	**z-average (nm)**	**PdI**	**Zeta Potential (mV)**
0	128.9	0.070	-0.46	128.9	0.070	-0.46
1	126.4	0.064	-4.79	142.4	0.116	-3.79
2	125.8	0.058	-8.87	158.1	0.127	-8.51
3	139.2	0.076	-17.60	160.2	0.148	-16.00
4	131.0	0.101	-27.10	161.6	0.164	-19.60
5	138.2	0.126	-29.20	159.2	0.171	-21.80
6	155.6	0.158	-34.4	182.0	0.175	-24.70

It is reported that in aqueous dispersions instability of the liposomes is due to aggregation and fusion of the liposomes [157, 158]. Particle size distribution of the liposomes is affected by attractive Vander Walls forces and repulsive electrostatic forces between colloidal particles. Liposomes tend to form large vesicles by attractive Vander Walls forces [157, 158]. PdI values of the liposomes indicate heterogeneity of the size distribution. The particles with PdI lower than 0.05 are called as monodisperse and with PdI between 0.05 and 0.08 are called as nearly monodisperse. The liposomes were initially monodisperse (PdI = 0.07). The decrease in PdI values indicates instability of the liposomes due to aggregation, fusion or precipitation.

The liposomes stored at 25^{o}C were less stable than the liposomes stored at 4^{o}C as they tend to aggregate more. Therefore, the liposomes should be stored at 4^{o}C in order to increase their shelf lives. They should be consumed within 5 months after production since they have better stability until 5th month having desired particle distribution. However, unlike size distribution results, zeta potentials indicated that stability is not preserved at 4^{o}C for a month period. The liposomes at 4^{o}C were tested for drug release after 6 months incubation. It is found that the liposomes released only 15.6% of the initially encapsulated drug, revealing that most of the drug remained in the liposomes. This concludes that the liposomes are quite stable at 4^{o}C after 6 months with good particle size distribution and drug encapsulation efficiency.

CHAPTER 4

CONCLUSION

The aim of this study was to design a brain targeted liposomal Levodopa delivery system to increase drug bioavailability and to maintain the required plasma level for a long time. The liposomes were prepared at different temperatures with different lipid compositions at the initial optimization studies. The liposomes were PEGylated in order to increase the bioavailability of the liposomes by reducing the reticuloendothelial uptake and macrophage encapture. The brain targeted liposomes were prepared with conjugation of maltodextrin to the long chain PEG molecule. The optimized targeted liposomes were later loaded with both Levodopa and GSH. Antioxidant was incorporated to improve liposome stability and drug bioavailability.

Size and surface charge of the liposomes were modified and optimized to increase the bioavailability and effectiveness of the liposomes. The liposomes were produced in sizes to be administrated intravenously in order to bypass gastrointestinal system.

In cell culture studies, toxicity of the liposomes on the 3T3 and SH-SY5Y cell lines was found low. Among all experimental groups, the developed and optimized dual loaded targeted liposomal formulation was found the optimum for Levodopa brain delivery system with the slowest *in vitro* Levodopa release, highest Levodopa passage through the PAMPA-BBB and highest binding to MDCK cells via receptor mediated association. This formulation also had good stability preserving size distribution and drug encapsulation efficiency when stored at 4^{o}C for 6 months.

These data suggest that designed liposomal system is promising in brain drug delivery with controlled and sustained drug release property, low cellular cytotoxicity, good BBB Levodopa delivery, good cellular binding, and good stability. This brain targeted liposomal delivery system will bring a novel approach for the delivery of Levodopa in brain with decreased drug side effects.

REFERENCES

[1] Davie, C. A. (2008). A review of Parkinson's disease. British medical bulletin, 86(1), 109-127.

[2] Levy, O. A., Malagelada, C., Greene, L. A. (2009). Cell death pathways in parkinson's disease: proximal triggers, distal effectors, and final steps. Apoptosis, 14(4), 478-500.

[3] Pahwa, R., Lyons, K., Koller, W.C., & Jankovic, J. (2007) Pathophysiology and assessment of parkinsonian symptoms and signs. In Pahwa, R., Lyons, K., Koller, W.C. (Ed.), Handbook of Parkinson's disease (pp. 79-104). New York: Taylor and Francis Group, LLC.

[4] Gelb, D. J., Oliver, E., & Gilman, S. (1999). Diagnostic criteria for Parkinson disease. Arch Neurol., 56(1), 33-39.

[5] Schapira, A. H. (2009). Neurobiology and treatment of Parkinson's disease. Trends Pharmacol Sci., 30(1), 41-47.

[6] Hasnain, M., Vieweg, W.V., Baron, M.S., Beatty-Brooks, M., Fernandez, A., & Pandurangi, A. K. (2009). Pharmacological management of psychosis in elderly patients with parkinsonism. Am. J. Med., 122 (7), 614-622.

[7] Singh, N., Pillay, V., & Choonara, Y.E. (2007). Advances in the treatment of Parkinson's disease. Progress in Neurobiology. 81(1), 29-44.

[8] Fan, S. (2008). The history of dopamine and Levodopa in the treatment of Parkinson's disease. Mov. Disord., 23 (3), 497–508.

[9] Wu, S. S., Frucht, S. J. (2005). Treatmant of Parkinson's disease. CNS Drugs, 19(9), 723-743.

[10] Warrior, D. A., Overby, A., & Jankovic, J. (2000). Postural control in Parkinson's disease after unilateral posteroventral pallidotomy. Brain, 123(10), 2141-2149.

[11] Hornykiewicz, O. (2002). L-DOPA: from a biologically inactive amino acid to a successful therapeutic agent. Amino Acids 23 (1–3), 65–70.

[12] John, D. F., & Madelyn, H. F. (2007). Tyrosine, phenylalanine, and catecholamine synthesis and function in the brain. J. Nutr., 137(6), 1539-1547.

[13] Krack, P., Benazzouz, A., Pollak, P., Limousin, P., Piallat, B., Hoffmann, D., Xie J., & Benabid, A.L. (1998). Treatment of tremor in Parkinson's disease by subthalamic nucleus stimulation. Mov Disord., 13(6), 907–914.

[14] Thanvi, B. R., & Lo, T. (2004). Long term motor complications of Levodopa: clinical features, mechanisms, and management strategies. Postgrad Med J, 80(946), 452-458.

[15] Loch-Neckel, G., & Koepp, J. (2010). The blood-brain barrier and drug delivery in the central nervous system. Rev Neurol., 51(3), 165-174.

[16] Hamilton, R.D., Foss, A. J., & Leach, L. (2007). Establishment of a human in vitro model of the outer blood–retinal barrier. Journal of Anatomy, 211 (6), 707-716.

[17] Habgood, M. D., Begley, D. J., & Abbott, N. J. (2000). Determinants of passive drug entry into the central nervous system. Cell. Mol. Neurobiol., 20 (2), 231–253.

[18] Abbott, N. J. (2010). Structure and function of the blood–brain barrier. Neurobiology of Disease, 37(1), 13-25.

[19] Begley, D. J. (2004). Delivery of therapeutic agents to the central nervous system: the problems and the possibilities. Pharmacol Ther., 4(1), 29-45.

[20] Hamilton, R. D., Foss, A. J., & Leach L. (2007). Establishment of a human in vitro model of the outher blood-retinal barrier. Journal of Anatomy, 211 (6), 707-716.

[21] Ballabh, Z., Braun, A., & Nedergaard, M. (June 2004). The blood–brain barrier: an overview: structure, regulation, and clinical implications. Neurobiology of disease 16 (1), 1–13.

[22] Kusuhara, H., & Sugiyama, Y. (2001). Efflux transport systems for drugs at the blood-brain barrier and blood–cerebrospinal fluid barrier (Part 1). Drug Discov. Today, 6 (3), 150-156.

[23] Abbott, N. J., Rönnbäck, L., & Hansson, E. (2006) Astrocyte–endothelial interactions at the blood–brain barrier. Nature Rev. Neurosci., 7 (1), 41–53.

[24] Mertsch, K., & Maas J. (2002) Blood–brain barrier penetration and drug development from an industrial point of view. Curr. Med. Chem., 2(15), 187–201.

[25] Nag, S., & Begley D. J. (2005) Blood–brain barrier, exchange of metabolites and gases. In Kalimo. H. (Ed.), Pathology and Genetics. Cerebrovascular Diseases (pp. 22-29). Basel:ISN Neuropath. Press.

[26] Shapira Y., Setton D., Artru A. A., Shohami E. (1993) Blood-brain barrier permeability, cerebral edema, and neurologic function after closed head injury in rats. Anesth Analg., 77(1), 141–148.

[27] Pardridge W. M. (2005). The blood-brain barrier and neurotherapeutics. The Journal of the American Society for Experimental NeuroTherapeutics, 2(1), 1-2.

[28] Yadollah O., Jaleh B. (2012). Impacts of blood-brain barrier in drug delivery and targeting of brain tumors. Bioimpacts, 2(1), 5-22.

[29] Masserini, M. (2013). Nanoparticles for brain drug delivery. ISRN Biochemistry, 2013(1), 1-18.

[30] Gabathuler, R. (2010). Approaches to transport therapeutic drugs across the blood – brain barrier to treat brain diseases. Neurobiology of Disease, 37(1), 48-57.

[31] Bangham, A. D.; Horne, R. W. (1964). Negative Staining of Phospholipids and Their Structural Modification by Surface-Active Agents As Observed in the Electron Microscope. Journal of Molecular Biology, 8(5), 660–668.

[32] Torchilin, V. (2006). Multifunctional nanocarriers. Advanced Drug Delivery Reviews, 58 (14), 1532–55.

[33] Gomezhens, A; Fernandezromero, J. (2006). Analytical methods for the control of liposomal delivery systems. TrAC Trends in Analytical Chemistry, 25 (2), 167.

[34] Torchilin, V. P. (2005). Recent advances with liposomes as pharmaceutical carriers. Nature Rev. Drug Discov., 4(2), 145-160.

[35] Koshkaryev, A., Sawant, R., Deshpande, M., & Torchilin, V. (2013). Immunoconjugates and long circulating systems: Origins, current state of the art and future directions. Advanced Drug Delivery Reviews, 65(1), 24-35.

[36] Senior J. (1982). Is half-life of circulating liposomes determined by changes in their permeability? FEBS Lett., 145(1), 109–14.

[37] Ishida, T., Harashima, H., & Kiwada, H. (2002). Liposome clearance. Biosci Rep., 22(2), 197–224.

[38] Veronese, F. M., & Pasut G. (2005). PEGylation, successful approach to drug delivery. Drug Discov. Today, 10(21), 1451–1457.

[39] Dreborg, S., & Akerblom, E.B. (1990). Immunotherapy with monomethoxy-polyethylene glycol modified allergenes. Crit Rev Ther Drug Carrier Syst., 6(4)315–65.

[40] Jing, L., & John K. (2003). Synthesis of polyethylene glycol (peg) derivatives and pegylated−peptide biopolymer conjugates. 4(4), 1055-1067.

[41] Johnstone, S.A., Masin, D., & Mayer, L., (2001). Surface associated serum proteins inhibit the uptake of phosphatidylserine and poly(ethylene glycol) liposomes by mouse macrophages. Biochim Biophys Acta., 1513(1), 25–37.

[42] Medina, O. P., Zhu, Y., & Kairemo, K. (2004). Targeted liposomal drug delivery in cancer. Curr Pharm Des., 10(24), 2981–2989.

[43] Gindy, M. E., Ji, S., Hoye, T. R., Panagiotopoulos, A. Z., & Prud'homme, R. K. (2008). Preparation of poly(ethylene glycol) protected nanoparticles with variable bioconjugate ligand density. Biomacromolecules, 9(10), 2705-2711.

[44] Gomezhens, A., & Fernandezromero, J. (2006). Analytical methods for the control of liposomal delivery systems. TrAC Trends in Analytical Chemistry, 25(2), 167-168.

[45] Yang, F., Jin, C., Jiang, Y., Li, J., Di, Y., Ni, Q., & Fu, D. (2011). Liposome based delivery systems in pancreatic cancer treatment: from bench to bedside. Cancer Treat Rev., 37(8), 633-642.

[46] Gulati, M., Grover, M., & Singh, S. (1998). Lipophilic drug derivatives in liposomes. Int J Pharm., 165(2), 129–68.

[47] Zhang, L., Gu, F. X., Chan, J. M., Wang, A. Z., Langer, R. S., & Farokhzad, O. C. (2008). Nanoparticles in Medicine: Therapeutic Applications and Developments. Clinical Pharmacology and Therapeutics, 83(5), 761–69.

[48] Gomezhens, A., & Fernandezromero, J. (2006). Analytical methods for the control of liposomal delivery systems. TrAC Trends in Analytical Chemistry, 25(2), 167.

[49] Shojia, Y., & Nakashima, H. (2004). Nutraceutics and Delivery Systems. Journal of Vitamin Delivery Targeting, 12(6), 385-91.

[50] Park, J. W. (2002). Liposome-based drug delivery in breast cancer treatment. Breast Cancer Res., 4(3), 95–99.

[51] Chaize, B., Colletier, J. P., Winterhalter, M., & Fournier, D. (2004). Encapsulation of Enzymes in Liposomes: High Encapsulation Efficiency and Control of Substrate Permeability. Artificial Cells, Blood Substitutes, and Biotechnology**,** 32(1), 67-75.

[52] Chang, H., & Yeh, M. (2012). Clinical development of liposome-based drugs: formulation, characterization, and therapeutic efficacy. International Journal of Nanomedicine, 7(1), 49-60.

[53] Patravale, V. B. & Mandawgade, S. D. (2008). Novel Cosmetic Delivery Systems: An Application Update. Internation al Journal of Cosmetic Science, 30(1), 19-33.

[54] Rahimpour, Y., & Hamishehkar, H. (2012). Liposomes in cosmeceutics. Expert Opin. Drug Deliv., 9(4), 443–455.

[55] Hattori, Y., Kawakami, S., Suzuki, S., Yamashita, F., & Hash, M. (2004). Enhancement of immune responses by DNA vaccination through targeted gene delivery using mannosylated cationic liposome formulations following intravenous administration in mice. Biochem. Biophys. Res. Commun., 317(4), 992-999.

[56] Gouin, S. (2004). Microencapsulation: Industrial appraisal of existing technologies and trends. Trends in Food Science Technology, 15(7-8), 330–347.

[57] Keller, B. C. (2001). Liposomes in nutrition. Trends Food Sci. Technol., 12 (1), 25-31.

[58] Mozafari, M. R., Johnson, C., Hatziantoniou, S., & Demetzos, C. (2008). Nanoliposomes and their applications in food nanotechnology. Journal of liposome research, 18(4), 309–27.

[59] Pinheiro, M., Lúcio, M., Lima, J., & Reis, S. (2011). Liposomes as drug delivery systems for the treatment of tb. Nanomedicine, 6(8), 1413-1428.

[60] Pandey, R., & Khuller, G. K. (2006). Nanotechnology based drug delivery systems for the management of tuberculosis. Indian J. Exp. Biol, .44(5), 357–366.

[61] Deol, P., & Khuller, G. K. (1997). Lung specific stealth liposomes: stability, biodistribution and toxicity of liposomal antitubercular drugs in mice. Biochim. Biophys. Acta., 1334(2-3), 161–172 .

[62] Pison, U., Welte, T., Giersing, M., & Groneberg, D. A. (2006). Nanomedicine for respiratoy diseases. Eur. J. Pharmacol., 533(1-3), 341–350.

[63] Gill, S., Löbenberg, R., Ku, T., Azarmi, S., Roa, W., & Prenner, E. J. (2007). Nanoparticles: characteristics, mechanisms of action, and toxicity in pulmonary drug delivery – a review. J. Biomed. Nanotechnol., 3(2), 107–119.

[64] Immordino, M. L., Dosio, F., & Cattel. L. (2006). Stealth liposomes: review of the basic science, rationale, and clinical applications, existing and potential. Int J Nanomedicine, 1(3): 297-315.

[65] Watanabe, K., Kaneko, M., & Maitani, Y. (2012). Functional coating of liposomes using a folate- polymer conjugate to target folate receptors. Int J Nanomedicine., 7(1), 3679-3688.

[66] Yamada, A., Taniguchi, Y., Kawano, K., Honda, T., Hattori, Y., & Maitani, Y. (2008). Design of folate-linked liposomal doxorubicin to its antitumor effect in mice. Clin Cancer Res., 14(24), 8161–8168.

[67] Daniels, A., Noor-Mahomed, N., Singh, M., & Ariatti, M. (2011). Cytofectin amine head group modification and degree of liposome pegylation: factors influencing gene transfer. Indian J Pharm Sci., 73(4), 381-386.

[68] Scherphof, G. L. (1985). Uptake and intracellular processing of targeted and nontargeted liposomes by rat Kupffer cells in vivo and in vitro. Ann N Y Acad Sci., 446(1), 368-384.

[69] Gabizon, Alberto; Goren, Dorit; Horowitz, Aviva T.; Tzemach, Dinah; Lossos, Alexander; Siegal, Tali, 1997: Long-circulating liposomes for drug delivery in cancer therapy A review of biodistribution studies in tumor-bearing animals. Advanced Drug Delivery Reviews. 24(2-3), 337-344.

[70] Damen J. (2005). Transfer and exchange of phospholipid between small unilamellar liposomes and rat plasma high-density lipoproteins: dependence on cholesterol and phospholipid composition. Biochim Biophys Acta., 665(3), 538-545.

[71] Damen, J. (2005). Transfer and exchange of phospholipid between small unilamellar liposomes and rat plasma high-density lipoproteins: dependence on cholesterol and phospholipid composition. Biochim Biophys Acta., 665(3), 538–545.

[72] Mantripragada, S. (2002). A lipid based depot (DepoFoam technology) for sustained release drug delivery. Prog Lipid Res., 41(5), 392-406.

[73] Senior, J. H. (1987). Fate and behavior of liposomes in vivo: a review of controlling factors. Crit Rev Ther Drug Carrier Syst., 3(2), 123–93.

[74] Seantier, B, Breffa, V., Félix, O., & Decher, G. (2004). In situ investigations of the formation of mixed supported lipid bilayers close to the phase transition temperature. Nano Letters, 4(1), 5–10,

[75] Lisa, M., Haysa, B., Crowea, J. H., Wolkersa, W., & Rudenkoc, S. (2001). Factors affecting leakage of trapped solutes from phospholipid vesicles during thermotropic phase transitions. Cryobiology, 42(2), 88–102,

[76] Vass, A. A., Barshick, S. A., Sega, G., Caton, J., Skeen, J. T., & Love J. C. (2002). Decomposition chemistry of human remains: a new

methodology for determining the postmortem interval of human remains. Journal of Forensic Sciences, 47 (3), 542–553.

[77] Kirby, C., Clarke, J., & Gregoriadis. (1980). Cholesterol content of small unilamellar liposomes controls phospholipid loss to high density lipoproteins in the presence of serum. FEBS Letters, 111(2),324.

[78] Spyratoua, E., & Makropoulou, M. (2012). Biophotonic techniques for manipulation and characterization of drug delivery nanosystems in cancer therapy. Cancer Letters, 327(1-2), 111-122.

[79] Litzinger, D.C., Buiting, A.M., van Rooijen, N., & Huang, L. (1994). Effect of liposome size on the circulation time and intraorgan distribution of amphipathic poly(ethylene glycol)-containing liposomes. Biochimica et Biophysica Acta, 190(1), 99-107.

[80] Park, Y. S., Maruyama, K., & Huang, L. (1992). Some negatively charged phospholipid derivatives prolong the liposome circulation in vivo. Biochim Biophys Acta., 1108(2), 257–60.

[81] Ishida, T., Harashima, H., & Kiwada, H. (2001). Interactions of liposomes with cells in vitro and in vivo: opsonins and receptors. Curr Drug Metab. 2(4), 397-409.

[82] Gosk, S., Vermehren, C., Storm, G., Moos, T., (2004). Targeting anti-transferrin receptor antibody (OX26) and OX26-conjugated liposomes to brain capillary endothelial cells using in situ perfusion. J. Cereb. Blood Flow Metab., 24(11), 1193-1204.

[83] Sies, H. (1997). Oxidative stress: Oxidants and antioxidants. Experimental physiology, 82 (2), 291-295.

[84] Sies, H. (1999). Glutathione and its role in cellular functions. Free radical biology and medicine., 27(9-10), 916-921.

[85] Scholz, R. W., Graham, K. S., Gumpricht, E., & Reddy, C. C. (1989). Mechanism of interaction of vitamin E and glutathione in the protection against membrane lipid peroxidation. Ann NY Acad. Sci., 570(1):514 - 517.

[86] Paromov, V., Kumari, S., Brannon, M., Kanaparthy, N. S., Yang, H., Smith, M. G., & Stone, W. L. (2011). Protective effect of liposome-

encapsulated glutathione in a human epidermal model exposed to a mustard gas analog. Journal of Toxicology, 2011(10), 1-11.

[87] Yang, H., Paromov, V., Smith, M., & Stone, W. L. (2008). Preparation, characterization, and use of antioxidant-liposomes. Methods Mol Biol., 477(1), 277-292.

[88] Sian, J., Dexter, D. T., Lees, A. J., Daniel, S., Agid, Y., Javoy-Agid, F., Jenner, P., & Marsden, C. D. (1994). Alterations in glutathione levels in Parkinson's disease and other neurodegenerative disorders affecting basal ganglia. Ann Neurol, 36(3), 348-355.

[89] Hasegawa, T., Matsuzaki, T., Tajika, Y., Ablimit, A., Suzuki, T., Aoki, T., Hagiwara, H., & Takata, K. (2007). Differential localization of aquaporin-2 and glucose transporter 4 in polarized MDCK cells. Histochem Cell Biol., 127(3):233-241.

[90] Poland, P. A., Rondanino, C., Kinlough, C. L., Heimburg-Molinaro, J., Arthur, C. M., Stowell, S. R., Smith, D. F., & Hughey, R. P. (2011). Identification and characterization of endogenous galectins expressed in Madin Darby canine kidney cells. J Biol Chem., 286(8), 6780-6790.

[91] Stewart, J. C. M. (1980). Colorimetric determination of phospholipids with ammonium ferrothiocyanate. Analytical Biochemistry, 104 (10), 10-14.

[92] Mendes, A. C.,Baran, E.T., Pereira, R.C.,Azevedo, H.S.& Reis, R. L. (2012) Encapsulation and survival of a chondrocyte cell line within xanthan gum derivative. MacromolBiosci., 12 (3), 350-359.

[93] Duvernay, F., Chiavassa, T., Borget, F., &Aycard, J. P. (2004). Experimental studyof water - ice catalyzed thermal isomerization of cyanamide into carbodiimide: Implication forprebiotic chemistry. J Am Chem Soc., 126(25), 7772-7773.

[94] Abramoff, M. D., Magalhaes, P. J., Ram, S. J. (2004). Image Processing with ImageJ. Biophotonics International, 11(7), 36-42.

[95] Torchilin, V. (2006). Multifunctional nanocarriers. Advanced Drug Delivery Reviews, 58 (14), 1532–1555.

[96] Nagle, J. F. & Nagle, S. (2000). Structres of lipid bilayers. Biochim. Biophys. Acta, 1469(3), 159-195.

[97] Somera, G. N. (1995). Proteins and temperature. Annu. Rev. Physiol., 57(3), 43-68.

[98] Gabathuler, R. (2010). Approaches to transport therapeutic drugs across the blood-brain barrier to treat brain diseases. Neurobiol Diseases, 37(1), 48-5.

[99] Segal, E., Shouse, P. J., Bradford, S. A., Skaggs, T. H., & Corwin, L. (2009). Measuring particle size distribution using laser diffraction: Implications for predicting soil hydraulic properties. Soil Science, 174(12), 639-645.

[100] Yurasov V. V., Podgornyi G. N., Kucheryanu V. G., Kudrin V. S., Nikushkin E. V., Zhigal'tsev I. V., Sandalov Yu G., Kaplun A. P., Shvets V. I., & Kryzhanovskii G. N. (1996). Effects of l-dopa-carrying liposomes on striatal concentration of dopamine and its metabolites and phospholipid metabolism in experimental parkinson's syndrome. Bulletin of Experimental Biology and Medicine, 122(6), 1180-1183.

[101] Nounou, M. M., El-Khordagui, L. B., & Khalafallah, N. (2005). Effect of various formulation variables on the encapsulation and stability of dibucaine base in MLVs. Acta Poloniae Pharmaceutica and Drug Research, 62(5), 369-379

[102] Patel, V. B. & Misra, A. N. (1999). Encapsulation and stability of clofazimine liposomes. J Microencapsul., 16(3), 357-367.

[103] Melzak, K. A., Melzak, S. A., Gizeli, E., & Toca-Herrera, J. L. (2012). Cholesterol organization in phosphatidylcholine liposomes: A surface plasmon resonance study. Materials, 5(11), 2306-2325.

[104] Masserini, M. (2013). Nanoparticles for Brain Drug Delivery. ISRN Biochemistry, 2013 (1), 1-18.

[105] Gaillard, P. J., Appeldoorn, C. C. M., Rip, J., Dorland, R., Pol, S. M. A., Kooij, G., Vries, H., & Reijerkerk, A. (2012). Enhanced brain delivery of liposomal methylprednisolone improved therapeutic efficacy in a model of neuroinflammation. Journal of Controlled Release, 164(3), 364-369.

[106] Anabousi, S., Kleemann, E., Bakowsky, U., Kissel, T., Schmehl, T., Gessler, T., Seeger, W., Lehr, C. M., & Ehrhardt, C. (2006). Effect of

PEGylation on the stability of liposomes during nebulisation and in lung surfactant. J Nanosci Nanotechnol., 6(9-10), 3010-3016.

[107] Pisal D. S., Kosloski M. P., & Balu-lyer S. V. (2010). Delivery of therapeutic proteins, Journal of Pharmaceutical Sciences, 99(6), 2557-2575.

[108] Yinghuan, L., Jie, W., & Yue, G. (2011). Relationships between Liposome Properties, Cell Membrane Binding, Intracellular Processing, and Intracellular Bioavailability. The AAPS Journal, 13(4), 585-597.

[109] Yang, T., Cui, F. D., Choi, M. K., Cho, J. W., Chung, S. J., Shim, C. K., & Kim, D. D. (2007). Enhanced solubility and stability of pegylated liposomal paclitaxel: in vitro and in vivo evaluation. Int J Pharm. , 338(1-2), 317-326.

[110] Reddy, K. R. (2000). Controlled-release, pegylation, liposomal formulations: new mechanisms in the delivery of injectable drugs. Ann Pharmacother., 34(7-8), 915-923.

[111] Crosasso, P., Ceruti, M., Brusa, P., Arpicco, S., & Cattel, L. (2000). Preparation, characterization and properties of sterically stabilized paclitaxel-containing liposomes. J. Control. Release, 63(1-2), 19-30.

[112] Song, H., Zhang, J., Han, Z., Zhang, X., Li, Z., Zhang, L., Fu, M., Lin, C., & Ma, J. (2006). Pharmacokinetic and cytotoxic studies of pegylated liposomal daunorubicin. Cancer Chemother. Pharmacol., 57(5), 591–598.

[113] Yang, T., Cui, F. D., Choi, M. K., Cho, J. W., Chung, S. J., Shim, C. K., & Kim, D. D. (2007). Enhanced solubility and stability of PEGylated liposomal paclitaxel: in vitro and in vivo evaluation. Int J Pharm., 338(1-2), 317-326.

[114] Gabizon, A., Goren, D., Horowitz, A. D., Tzemach, D., Lossos, A., & Siegal, T. (1997). Long-circulating liposomes for drug delivery in cancer therapy: a review of biodistribution studies in tumor-bearing animals. Adv. Drug Del. Rev., 24 (2-3), 337–344.

[115] Dodi, G., Hritcu, D., &Popa, M. I. (2011). Carboxymethylation of guar gum: Synthesis and characterization. Cellulose Chem. and Technol., 45 (3-4), 171-176.

[116] Tijsen, C. J., Kolk, H. J., Stamhuis, E. J., &Beenackers, A. (2001).An experimental study on carboxymethylationof granular potato starch in non-aqueous media.CarbohydPolym, 45(3), 219-226.

[117] Bohari, Y., Mohd, C., Kamaruddin, H., &Bukhori, A. (2011). Optimization of Reaction Conditions for Carboxylmethylated Sago Starch. Iranian Polymer Journal, 20 (3), 195-204.

[118] Bono, A., Ying, P. H., Yan, F. Y., Muei, C. L., Sarbatly, R., &Krishnaiah, D. (2009). Synthesis andCharacterization of Carboxylmethyl Cellulose from Palm Kernel Cake.Adv. in Nat. Appl. Sci., 3(1), 5-11.

[119] Yoo, H. S. &Park, T. G. (2004). Folate-receptor-targeted delivery of doxorubicin nano-aggregates stabilized by doxorubicin–PEG–folate conjugate. Journal of Controlled Release., 100 (2), 247–256.

[120] Wu, J., Liu, Q., &Lee, R. J. (2006). A folate receptor-targeted liposomal formulation for paclitaxel.Int J Pharm., 316(1-2):148-153.

[121] Jin, R., Hiemstra, C., Zhong, Z., &Feijen, J. (2007). Enzyme-mediated fast in situ formation of hydrogels from dextran-tyramine conjugates. Biomaterials, 28(18); 2791-2800.

[122] Huang, J., Gao, F., Tang, X., Yu, J., Wang, D., Liu, S., & Li, Y. (2010). Liver-targeting doxorubicin-conjugated polymeric prodrug with pH-triggered drug release profile.Polymer International, 59(10), 1390-1396.

[123] Nakajima, N. & Ikada, Y. (1995). Mechanism of amide formation by carbodiimide for bioconjugation in aqeous media, Bioconjugate Chem., 6(1), 123-130.

[124] Perry, T. L., Godin, D. V., & Hansen, S. (1982). Parkinson'sdisease: a disorder due to nigral glutathione deficiency? NeurosciLett., 33(3), 305-310.

[125] Black, K. J., Carl, J. L., Hartlein, J. M., Warren, S. L., Hershey, T., & Perlmutter, J. S. (2003). Rapid intravenous loading of levodopa for human research: clinical results. J Neurosci Methods., 127(1), 19-29.

[126] Michelet, F., Gueguen, R., Leroy, P., Wellman, M., Nicolas, A., & Siest, G. (1995). Blood and plasma glutathione measured in healthy subjects by HPLC: relation to sex, aging, biological variables, and life habits. Clin Chem., 41(10), 1509-1517.

[127] Xiang, Y., Wu, Q., Liang, L., Wang, X., Wang, J., Zhang, X., Pu, X., & Zhang, Q. (2012). Chlorotoxin-modified stealth liposomes encapsulating levodopa for the targeting delivery against Parkinson's disease in the MPTP-induced mice model. J Drug Target. 20(1), 67-75.

[128] Sihorkar, V. & Vyas, S. P. (2001). Potential of polysaccharide anchored liposomes in drug delivery, targeting and immunization. J Pharm Pharm Sci., 4(2), 138-158.

[129] Umezawa, F. & Eto, Y. (1988). Liposome targeting to mouse brain: mannose as a recognition marker. Biochem Biophys Res Commun.,153(3), 1038-1044.

[130] Galea, I., Palin, K., Newman, T. A., Van Rooijen, N., Perry, V. H., & Boche, D. (2005). Mannose receptor expression specifically reveals perivascular macrophages in normal, injured, and diseased mouse brain. Glia., 49(3), 375-384.

[131] Nishimura, M., Kohara, J., & Kuroda Y. (2013). Oligomannose-coated liposome-entrapped dense granule protein 7 induces protective immune response to Neospora caninum in cattle. Vaccine, 31(35), 3528–3535.

[132] Ochi, A., Shibata, S., Mori, K., Sato, T., & Sunamoto, J. (1990). Targeting chemotherapy of brain tumors using liposome encapsulated cisplatin. Part 2. Pullulan achored liposomes to target brain tumor. Drug Delivery Syst., 5(4), 261-271.

[133] Cheng, N., Maeda, T., & Kume, T. (1996). Differential neurotoxicity induced by Levodopa and dopamine in cultured striatal neurons. Brain Research, 743 (1–2), 278–283.

[134] Mytilineou, C., Han, S. K., & Cohen, G. (1993). Toxic and protective effects of Levodopa on mesencephalic cell cultures. Journal of Neurochemistry, 61 (4), 1470–1478.

[135] Jin C. M., Yang, Y. J., Huang, H. S., Kai, M., & Lee, M. K. (2010). Mechanisms of Levodopa-induced cytotoxicity in rat adrenal pheochromocytoma cells: implication of oxidative stress-related kinases and cyclic amp. Neuroscience., 170(2):390-398.

[136] Raffray, M., & Gerald M, C. (1997) Apoptosis and necrosis in toxicology: A continuum or distinct modes of cell death? Pharmacology & Therapeutics, 75(3), 153-177.

[137] Pardo, B., Mena, M. A., Casarejos, M. J., Paíno, C. L., & De Yébenes, J. G. (1995). Toxic effects of Levodopa on mesencephalic cell cultures: protection with antioxidants. Brain Research, 682 (1–2), 133–143.

[138] Scholz, R. W., Graham, K. S., Gumpricht, E., & Reddy, C. C. (1989). Mechanism of interaction of vitamin E and glutathione in the protection against membrane lipid peroxidation. Annals of the New York Academy of Sciences, 570(1), 514-517.

[139] Pompella, A., Visvikis, A., Paolicchi, A., Tata, V., & Casini, A. F. (2003). The changing faces of glutathione, a cellular protagonist. Biochemical Pharmacology, 66 (8), 1499–1503.

[140] Wang X. J., & Xu, J. X. (2005). Possible involvement of Ca^{2+} signaling in rotenone-induced apoptosis in human neuroblastoma SH-SY5Y cells. Neurosci. Lett., 376 (2), 127–132.

[141] Yu. Z., Li, W., Hillman, J., & Brunk, U. T. (2004). Human neuroblastoma (SH-SY5Y) cells are highly sensitive to the lysosomotropic aldehyde 3-aminopropanal. Brain Res., 1016(2),163-169.

[142] Kim, S. S., Park, R. Y., Jeon, H. J., Kwon, Y. S., & Chun, W. (2005). Neuroprotective effects of 3,5-dicaffeoylquinic acid on hydrogen peroxide-induced cell death in SH-SY5Y cells. Phytotherapy Research, 19 (3), 243-245.

[143] Rafiyath, S. M., Rasul, M., Lee, B., Wei, G., Lamba, G., & Liu, D. (2012). Comparison of safety and toxicity of liposomal doxorubicin vs. conventional anthracyclines: a meta-analysis. Exp Hematol Oncol., 1(1), 1-10.

[144] Katayama, K., Sunamoto, J., Takada, M., & Yuzuriha, T. (1983). Coated ubidecarenone-containing liposome. U.S. Patent No. 4,636,381. California, CA: U.S. Patent and Trademark Office.

[145] Rooy, I., Mastrobattista, E., Storm, G., Hennink, W. E., &Schiffelers, R. M. (2011). Comparison of five different targeting ligands to enhance accumulation of liposomes into the brain. Controlled Release, 150(1), 30-36.

[146] Pappert, E. J., Buhrfiend, C., Lipton, J. W., Carvey, P. M., Stebbins, G. T., &Goetz, C. G. (1996). Levodopa stability in solution: time course, environmental effects, and practical recommendations for clinical use. Mov. Disord., 11(1), 24-26.

[147] Dagenais, C., Avdeef, A., Tsinman, O., Dudley, A., &Beliveau, R.(2009). P-glycoprotein deficient mouse in situ blood-brain barrier permeability and its prediction using an in combo PAMPA model.Eur J Pharm Sci., 38(2), 121-137.

[148] Contin, M., Riva, R., Martinelli, P., Cortelli, P., Albani, F., & Baruzzi, A. (1994). Longitudinal monitoring of the levodopa concentration-effect relationship in Parkinson's disease. Neurology., 44(7),1287-1292.

[149] Xie, Y., Ye, L., Zhang, X., Cui, W., Lou, J., Nagai, T., &Hou, X. (2005). Transport of nerve growth factor encapsulated into liposomes across the blood-brain barrier: in vitro and in vivo studies. J Control Release., 105(1-2), 106-119.

[150] Bachmeier, C. J., Trickler, W. J., &Miller, D. W. (2006). Comparison of drug efflux transport kinetics in various blood-brain barrier models. Drug MetabDispos., 34(6), 998-1003.

[151] Jeffrey, P. & Summerfield, S. G. (2007). Challenges for blood–brain barrier (BBB) screening. Xenobiotica, 37(10–11), 1135–1151.

[152] Orthmann, A., Zeisig, R., Koklic, T., Sentjurc, M., Wiesner, B., Lemm, M., &Fichtner, I. (2010). Impact of membrane properties on uptake and transcytosis of colloidal nanocarriers across an epithelial cell barrier model. J Pharm Sci., 99(5), 2423-2433.

[153] Ambroziak, K., Kuteykin-Teplyakov, K., Luna-Tórtos, C., Al-Falah, M., Fedrowitz, M., &Löscher, W. (2010). Exposure to antiepileptic drugs does not alter the functionality of P-glycoprotein in brain capillary endothelial and kidney cell lines. Eur J Pharmacol., 628(1-3), 57-66.

[154] Wang, Q., Rager, J. D., Weinstein, K., Kardos, P. S., Dobson, G. L., Li, J., &Hidalgo, I. J. (2005). Evaluation of the MDR-MDCK cell line as a permeability screen for the blood-brain barrier. Int J Pharm., 288(2), 349-359.

[155] Hirase, T., Staddon, J. M., Saitou, M., Ando-Akatsuka, Y., Itoh, M., Furuse, M., Fujimoto, K., Tsukita, S., &Rubin, L. L. (1997). Occludin as a possible determinant of tight junction permeability in endothelial cells. J Cell Sci., 10(14), 1603-1613.

[156] Hombach, J., & Bernkop-Schnürch, A. (2009). Chitosan solutions and particles: evaluation of their permeation enhancing potential on MDCK cells used as blood brain barrier model. Int J Pharm., 376(1-2), 104-109.

[157] Senior, J. H. (1987). Fateandbehavior of liposomes*in vivo*: a review of controlling factors. Crit Rev Ther Drug Carrier Syst., 3(2), 123–193.

[158] Swaroop, K., Jyothi, T., Nagendar, S., Devipriya, S., Vijaya, K., & Sudhakar, B. (2011). Stability of liposomes. Pharmanest, 2(4), 301-307.

[159] Pardridge, W. M. (2005). The blood-brain barrier: bottleneck in brain drug development. NeuroRx., 2 (1), 3-14.

[160] Boer, A. G. & Gaillard, P. J. (2007). Drug Targeting to the Brain. Annu Rev Pharmacol Toxicol., 47 (1) 323-355.

[161] Kang, Y. S. & Pardridge, W. M. (1994). Brain delivery of biotin bound to a conjugate of neutral avidin and cationized human albumin. Pharm Res., 11(9),1257-1264.

[162] Béduneau, A., Saulnier, P., & Benoit, J. P. (2007). Active targeting of brain tumors using nanocarriers. Biomaterials, 28(33), 4947-4967.

[163] Bickel, U., Yoshikawa, T., & Pardridge, W. M. (2001). Delivery of peptides and proteins through the blood-brain barrier. Adv Drug Deliv Rev., 46(1-3):247-279.

[164] Ponka, P. & Lok, C. N. (1999). The transferrin receptor: role in health and disease. Int J Biochem Cell Biol.,31(10), 1111-1137.

[165] Gosk, S., Vermehren. C., Storm. G., & Moos, T. (2004). Targeting anti-transferrin receptor antibody (OX26) and OX26-conjugated liposomes to brain capillary endothelial cells using in situ perfusion. J Cereb Blood Flow Metab., 24(11), 1193-1204.

[166] Qin, Y., Fan, W., Chen, H., Yao, N., Tang, W., Tang, J., Yuan, W., Kuai R., Zhang, Z., Wu, Y., He, Q. (2010). In vitro and in vivo investigation of glucose-mediated brain-targeting liposomes. J Drug Target., 18(7), 536-549.

[167] Reidelberger, R., Haver, A., & Chelikani, P. K. (2013). Role of peptide YY(3-36) in the satiety produced by gastric delivery of macronutrients in rats. Am J Physiol Endocrinol Metab., 304(9), 944-950.

[168] Jallouli, Y., Paillard, A., Chang, J., Sevin, E., & Betbeder, D. (2007). Influence of surface charge and inner composition of porous nanoparticles to cross blood-brain barrier in vitro. Int J Pharm., 344(1-2), 103-109.

[169] Marchesini, G., Marzocchi, R., Noia, M., & Bianchi, G. (2005). Branched-chain amino acid supplementation in patients with liver diseases. J Nutr., 135(6), 1596-1601.

[170] Merli, V., Adrienne, P., & Aronhime, K. J. (2006). Polymorphs of memantine hydrochloride. U.S. Patent No. 7462743. California, CA: U.S. Patent and Trademark Office.

[171] Tsuchiya, T., Ikarashi, Y., Hata, H., Toyoda, K., Takahashi, M., Uchima, T., Tanaka, N., Sasaki, T., & Nakamura, A. (1993). Comparative studies of the toxicity of standard reference materials in various cytotoxicity tests and in vivo implantation tests. J Appl Biomater., 4(2), 153-156.

[172] Xie, H. R., Hu, L. S., & Li, G. Y. (2010). SH-SY5Y human neuroblastoma cell line: in vitro cell model of dopaminergic neurons in Parkinson's disease. Chin Med J (Engl)., 123(8), 1086-1092.

[173] Di, L., Kerns, E. H., Bezar, I. F., Petusky, S. L., & Huang, Y. (2009). Comparison of blood-brain barrier permeability assays: in situ brain perfusion, MDR1-MDCKII and PAMPA-BBB. J Pharm Sci., 98(6), 1980-1991.

APPENDIX A

CALIBRATION CURVES

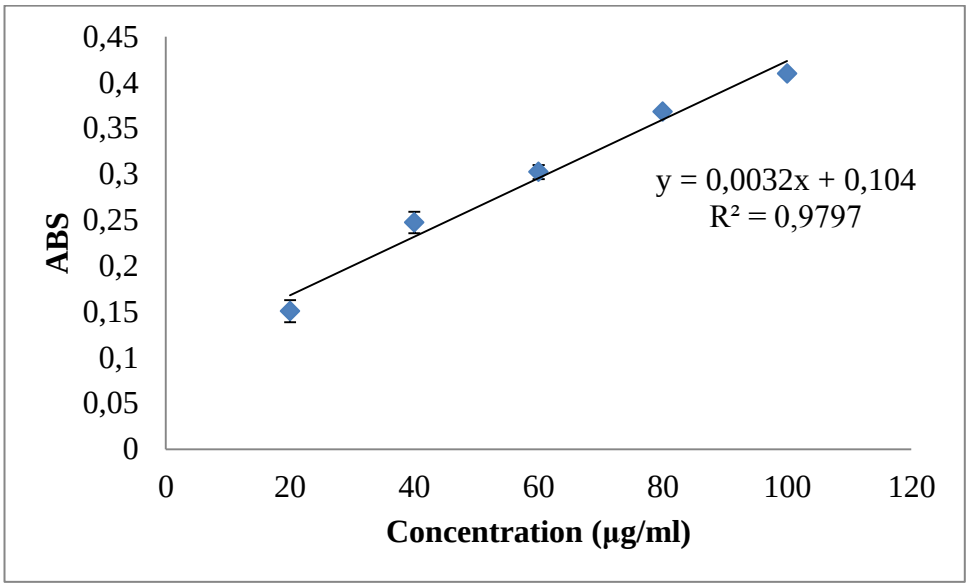

Figure A1 – DPPC calibration curve

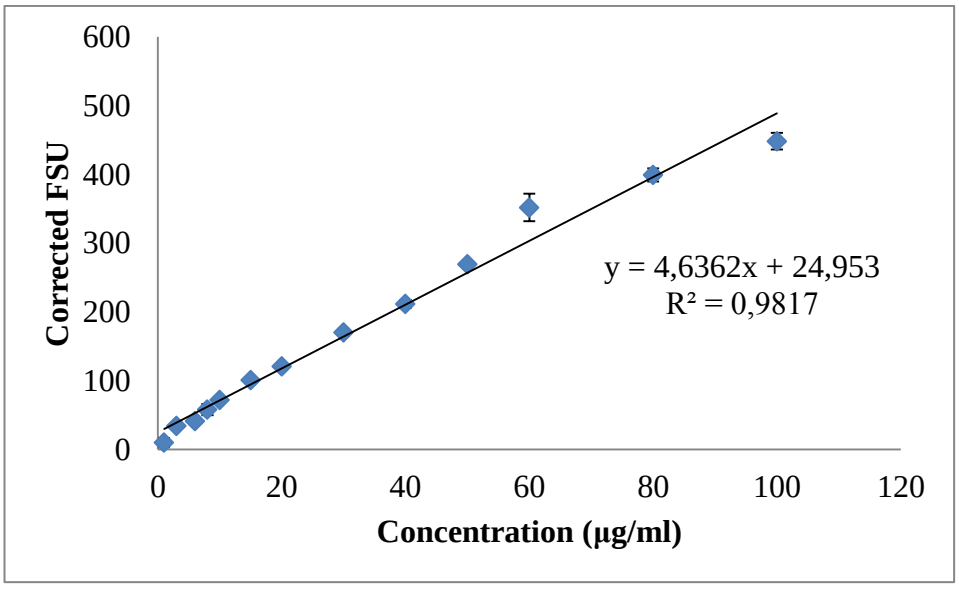

Figure A2 – Levodopa calibration curve

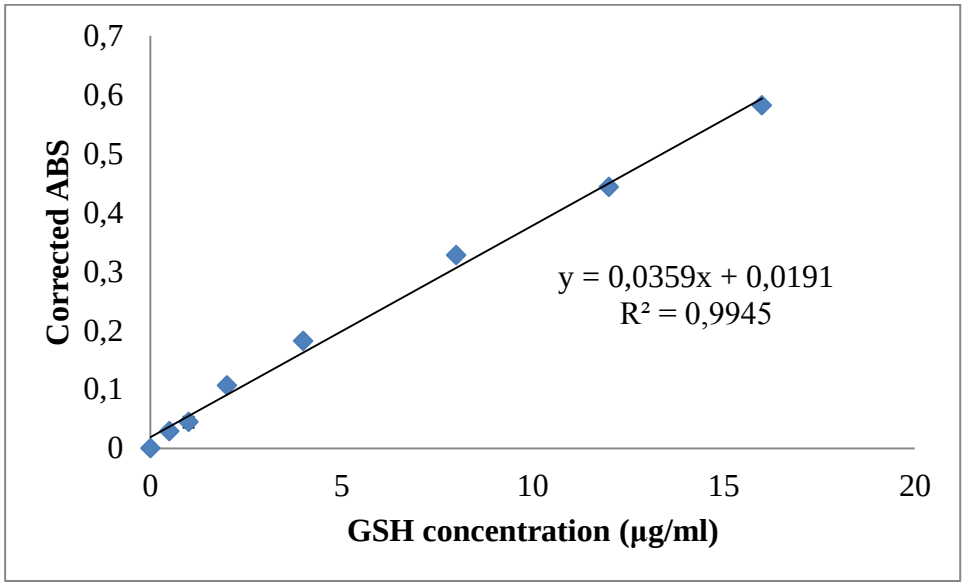

Figure A3 – GSH calibration curve

APPENDIX B

FLUORESCENCE EXCITATION AND EMISSION SPECTRA

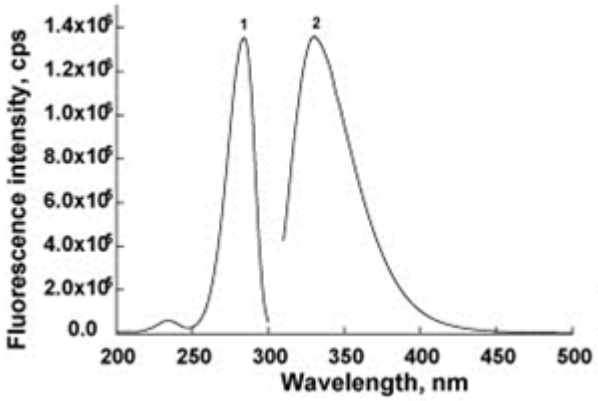

Figure B1 – Fluorescence (1) excitation (λ_{ex} = 284 nm)and (2) emission (λ_{em} = 331 nm) spectra of Levodopa

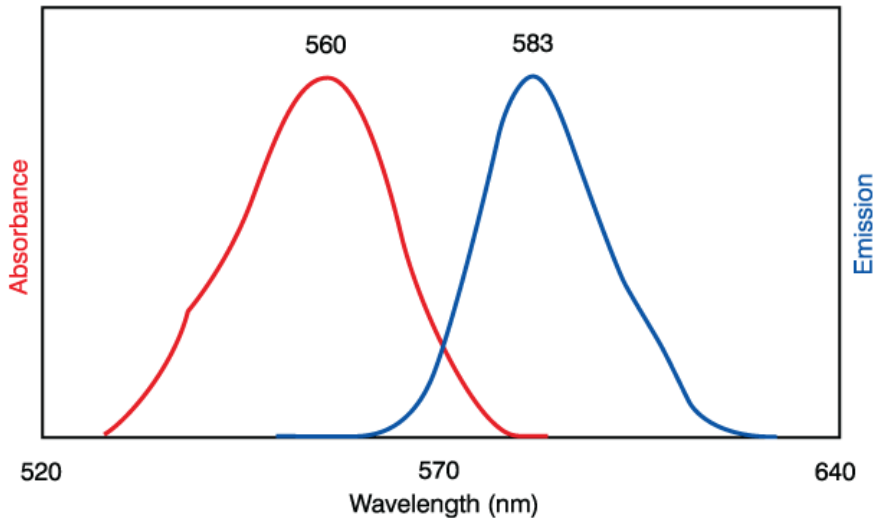

Figure B2 – Fluorescence excitation and emission spectra of Lissamine-Rhodamine PE (λ_{ex} = 560 nm) andemission (2) (λ_{em} = 583 nm)